



**US Army Corps
of Engineers®**
Engineer Research and
Development Center

Feasibility Investigation into Strengthening of Timber Bridge Stringers

Anthony J. Lamanna, Arda Akbiyik, James C. Ray,
and Gerardo I. Velázquez

May 2007

Feasibility Investigation into Strengthening of Timber Bridge Stringers

Anthony J. Lamanna and Arda Akbiyik

Department of Civil and Environmental Engineering

201 Walter E. Blessey Hall

Tulane University

New Orleans, LA 70118

James C. Ray and Gerardo I. Velázquez

Geotechnical and Structures Laboratory

U.S. Army Engineer Research and Development Center

3909 Halls Ferry Road

Vicksburg, MS 39180-6199

Final report

Approved for public release; distribution is unlimited.

Prepared for Headquarters, U.S. Army Corps of Engineers
Washington, DC 20314-1000

Abstract: The majority of timber bridges in the United States are nearing the end of their service life. They exhibit several types of damage, which occurs in their structural elements such as timber stringers. The most commonly encountered damage type in timber stringers in bridge structures is horizontal splits. Researchers investigated the feasibility of repairing timber stringers that showed signs of horizontal splitting along the length of the member. Timber stringer damage types were reviewed with particular attention to horizontal splits along the span, and the factors contributing to these failure types were studied. Typical timber stringers recently taken from service were examined to understand the effects of horizontal split damage and its impact on the effectiveness of the repair methods. Several methods for repairing horizontal splits along the span of timber stringers were employed, including fiber reinforced polymer plates attached to the vertical sides of the stringers with lag screws. Thirteen stringers were repaired with approximately 44% increase of the unstrengthened postfailure load capacity. It was proven that the methods examined in this study may be feasible to repair timber stringers with horizontal splits.

DISCLAIMER: The contents of this report are not to be used for advertising, publication, or promotional purposes. Citation of trade names does not constitute an official endorsement or approval of the use of such commercial products. All product names and trademarks cited are the property of their respective owners. The findings of this report are not to be construed as an official Department of the Army position unless so designated by other authorized documents.

DESTROY THIS REPORT WHEN NO LONGER NEEDED. DO NOT RETURN IT TO THE ORIGINATOR.

Contents

Figures and Tables	vi
Preface	x
Unit Conversion Factors	xi
1 Introduction	1
Defects in timber stringers	2
Objective and scope	2
Methodology	3
Study outline.....	4
2 Literature Review	5
Structural behavior of timber.....	5
<i>Flexural failure modes</i>	5
<i>Natural defects in wood</i>	6
Shear strength of wood beams	8
<i>Wood shear strength without splits</i>	8
<i>Effects of splits and checks on shear strength</i>	9
Timber bridge maintenance.....	10
<i>Replacement</i>	10
<i>Repairs</i>	10
<i>Preservative maintenance</i>	12
Studies on timber members recycled from old timber structures.....	12
Previous studies on timber strengthening and repairing.....	13
<i>Strengthening with aluminum and steel</i>	13
<i>Strengthening of timber railroad ties</i>	13
<i>Strengthening with FRP materials</i>	14
3 Experimental Program	16
Materials	18
<i>Timber stringers</i>	18
<i>Hex bolts and lag screws</i>	20
<i>FRP material</i>	22
<i>Plywood</i>	23
<i>Epoxy resin</i>	23
<i>Drilling tools</i>	23
Timber specimens	25
<i>Specimen C1</i>	25
<i>Specimen C2</i>	26
<i>Specimen C3</i>	26
<i>Specimen C4</i>	26
<i>Specimen C5</i>	27

<i>Specimen C6</i>	28
<i>Specimen C7</i>	29
<i>Specimen C8</i>	30
<i>Specimen C9</i>	30
<i>Specimen C10</i>	30
<i>Specimen C11</i>	31
<i>Specimen C12</i>	32
<i>Specimen C13</i>	33
<i>Specimen C14</i>	33
<i>Specimen C15</i>	34
<i>Specimen C16</i>	35
Repair systems for stringers	35
Number of hex bolts and lag screws	36
Number of lag screws to attach side plates	37
Stringers repaired with hex bolts	39
Specimens C2-R and C3-R	39
Specimen C4-R	41
Specimen C5-R	42
Stringers repaired with lag screws	44
Specimen C6-R	44
Specimens C7-R and C10-R	44
Specimens C11-R and C15-R	46
Stringer C13-R repaired with plywood side plates	46
Stringers repaired with FRP side plates or FRP strip	48
Specimens C14-R and C16-R	48
Specimen C12-R	50
4 Testing Methods and Procedure	52
Testing frame	52
Load application	53
Data acquisition for tests	54
Loading application	57
5 Test Results and Discussion	59
Test results of original stringers	64
<i>Specimen C1</i>	64
<i>Specimen C2</i>	65
<i>Specimen C3</i>	66
<i>Specimen C4</i>	67
<i>Specimen C5</i>	69
<i>Specimen C6</i>	71
<i>Specimen C7</i>	72
<i>Specimen C8</i>	74
<i>Specimen C9</i>	75
<i>Specimen C10</i>	77
<i>Specimen C11</i>	77

<i>Specimen C12</i>	78
<i>Specimen C13</i>	80
<i>Specimen C14</i>	80
<i>Specimen C15</i>	82
<i>Specimen C16</i>	82
Discussion of original timber stringers	83
Test results of repaired stringers.....	88
<i>Stringers repaired with hex bolts</i>	90
<i>Stringers repaired with lag screws</i>	95
<i>Specimen C13-R repaired with plywood side plates</i>	100
<i>Stringers repaired with FRP side plates or FRP strip</i>	102
Overall discussion	107
6 Summary and Conclusions.....	110
Summary of study	110
Conclusions	111
Recommendations for future studies	112
References.....	113
Appendix A: Structural Analysis of Timber Stringers	117
Appendix B: Number of Hex Bolts and Lag Screws	121
Appendix C: Number of Lag Screws to Attach Side Plates.....	126
Report Documentation Page	

Figures and Tables

Figures

Figure 1. Schematic of stringer damage types.....	2
Figure 2. Failure types in static bending (adapted from ASTM D 143 (1999) and ASTM D 198 (1999)).....	6
Figure 3. Failure in bending caused by knots (adapted from Bodig and Jayne (1982)).	6
Figure 4. Schematic of typical wane and shakes.....	7
Figure 5. Schematic of typical checks and splits.	8
Figure 6. Schematic of heart checks (adapted from Green, Falk, and Lantz (2001)).....	8
Figure 7. Typical cross-sectional view of a railroad bridge (adapted from Wipf, Ritter, and Wood (2000))......	11
Figure 8. Several checks along the length of a timber stringer.	18
Figure 9. Several checks at the end of a timber stringer.....	19
Figure 10. Timber stringers with end splits.	19
Figure 11. Horizontally drilled holes at the ends of the stringers.....	20
Figure 12. Two different length hex bolts.....	21
Figure 13. Three different length lag screws.....	22
Figure 14. Hilti drill model TE 2 and drill bit.....	24
Figure 15. Hilti drill model TE 35.	24
Figure 16. Checks along the length of specimen C1.....	25
Figure 17. Checks at the end and along the length of specimen C2.	26
Figure 18. Damaged area at the loading point of specimen C4.	27
Figure 19. Damaged area close to the support and knots on specimen C5.	28
Figure 20. Splitting at the ends and along the length of specimen C6.	28
Figure 21. Splitting at the ends and along the length of specimen C6.....	29
Figure 22. Cross-grain tension crack on specimen C7.	29
Figure 23. Damaged area at the end of specimen C9.	30
Figure 24. Heart checks on specimen C10.	31
Figure 25. Rotting, shakes, and splits at the support end on specimen C11.....	31
Figure 26. End splitting on specimen C11.....	32
Figure 27. A view of specimen C12.....	32
Figure 28. End splitting on specimen C13.	33
Figure 29. Heart checks on specimen C14.	34
Figure 30. End splitting on specimen C15.	34
Figure 31. Initiation of end splitting on specimen C16.....	35
Figure 32. Shear stress distribution on a cross section of timber stringers.....	36
Figure 33. Single shear connection model for hex bolts and lag screws.....	37

Figure 34. Single shear connection model for side plates attached using lag screws.	38
Figure 35. Holes being drilled with TE 2.	39
Figure 36. Schematic of cross section of specimens C2-R and C3-R.	40
Figure 37. Epoxy being applied to the hex bolts.	40
Figure 38. Specimen C3-R repaired using hex bolts and epoxy.	41
Figure 39. Schematic of hex bolt layout for specimens C2-R and C3-R.	41
Figure 40. Schematic of hex bolt layout for specimen C4-R.	42
Figure 41. Specimen C4-R repaired with hex bolts.	42
Figure 42. Specimen C5-R repaired with hex bolts and steel plates from top view.	43
Figure 43. Specimen C5-R repaired with hex bolts and steel plates from underneath.	43
Figure 44. Schematic of hex bolt layout for specimen C5-R.	44
Figure 45. Schematic of lag screws layout for specimen C6-R.	44
Figure 46. Schematic of lag screws layout for specimen C7-R.	45
Figure 47. Schematic of lag screws layout for specimen C10-R.	45
Figure 48. Specimen C7-R repaired with lag screws.	46
Figure 49. Schematic of lag screws layout for specimens C11-R and C15-R.	46
Figure 50. Lag screws being installed to specimen C13-R.	47
Figure 51. Lag screws being installed.	47
Figure 52. Schematic of plywood side plates for specimen C13-R.	48
Figure 53. Specimen C13-R repaired with plywood side plates.	48
Figure 54. FRP plates being cut to size.	49
Figure 55. Schematic of FRP side plates for specimens C14-R and C16-R.	49
Figure 56. Specimen C14-R repaired with FRP plates.	50
Figure 57. Stringer C12-R repaired at tension zone with FRP strip.	51
Figure 58. Configuration for the four-point bending test.	52
Figure 59. Typical cross section of timber stringers.	53
Figure 60. Typical configuration of the support plates.	53
Figure 61. Placement of monitoring equipment on test specimens.	54
Figure 62. Monitoring equipment on timber stringers.	55
Figure 63. The load cell-hydraulic ram setup with spreader beam.	56
Figure 64. The MTS actuator and spreader beam.	56
Figure 65. Effectiveness of a repair method.	57
Figure 66. Schematic of idealized sliding on support face.	61
Figure 67. Load-deflection curve for stringer C1.	64
Figure 68. Horizontal sliding on support face after shear failure of stringer C1.	65
Figure 69. Load-deflection curve for stringer C2.	65
Figure 70. Load-deflection curve for stringer C3.	66
Figure 71. Splinter at the midspan on stringer C3.	67
Figure 72. Load-deflection curve for stringer C4.	68
Figure 73. Cross-grain tension failure at 222 kN (50 kips) on stringer C4.	68

Figure 74. Horizontal shear failure on stringer C4	69
Figure 75. Load-deflection curve for stringer C5.....	70
Figure 76. Horizontal and tension cracks at failure for stringer C5.....	70
Figure 77. Load-deflection curve for stringer C6.....	71
Figure 78. Tension crack at failure for stringer C6.....	72
Figure 79. Load-deflection curve for stringer C7.....	73
Figure 80. Horizontal shear failure and tension crack on stringer C7.....	73
Figure 81 Load-deflection curve for stringer C8.....	74
Figure 82. Tension failure initiated by a knot on stringer C8	75
Figure 83. Load-deflection curve for stringer C9.....	76
Figure 84. Tension failure caused by a knot on stringer C9.....	76
Figure 85. Load-deflection curve for stringer C10	77
Figure 86. Load-deflection curve for stringer C11	78
Figure 87. Load-deflection curve for stringer C12.....	79
Figure 88. Cross-grain tension failure on stringer C12.....	79
Figure 89. Load-deflection curve for stringer C13	80
Figure 90. Load-deflection curve for stringer C14	81
Figure 91. Horizontal shear failure on stringer C14.....	81
Figure 92. Load-deflection curve for stringer C15	82
Figure 93. Load-deflection curve for stringer C16	83
Figure 94. Distribution of ultimate load for original stringers without end splitting.....	84
Figure 95. Unstrengthened postfailure capacity and repaired ultimate load capacities.....	89
Figure 96. Ultimate load of original and repaired stringers without end split before testing.....	89
Figure 97. Load-deflection curves for stringers C2 and C2-R.....	90
Figure 98. Tension cracks at the failure on stringer C2-R.....	91
Figure 99. Load-deflection curves for stringers C3 and C3-R.....	91
Figure 100. Load-deflection curves for stringers C4 and C4-R.....	93
Figure 101. Cross-grain tension failure and tension splinters at the midspan on stringer C4-R	93
Figure 102. Load-deflection curves for stringers C5 and C5-R.....	95
Figure 103. Load-deflection curves for stringers C6 and C6-R.....	96
Figure 104. Load-deflection curves for stringers C7 and C7-R.....	97
Figure 105. Load-deflection curves for stringers C10 and C10-R.....	98
Figure 106. Load-deflection curves for stringers C11 and C11-R.....	99
Figure 107. Load-deflection curves for stringers C15 and C15-R.....	100
Figure 108. Load-deflection curves for stringers C13 and C13-R.....	101
Figure 109. Buckling of the side plate on stringer C13-R	101
Figure 110. Load-deflection curves for stringers C14 and C14-R	103
Figure 111. Compression failures due to excessive deformations on stringer C14-R	103
Figure 112. Minor bearing damages at the holes on FRP plates.....	104
Figure 113. Load-deflection curves for stringers C16 and C16-R	104

Figure 114. Load-deflection curves for stringers C12 and C12-R.....	106
Figure 115. Horizontal shear crack after the failure of stringer C12-R.....	106

Tables

Table 1. Repair methods applied to timber stringers.	17
Table 2. Ultimate loads, bending and shear stresses at the ultimate load and unstrengthened postfailure capacity of original timber stringers.....	59
Table 3. Deflections at ultimate moment for original timber stringers.	60
Table 4. Failure modes of original timber stringers.	60
Table 5. Repaired ultimate load, bending and shear stresses at the repaired ultimate load, and effectiveness of repair methods.	62
Table 6. Deflections at ultimate moment for repaired timber stringers.....	63
Table 7. Failure modes of repaired timber stringers.	63
Table 8. Maximum, minimum, and average bending and shear stresses at ultimate load for original timber stringers with checks.	85
Table 9. Comparison of bending and shear stresses to LRFD (AFPA 1996) reference strength values for dense select structural southern pine.	85
Table 10. Comparison of bending and shear stresses of timber stringers with end splitting to LRFD (AFPA 1996) reference strength values for dense select structural southern pine.....	86
Table 11. Maximum, minimum, and average bending and shear stresses at ultimate load for original timber stringers with end splitting.	86
Table 12. Timber stringers which failed due to presence of knots.	88

Preface

This study was conducted by personnel of the Department of Civil and Environmental Engineering, Tulane University, under contract DACA 42-03-P-0212, and of the U.S. Army Engineer Research and Development Center (ERDC), Geotechnical and Structures Laboratory (GSL), Vicksburg, MS. The study was part of the Department of the Army Project No. 4A162784AT40, Work Package 168A, "BattleSpace Gap Definition and Defeat," Work Unit BG005, "Advanced Gap Defeat Concepts," which is sponsored by Headquarters, U.S. Army Corps of Engineers.

James C. Ray and Gerardo I. Velázquez were ERDC project investigators for this effort. Professor Anthony J. Lamanna was the Principal Investigator, and Arda Akbiyik was research assistant for Tulane University. Corine E. Pugh, GSL contractor (Bowhead Information Technology Services, Inc.), assisted the authors in the preparation of this report.

The experimental work was accomplished under the general supervision of Dr. David W. Pittman, Director, GSL; Dr. William P. Grogan, Deputy Director, GSL; Dr. Robert L. Hall, Chief, Geosciences and Structures Division; and James S. Shore, Chief, Structural Engineering Branch, GSL.

COL Richard B. Jenkins was Commander and Executive Director of ERDC. Dr. James R. Houston was Director.

Unit Conversion Factors

Multiply	By	To Obtain
degrees (angle)	0.01745329	radians
feet	0.3048	meters
horsepower (550 foot-pounds force per second)	745.6999	watts
inches	0.0254	meters
inch-pounds (force)	0.1129848	newton meters
miles (U.S. statute)	1,609.347	meters
square feet	0.09290304	square meters
square inches	6.4516 E-04	square meters
square miles	2.589998 E+06	square meters
square yards	0.8361274	square meters
tons (force)	8,896.443	newtons
tons (2,000 pounds, mass)	907.1847	kilograms

1 Introduction

Wood is one of the oldest construction materials in the world and has been widely used to build a variety of structures. Some important structures constructed with wood are bridges, residential buildings, and substructures. Wood is very popular as a building material because of its availability in most parts of the world, and its light weight compared to materials like concrete and steel. Wood has a high strength and is a renewable

resource. Wood has disadvantages, such as deterioration caused by decay, and swelling and shrinkage with changing atmospheric humidity. Another drawback of using wood is its poor strength perpendicular to the grain, sometimes resulting in situations where shear resistance parallel to the grain becomes critical (Triantafillou 1997).

There are several reasons for using timber as a material in bridge construction. Timber presents a natural and aesthetically pleasing appearance. A timber bridge can be constructed in any weather, including cold and wet conditions, without detrimental effects. Timber bridges possess resistance to the effects of deicing agents, can sustain overloads for short periods of time, and require less repair and rehabilitation efforts because of the relative light weight of timber (Ou and Weller 1986).

According to the National Bridge Inventory (NBI 2005), there are a total of 29,660 timber bridges in the United States. Of bridges that have a span of more than 6 m (20 ft), 12.6% are made of timber. Railroads also have more than 2,415 km (1,500 miles) of timber bridges and trestles in service (Ou and Weller 1986). The number of timber bridges is much larger in Canada and Australia. Most of the timber bridges in the United States were built 30-40 years ago. The age of a timber structure is the largest factor in gauging the deterioration of the bridge members. The majority of timber bridges in the United States are nearing, or at the end of their service life, which means they exhibit several types of damage. This occurs mostly on structural elements such as timber stringers (Svecova and Eden 2004).

Defects in timber stringers

Timber stringers exhibit five types of damage, shown schematically in Figure 1. The first damage type is interior decay along the span. The second damage type is top, bottom, corner damage, or full width vertical splitting inclined toward the bottom face. The third damage type is side or corner damage or full width vertical splits inclined toward the side face. The fourth damage type is horizontal splitting not within 3 in. of the top and bottom faces through the full width. The fifth type encompasses any damage within 130 mm (15 in.) from the face of the pier cap, including interior decay, side damage, crushing, and splitting.

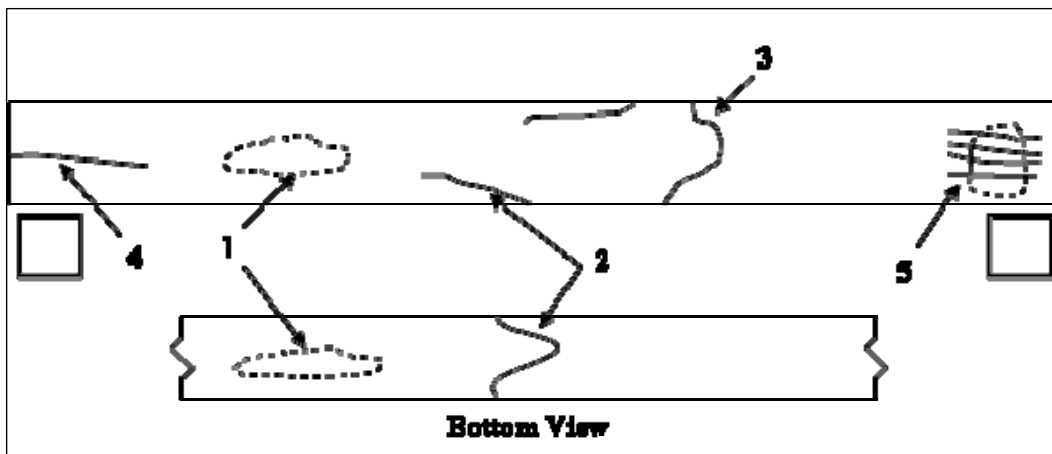


Figure 1. Schematic of stringer damage types.

The most commonly encountered damage type in timber stringers in bridge structures is type 4, horizontal splitting. These horizontal splits often stretch the entire length of the span. This splitting is induced by shear stresses and severely impacts the strength of the timber member.

Objective and scope

The main objective of this project was to investigate the feasibility of repairing timber stringers that show signs of horizontal splitting along the length of the member. An experimental program was conducted in order to examine the existing repair methods and to investigate the feasibility and effectiveness of attaching FRP strips to the sides of the stringers with mechanical fasteners.

The specific objectives of this investigation were to:

- Review of timber stringer damage types in the literature with particular emphasis on horizontal splits along the span to identify the factors contributing to these types of failures
- Examine timber stringers pulled recently from service in order to understand the stringer damage types
- Develop a method of repairing the horizontal splits along the span of the timber stringers including FRP plates attached to the vertical sides of the stringers using mechanical fasteners
- Verify the proposed repairing system experimentally on stringers, subjected to four-point bending.

Methodology

This study consists of an experimental investigation of repairing sawn timber bridge stringers with horizontal splits. All tests were performed according to ASTM D198 (1999). The experimental program was carried out involving sixteen 191 mm by 406 mm by 4.6 m (7.5 in. by 16 in. by 15 ft) timber stringers. The timber stringers were obtained from a railroad bridge recycling yard near San Marcos, TX. Four-point loading was used to determine shear and bending strength properties of the timber stringers. A stringer was used as a control and thirteen stringers were repaired with different methods. Hex bolts and lag screws were used in several configurations and spacings to repair the timber stringers, and they were inserted from the top of the stringers. Plywood and FRP plates were attached to the sides of the timber stringers using lag screws to repair the timber stringers. Based on the limited number specimens, it is appropriate to determine trends rather than concentrating on specific values such as the average.

A few timber stringers which did not exhibit horizontal splits, but had checks along the length, were tested to shear failure. Repair methods were then applied. Timber stringers which already had horizontal end splits were tested to determine the residual strength after splitting, called the postfailure load capacity. All of the stringers were tested to failure, after undergoing repair, to determine the effectiveness of the repair method. The effectiveness of a repairing method was determined by comparing the unstrengthened postfailure capacity of original stringer to ultimate strength of repaired stringer.

Study outline

An overview of the contents of the study is provided:

Chapter 2, “Literature Review” - General wood properties, failure modes in bending, and defects observed in wood. The effects of splits and checks on shear strength, timber bridge maintenance, strength properties of recycled timber members, and a review of published studies of repairing and strengthening of timber structures.

Chapter 3, “Experimental Program” - Details of the experimental program which includes repair methods applied to timber stringers.

Chapter 4, “Testing Methods and Procedures” - Testing setup, location of sensors on the specimens and properties of the data acquisition system and sensors used in the tests and the loading pattern.

Chapter 5, “Test Result and Discussion” - Test results and discussion for the timber stringers and the repair methods. The effectiveness of the repair method is determined by comparing the strength increase of the repaired specimen.

Chapter 6, “Summary and Conclusions” - Summary of the research program, conclusions resulting from this study, and recommendations for further research.

2 Literature Review

This chapter presents a brief summary of the structural behavior of wood, failure modes of timber stringers in bending, typical defects observed in wood, effects of splits and checks on shear strength, timber bridge maintenance, and the strength properties of recycled timber members. The chapter concludes with a review of previous studies of repairing and strengthening of timber structures.

Structural behavior of timber

Wood is an orthotropic material. It possesses different properties in different directions that are longitudinal, radial, or tangential to the grain. Wood strength is greatest in the longitudinal, or parallel-to-grain, direction and weakest perpendicular to the grain. Wood is different from other structural materials as its strength and other mechanical properties such as modulus of elasticity or compressive strength are extremely variable. Material properties of a given structural member are dependent on the wood species and variety, the locality from which the wood is obtained, its density, moisture content, and the presence of defects and their locations. The strength properties are, therefore, determined by a number of wood characteristics, including slope of a grain, knots and their locations, pitch, wane, density, checks or splits from uneven drying, and size variations (Bodig and Jayne 1982, Ou and Weller 1986).

Flexural failure modes

Defect-free wood specimens are called clear specimens. Several failure types for clear wood in bending have been observed during testing. The most common failure modes were horizontal shear, cross-grain tension, simple tension, and compression, as shown schematically in Figure 2. When cross-grain is present, a typical failure pattern is cross-grain tension. Compression failure typically occurs in low-density wood. Shear failure near the neutral plane occurs in species containing checks and shakes which can act as planes of weakness for shear failure (Bodig and Jayne 1982, ASTM D 143 1999, ASTM D 198 1999).

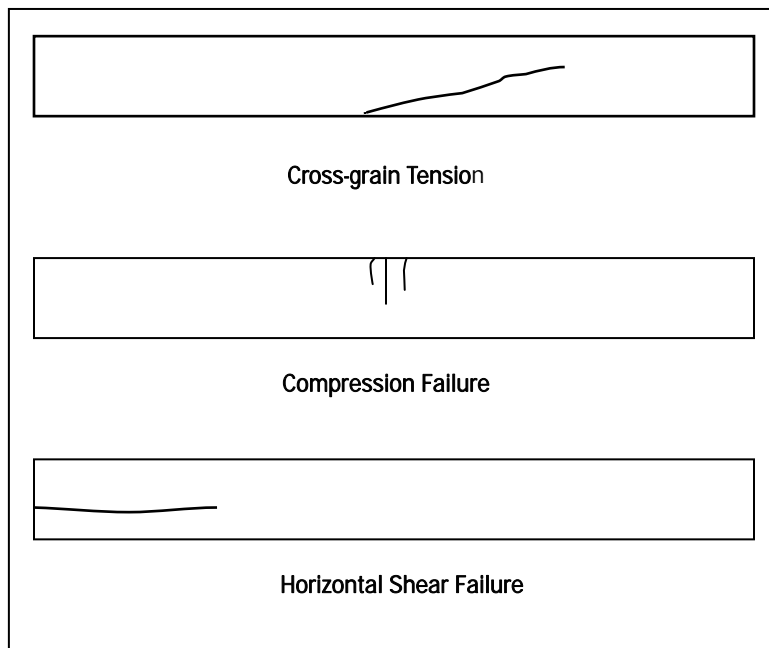


Figure 2. Failure types in static bending (adapted from ASTM D 143 (1999) and ASTM D 198 (1999)).

Natural defects in wood

Different types of defects in wood decrease the strength and durability of timber members. Commercial timber is a defect-filled natural composite; therefore, timber is visually graded according to the natural defects (Johns and Lacroix 2000). The most common types of defects that might occur in wood are knots, wanes, shakes, checks, splits, and rots or decay.

The discontinuity introduced by knots lowers the strength of the wood material. The effect of the presence of a knot on the tensile strength is greater than the effect on the compressive strength. Consequently, a knot near the bottom surface of a simple beam is less desirable than the same knot near the top surface of the beam, as shown in Figure 3.

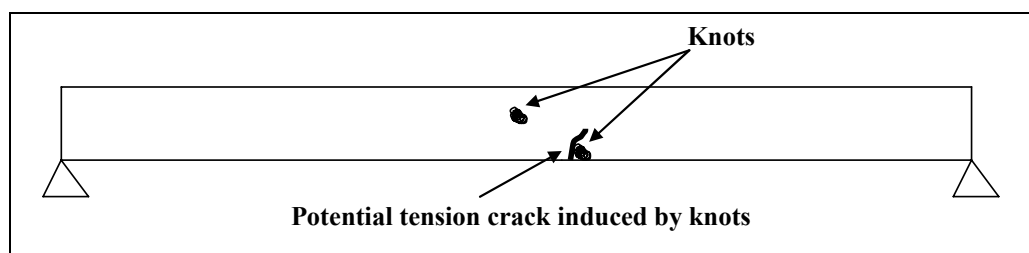


Figure 3. Failure in bending caused by knots (adapted from Bodig and Jayne (1982)).

A wane is lack of wood on the edge or corner of wood members, and shakes are lengthwise separations in the wood occurring between annual rings, shown schematically in Figure 4. Rots are usually evidence of disintegration caused by bacterial action. Wood is susceptible to damage from fungus or insects, thus hardness and mechanical strength in the presence of rot are decreased. Several preservative treatments have practically eliminated decay; splits are usually the reason for the replacement of wood members. Checking and splitting can penetrate to the interior of the member, resulting in exposing untreated wood to decay fungi and insects, which negates the beneficial effects of preservative treatments.

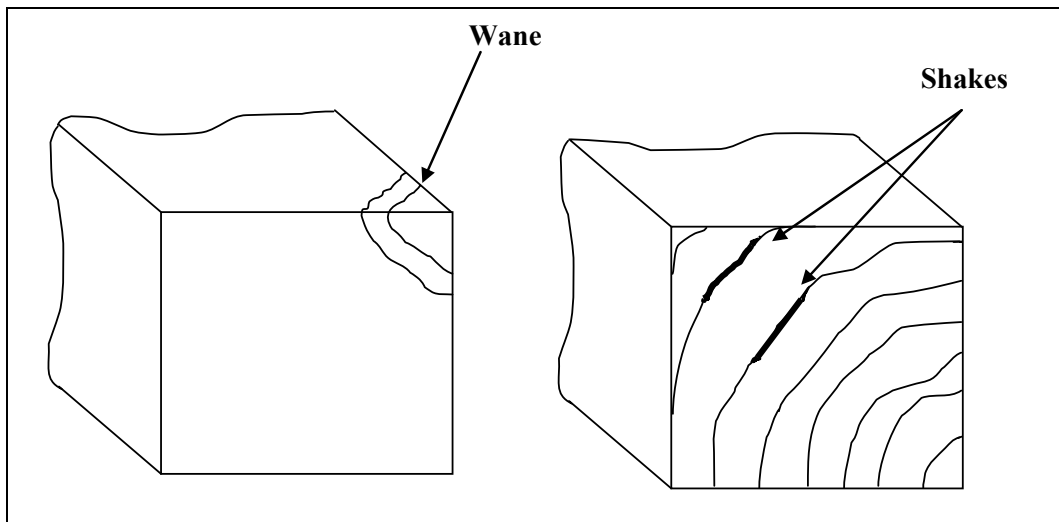


Figure 4. Schematic of typical wane and shakes.

Checks and splits are lengthwise separations in the wood, occurring across the annual rings, as shown in Figure 5. Under typical conditions, wooden beams and columns may develop splits and checks. These splits and checks are a result of swelling and shrinkage from drying as the member equilibrates to the surrounding moisture condition, or from repeated wet/dry moisture cycling. Splits and checks are commonly encountered in exposed timber bridge stringers and in timber columns (Rammer and McLean 1996; Rammer, McLean, and Cofer 1998). Heart checks are a result of stresses set up by differences in tangential and radial shrinkage of wood around pith, as shown in Figure 6. (Green, Falk, and Lantz 2001).

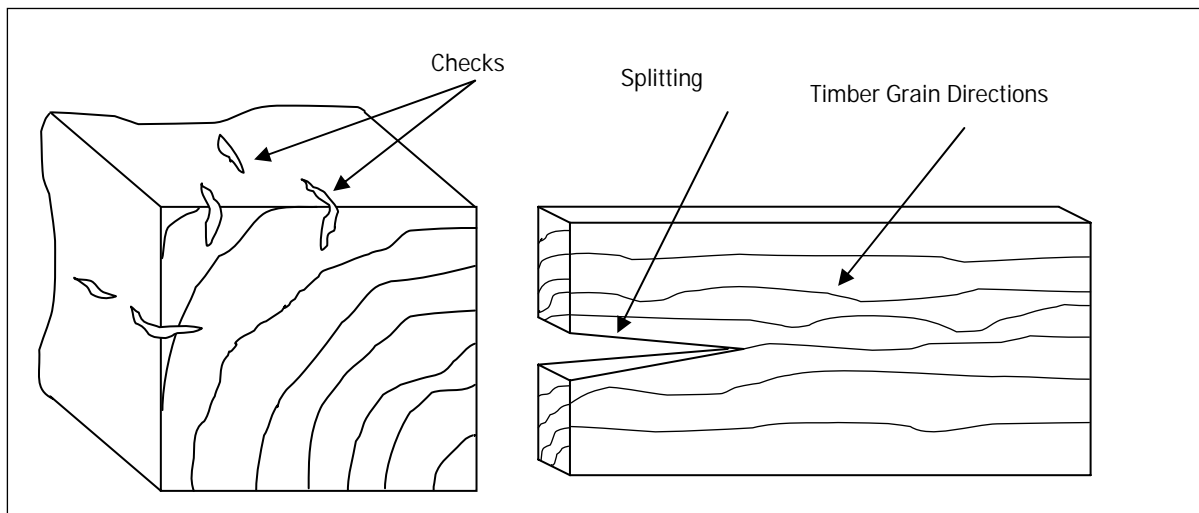


Figure 5. Schematic of typical checks and splits.

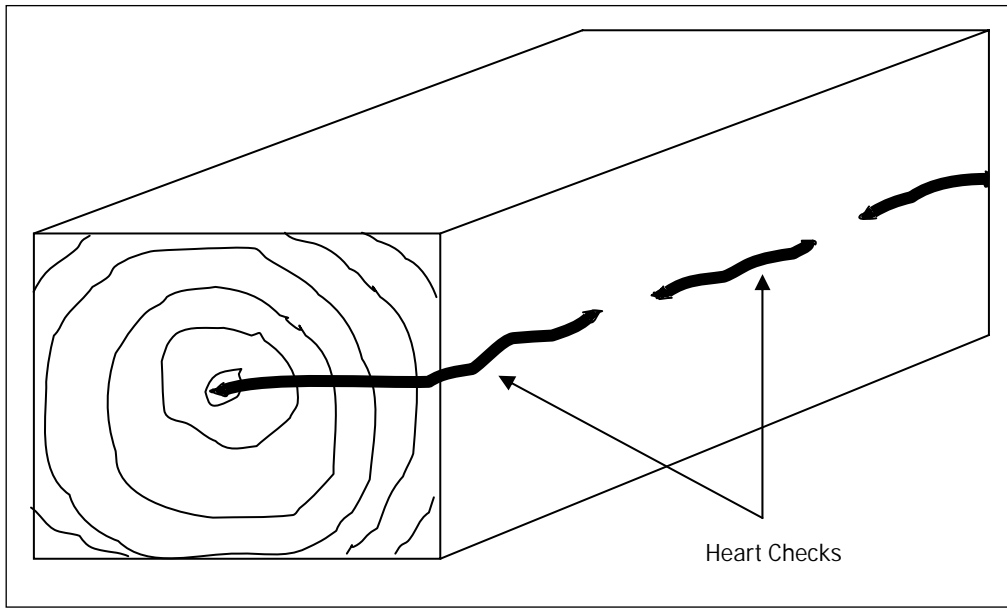


Figure 6. Schematic of heart checks (adapted from Green, Falk, and Lantz (2001)).

Shear strength of wood beams

Several studies have been conducted to understand the shear strength of wood beams. The studies concentrated on the strength of an unsplit member and the strength of a split or checked member.

Wood shear strength without splits

Shear design values for solid-sawn structural members are presently derived from small, straight-grained, clear ASTM shear block specimens (ASTM 1999). Predictions of the actual shear strength of wood beams from

shear block tests have long been questioned. Timber beams have been tested using different testing setups in order to compare the results with ASTM shear block tests of small clear specimens and finite element analysis. Studies showed that shear strength was related to size of the member; the longitudinal shear strength of beams was lower than the shear strength obtained from shear blocks. The size effect that was apparent in experimental tests has not yet been reproduced in the finite element analysis (Foschi and Barrett 1976; Longworth 1977; Rammer and Lebow 1997; Cofer, Proctor, and McLean 1997; Lam, Yee, and Barrett 1997). Shear strength values provided in the design codes do not consider the member size effects. Current shear design values are the values obtained from ASTM clear shear block tests and are reduced by a factor of safety to account for member size effects (Rammer and McLean 1996; Rammer, McLean, and Cofer 1998).

Effects of splits and checks on shear strength

In an uncontrolled environment, the occurrence and degree of splitting vary widely and are difficult to predict. The effect of checks and splits on the shear strength of a member depends on the proximity and closeness of the defect alignment to the neutral plane of the structural member. The resistance to shear stress and the moment of inertia are reduced noticeably when a complete separation occurs along the neutral plane, thus, affecting bending strength. Published shear design values account for this uncertainty by assuming a worst case scenario, i.e., the stringer has a lengthwise split at the neutral axis (Bodig and Jayne 1982; Rammer and McLean 1996; Rammer, McLean, and Cofer 1998).

Several theoretical approaches have been proposed to account for the effects of checks and splits on shear strength. In the early 1930s, the two-beam theory was proposed. The position of the load, beam depth, and span was considered without taking into account the length and depth of checks; however, it was realized that the fundamental assumptions of two-beam shear behavior were incorrect (Keenan 1974). Fracture mechanics approaches have also been proposed for investigation of the effects of checks and splits on the shear strength (Murphy 1979). Rammer and McLean (1996) and Rammer, McLean, and Cofer (1998) investigated the shear strength on both unsplit and split/checked beam specimens. Different size beams with various loading configurations were tested. They found that the shear strength without splits and checks decreases with the beam size. The effects of beam splitting and checking on the measured

shear strength were smaller than predicted by current code procedures or by fracture mechanics.

Timber bridge maintenance

The age of a structure is a crucial factor in the level of deterioration of a bridge. Since the typical service life of a timber bridge is approximately 30–40 years, the majority of timber bridges in the United States are nearing the end of their service life, resulting in the formation of several types of damage in the timber members (Svecova and Eden 2004). Timber bridge maintenance is therefore important. Timber bridge maintenance falls into three categories: replacement, repair and preventative maintenance (Ou and Weller 1986).

Replacement

Replacement includes the removal of damaged timber bridge members such as stringers, plank decks, and defective piling; however, replacement is time consuming and is not cost effective (Radford et al. 2002). It may be preferable to have in situ repair methods of timber bridge members available in certain cases.

Repairs

There are several reasons for repairing structures. Most of the reasons to repair timber bridges are aimed at extending the service life of the bridge, increasing or maintaining the load-carrying capacity, or improving the bridge safety. For example, the design axle load of railcars was 30 tons (66 kips) for many years. Double stack container trains have recently increased the axle loading from 30 tons (66 kips) to 35.7 tons (79 kips) (Radford et al. 2002). The load-carrying capability of the structure should therefore be increased to carry increasing loads safely. Since the cost of replacing the timber structures with concrete or steel is high, repair and strengthening of timber structures becomes an important issue to sustain increasing load levels safely while extending the service life of timber structures (Gentile, Svecova, and Rizkalla 2002; Radford et al. 2002).

Repairs range from strengthening existing timber pier caps to fixing cracked or split timber stringers. The appropriate methods of repair can vary depending on the location and function of the member in the structure and the severity of the damage. Repair methods include

replacement, reinforcing a member by adding a sister member, stitch bolting, inserting steel or fiberglass dowels, adding reinforcing FRP strips or reinforcing plates to the sides of exposed timber beams, addition of a fiberglass wrap, posttensioning, repairing with epoxy, and using preservatives (Avent 1985 and 1986; Ou and Weller 1986; Ebeling and Fellow 1990; Plevris and Triantafillou 1992; Triantafillou 1997; Triantafillou and Deskovic 1992; Triantafillou 1998; Johns and Lacroix 2000; Redford et al. 2002; Svecova and Eden 2004; Ehsani, Larsen, and Palmer 2004). In situ application of reinforced plates to the sides of timber members or wrapping may be problematic, because of the close proximity of members to one another, such as the case of member stacking in railroad bridges. This situation can be seen in Figure 7. Only the outer faces of the outer members would be readily accessible, and the inside members could only be reached by removing the outer stringers (Wipf, Ritter, and Wood 2000). In situ wrapping and reinforced side plates are therefore difficult to apply to interior members. From this viewpoint, the effectiveness of using steel or fiberglass dowels for shear reinforcement is crucial to reduce the amount of effort and time required in the field.

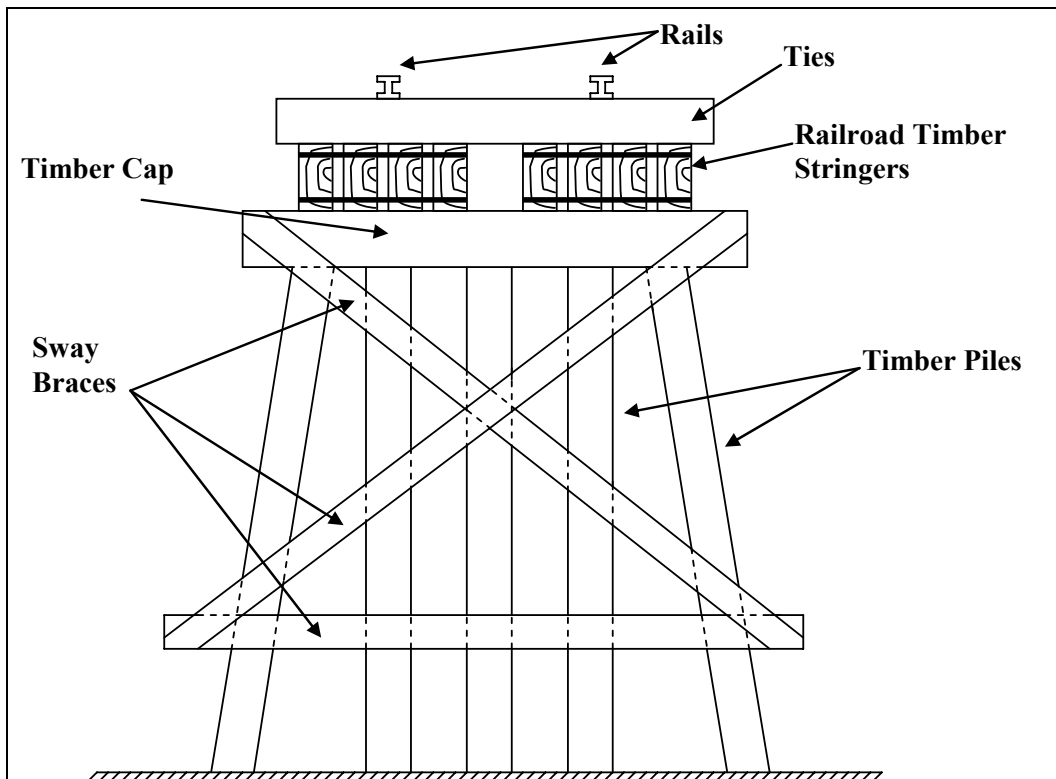


Figure 7. Typical cross-sectional view of a railroad bridge
(adapted from Wipf, Ritter, and Wood (2000)).

Preservative maintenance

Preservative maintenance is carried out either by field preservative treatments or through moisture control. Field preservatives are applied to members of the structure. Moisture control should be frequently undertaken to prevent decay in timber members of a structure (Ou and Weller 1986).

Studies on timber members recycled from old timber structures

The shear strength of timber stringers that have been in service for a considerable period of time is of concern because these members are likely to have experienced strength loss as a result of checking, splitting, and deterioration. Determination of the residual strength of wood existing in old structures is important to assess the safety of such structures.

Rammer (1999) investigated the residual shear capacity of large solid sawn Douglas-fir timber beams used in a military facility in Ardeen Hills, MN. Timber beams had dimensions of 152 mm by 356 mm (6 in. by 14 in.) and 254 mm by 457 mm (10 in. by 18 in.). Twenty members were selected that had little visual evidence or significant checking and splitting along the length for each beam size. The beams were tested at 5-point and 4-point testing setups (Rammer 1999). The 5-point test configuration was used to investigate the shear strength near the middle of the beam, typically where a member is only affected by checks, without severe end splits. The four-point test was used to create a constant shear force where the greatest occurrence of splits and checks are located at the ends of the beam. Shear failure occurred in 36 out of 40 specimens of both beam sizes in the 5-point bending test. Of the beams tested in the 4 point bending, twelve of fifteen 152 mm by 356 mm (6 in. by 14 in.) beams failed in bending. All of the 254 mm by 457 mm (10 in. by 18 in.) members tested in 4-point bending failed in shear. The test results indicated that shear strength was affected by the presence of splits and checks when compared to uncheck material strength. Shear strength was lower than the allowable shear design values for Douglas-fir for the split specimens.

The effects of heart checks and splits on the strength of timber stringers columns were also investigated. The results showed that heart checks and splits lowered the modulus of rupture by about 15%, but have no direct effect on modulus of elasticity of stringers. The effects of splits and checks in the recycled timber columns were not significant. The measured

modulus of elasticity and compressive strength were greater than design values (Falk and Green 1999; Falk et al. 2000; Green, Falk, and Lantz 2001).

Previous studies on timber strengthening and repairing

Several timber structures such as monumental timber structures and timber trusses have been repaired and strengthened with different techniques over the past 40 years. Although there have been several studies conducted to strengthen and rehabilitate the timber structures, studies on solid sawn timber stringers were uncommon (Johns and Lacroix 2002). The following sections describe previous studies into the strengthening and repairing of timber members.

Strengthening with aluminum and steel

Early investigations of reinforcing timber beams examined the use of metals for reinforcement. Aluminum sheets were placed at the top and bottom faces of timber beams. The aluminum sheets were also used horizontally and vertically between selected laminates of glulam beams to increase their strength and stiffness (Mark 1961, 1963; Sliker 1962).

Prestressing of wood beams in the tension zone with unbonded and bonded steel strands enhanced the strength of the beams by 76%. There was also a 26% increase in stiffness. However, both the stiffness and strength increases were observed only with bonded steel strands (Bohannan 1962, Peterson 1965). Steel reinforcements were also utilized at different positions in timber beams. Light gage steel local reinforcements were placed between wood laminates horizontally and vertically, and steel rebars were embedded near the top and bottom of the laminations to enhance the strength of glulam beams (Coleman and Hurst 1974; Lantos 1970; Bulleit, Sandberg, and Woods 1989). These methods showed about 24% increase in stiffness and 32% increase in ultimate load capacity.

Strengthening of timber railroad ties

Splitting and other damage has been the predominant reason for the need to replace timber railroad ties every few years. One or two dowels installed at each end from top to bottom and diagonally were used to increase the shear strength of ties which had splits and checks. The timber ties were compressed in a press to close the splits before inserting the dowels.

Satisfactory results were observed after nine years in service with the use of dowels, and further research was recommended (Code 1963).

Veneer caps were applied with an adhesive to timber members with checks which caused end splitting. The caps were intended to prevent the timber's surface from shrinking enough to check and split. The timber specimens with caps did not show any splits after several months in an uncontrolled environment. Uncapped control specimens developed deep splits (Higgins 1970).

Strengthening with FRP materials

Research on the strengthening of timber structures, bridges, railroad ties, and historic buildings with FRP materials has increased (Zaboklicki and Gebski 1997; Gentile, Svecova, and Rizkalla 2002). FRP materials have been applied in different configurations in attempts to increase the strength of timber ties. Wrapping timber ties in glass fiber reinforced composite fabrics enhanced both their stiffness and strength by as much as 25% and 70%, respectively (Sonti and GangaRao 1996; Qiao, Davalos, and Zipfel 1998; Davalos, Zipfel, and Qiao 1999; Chamarthy and GangaRao 2003).

The use of glass fiber reinforced polymers (GFRP) to strengthen timber beams has been widely investigated. FRP enhanced the stiffness and strength of the members by 17% to 21% when it was wrapped on the outside of a solid or laminated timber beams or when it was placed between horizontal laminates (Biblis 1965; Theakston 1965; Saucier and Holman 1975; Spaun 1981; Rowlands et al. 1986; Moulin, Pluvinage, and Jodin 1990; Sonti, Zipfel, and GangaRao 1995; Sonti et al. 1995; Dorey and Cheng 1996). FRP layers that have been applied to the top and bottom faces of the timber members have increased the ultimate load-carrying capacity of wood connections by 33% (Soltis, Ross, and Windorski 1998).

Prestressed FRP sheets have been used on the tension zone of the timber members successfully as an external reinforcement. Small amounts of nonprestressed and prestressed FRP materials as external reinforcement have been shown to enhance the stiffness up to 60% (Triantafillou and Deskovic 1992).

GFRP bars have been successfully used as near-surface-mounted reinforcement to increase the flexural strength of sawn timber beams by

up to 46% (Gentile, Svecova, and Rizkalla, 2002). Timber stringers have been successfully reinforced in bending and shear using FRP sheets bonded to the tension zone and sides of the members. Reinforced stringers showed 67% increase in strength over unreinforced samples; however, the strength increase was far greater than that predicted by simple transformed-section analysis and direct use of code strength values (Johns and Lacroix 2000; Gilfillan, Gilbert, and Patrick 2003; Ehsani, Larsen, and Palmer 2004). Nonlinear models for the analysis of FRP strengthened timber beams were in good agreement with experimental results (Chen and Balaguru 2002). An analytical model in good agreement with experimental results was also developed to predict the creep behavior of FRP-reinforced wood members (Plevris and Triantafillou 1995).

Research on repairing timber stringers in shear has been limited. GFRP materials in the form of laminates or fabrics have been externally bonded using epoxy to shear-critical zones at various configurations and areas of shear reinforcement. The experimental results for the shear capacity were in good agreement with the analytical predictions, and the most effective FRP reinforcement was by longitudinal placement of fibers (Triantafillou 1997, 1998).

More recently, composite rods and GFRP side plates have been used as shear reinforcement. Using scaled beam tests, shear reinforcement was applied from the bottom to top of two 51 mm by 51 mm (2 by 2 in.) which were stacked top of each other in order to investigate their strength and stiffness increase. Composite rods inserted from bottom to top of the timber beams with adhesive increased the modulus of the timber beams by 262% (Radford et al. 2002). FRP plates bonded to the sides of the timber beams have proven to be the most effective in maximizing the stiffness of the beams by 377% (Radford et al. 2002). The effectiveness of the GFRP bars as a repair method depended on the number and the position of the bars in timber stringers. Setting the shear bars spacing equal to the depth of the section provided the most effective option for shear reinforcement of timber stringers (Svecova and Eden 2004).

3 Experimental Program

The main objective of this experimental program was to investigate the feasibility of repairing sawn timber stringers that show signs of horizontal checking and splitting along the length of the member. The experimental program was conducted in order to examine the existing repair methods and to investigate the feasibility and effectiveness of attaching FRP plates to the sides of the stringers.

A total of twenty nine experiments were conducted on sixteen timber stringers. The timber stringers were labeled as C1, C2, C2-R, etc. The R in C2-R stands for a repaired member, i.e., C2-R is the repaired stringer C2. Specimen C1 was used as the control specimen. Specimens C2-R and C3-R were repaired with 406 mm (16 in.) long hex bolts and epoxy and seven hex bolts were used at every 610 mm (2 ft). Specimen C4-R was repaired with thirteen 406 mm (16 in.) long hex bolts at every 305 mm (1 ft). Specimen C5-R was repaired with thirteen 508 mm (20 in.) long hex bolts and steel plates. Specimen C6-R was repaired with thirteen 406 mm (16 in.) long lag screws at every 305 mm (1 ft). Specimen C11-R and C15-R were repaired with seven 406 mm (16 in.) long lag screws at every 610 mm (2 ft). Specimen C7-R and C10-R were repaired with ten 610 mm (2 ft) long lag screws, inserted 45° along the transverse direction. Specimen C12-R was reinforced with FRP strips and 406 mm (16 in.) long lag screws. The FRP strips were attached to the tension zone with lag screws. Specimen C13-R was repaired with four plywood side plates mechanically attached to the stringer using 76 mm (3 in.) long lag screws. Specimen C14-R and C16-R were repaired with four FRP plates mechanically attached to the stringer using 76 mm (3 in.) long lag screws. All specimen repair information is provided in Table 1.

Table 1. Repair methods applied to timber stringers.

Timber Stringers	Repair Method	Schematic Presentation of Repair Method
C1	Control specimen, no repair method applied	
C2-R C3-R	406 mm (16 in.) long hex bolts and epoxy over the entire length at 610 mm (2 ft) spacing	
C4-R	406 mm (16 in.) long hex bolts and epoxy over the entire length at 305 mm (1 ft) spacing	
C5-R	508 mm (20 in.) long hex bolts and steel plates over the entire length at 305 mm (1 ft) spacing	
C6-R	406 mm (16 in.) long lag screws over the entire length at 305 mm (1 ft) spacing	
C11-R C15-R	406 mm (16 in.) long lag screws over the entire length at 610 mm (2 ft) spacing	
C7-R C10-R	610 mm (24 in.) long lag screws over the entire length 45° to transverse direction	
C12-R	406 mm (16 in.) long lag screws in shear and flexural repair	
C13-R	Plywood side plates mechanically attached	
C14-R C16-R	GFRP side plates mechanically attached	

Timber stringers which did not have horizontal splits, but had checks along the length, were tested without any repair to failure to observe the failure type and unstrengthened postfailure capacity. Repair methods were then applied. Timber stringers which already had horizontal splits were tested to determine unstrengthened postfailure capacity. All of the stringers except C1 were tested to failure after repairing to determine the effectiveness of the repair technique. Based on previous research it was anticipated that using hex bolts and lag screws and attaching FRP side plates would increase unstrengthened postfailure capacity of the original stringers (Radford et al. 2002). This chapter provides details of the timber

stringers, the materials used for the repair methods applied for various timber stringers.

Materials

Properties of the timber stringers, strengthening materials and tools used in the laboratory work are provided in this section.

Timber stringers

Sixteen 191 mm by 406 mm by 4.6 m (7.5 in. by 16 in. by 15 ft) timber stringers were obtained from a railroad bridge recycling yard near San Marcos, TX. The timber specimens were classified as beams and stringers (AFPA 1996). Most of the stringers had signs of checking and horizontal splitting. An example of checking is shown in Figures 8 and 9. Some timber stringers had severe horizontal end splits, as shown in Figure 10. All timber stringers were graded select structural and were pressure treated with creosote. All of the timber stringers tested in this study had two horizontally drilled holes at their ends, as shown in Figure 11. These holes were drilled to connect stringers together when they were put into service in a railroad bridge.

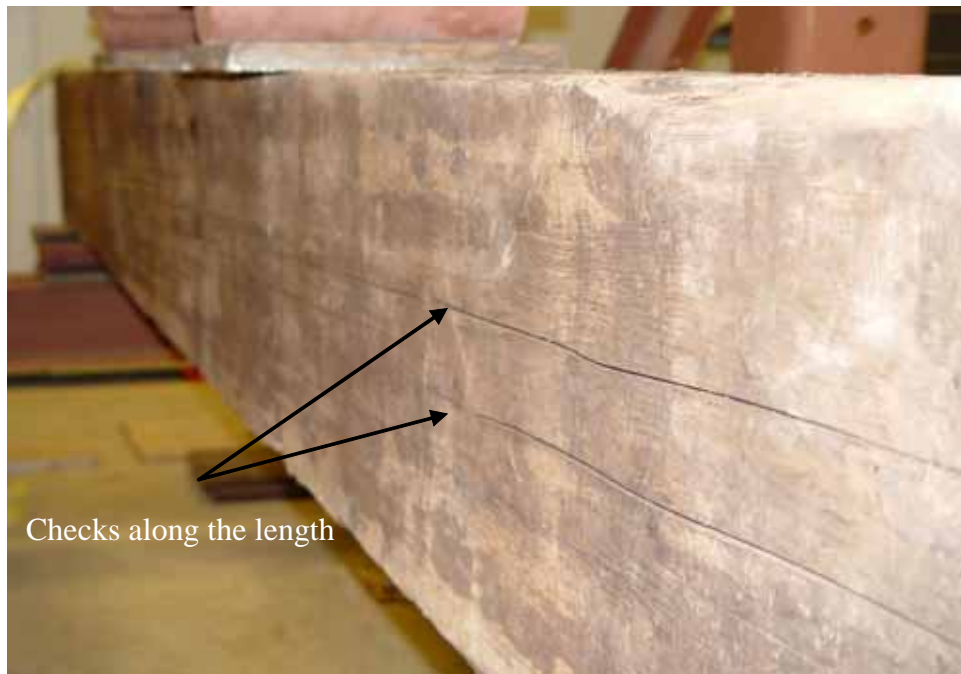


Figure 8. Several checks along the length of a timber stringer.

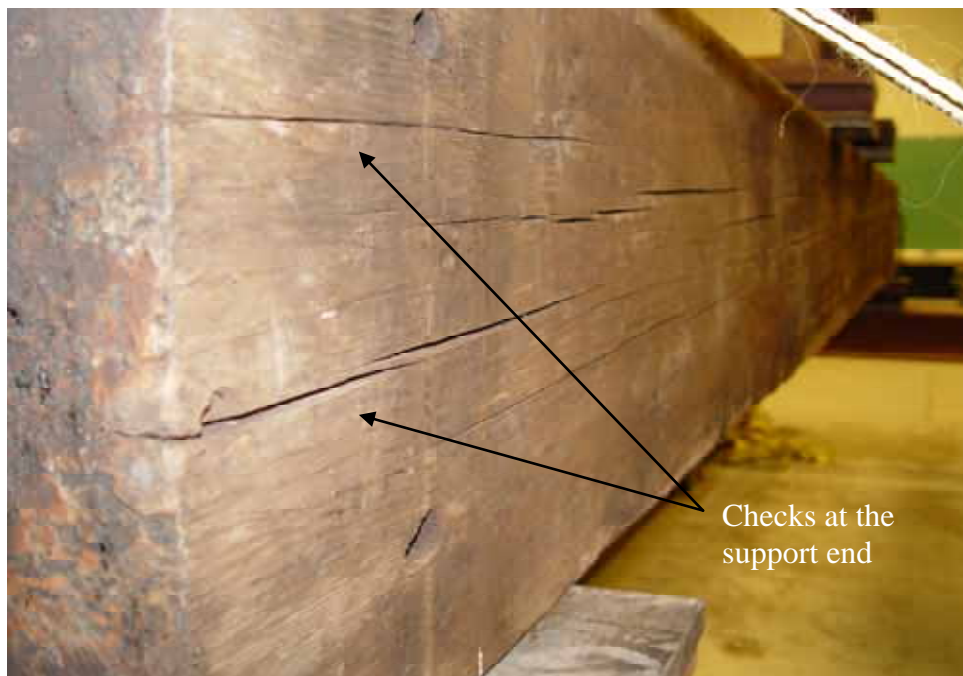


Figure 9. Several checks at the end of a timber stringer.



Figure 10. Timber stringers with end splits.



Figure 11. Horizontally drilled holes at the ends of the stringers.

Hex bolts and lag screws

Partially threaded steel hex-head hex bolts and lag screws were obtained from McMaster-Carr and Barnhill Bolt Co., Inc. Hex bolts were 13 mm (0.5 in.) in diameter. Two different lengths, 406 mm and 508 mm (16 in. and 20 in.), shown in Figure 12, were used to repair the timber stringers which had horizontal splitting. Hex bolts had 1/2 in.-13 threads. Minimum tensile and shear strength of the hex bolt material were 414 MPa (60,000 psi) and 232 MPa (33,600 psi), respectively.

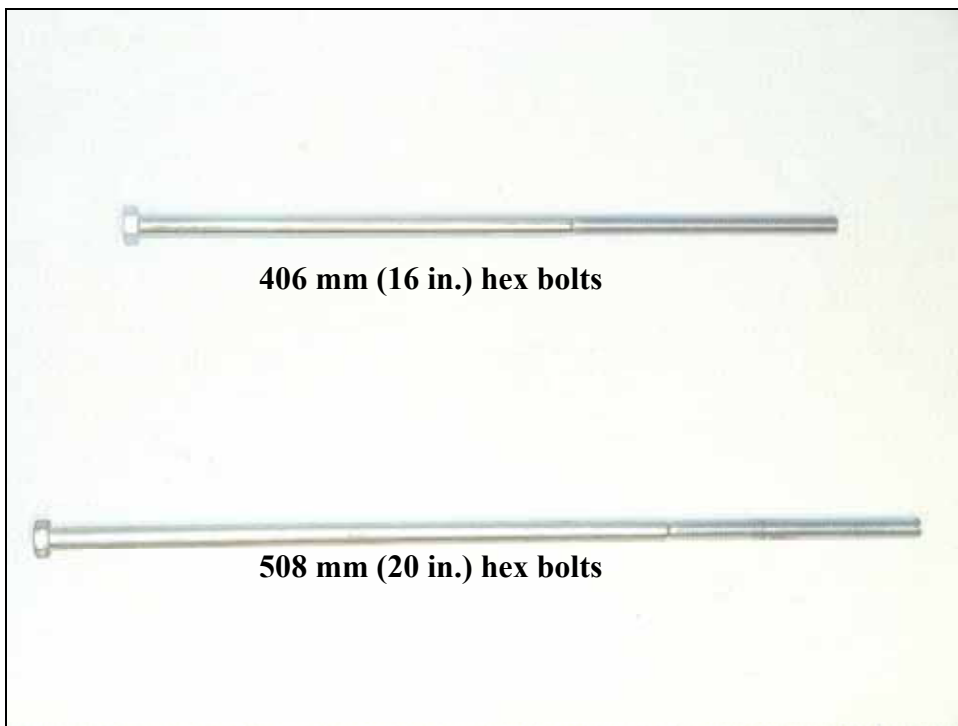


Figure 12. Two different length hex bolts.

The lag screws used in this study were 13 mm (0.5 in.) in diameter. Lengths of the lag screws were 76 mm, 406 mm, and 610 mm (3 in., 16 in., and 24 in.), as shown in Figure 13. The lag screws were not only used perpendicular to the timber fiber direction, but also as inclined reinforcing members in the timber stringers. The 406 mm and 610 mm (16 in. and 24 in.) lag screws were used directly for repairing and strengthening, while the 76 mm (3 in.) long lag screws were used to attach side plates to the timber stringers. The lag screws had 1/2 in.-13 threads. They are made of zinc plated grade 2 steel and were not corrosion resistant. Tensile and shear strength of the lag screws were 310 MPa (45,000 psi) and 174 MPa (25,200 psi) (AFPA 1996), respectively.

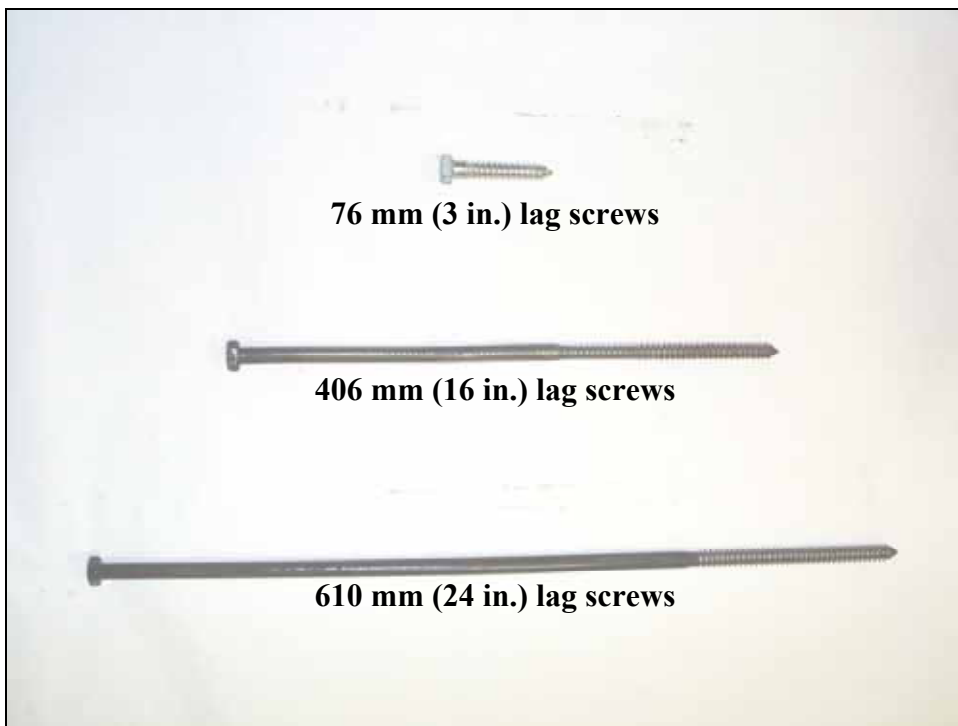


Figure 13. Three different length lag screws.

FRP material

FRP is an advanced composite material that consists of two main components: fibers and resin. The high strength fibers are the load-carrying component of the FRP. The polymer matrix binds, separates, and protects the fibers against abrasion. It also transmits load between the fibers. There are three commonly used types of fibers: glass, carbon, and aramid. The strength of a FRP material depends on the amount, types, and orientation of the fibers used. GFRP plates used to repair the timber stringers in shear were obtained from Gulf Wandes Plastics, a distributor of Creative Pultrusions, Inc. There were two reasons using glass fiber instead of carbon. First reason was the cost. Second one was to prevent the galvanic corrosion of bolts used to attach FRP plates. The thickness of the GFRP plates was 6.4 mm (0.25 in.). The plates were delivered in 1.2 m by 2.4 m (4 ft by 8 ft) sheets and were cut to the required dimensions before testing. The GFRP plates were attached to the sides of the stringers with 76 mm (3 in.) long and 13 mm (0.5 in.) diameter lag screws.

To reinforce a stringer in the tension zone, a 3.2 m (126 in.) long and 3.18 mm (1/8 in.) thick fiber reinforced strip was used. The fiber reinforced strip had a tensile strength of 695 MPa (101 ksi) and modulus of elasticity of 26.3 GPa (3,814 ksi), based on manufacturer's data.

Plywood

Plywood sheets 6.4 mm (0.25 in.) thick 1.2 m by 2.4 m (4 ft by 8 ft) were used for shear strengthening. The plywood sheets were cut into required plate dimensions to be used as side reinforcement. The plywood plates were attached to the sides of the stringers using 76 mm (3 in.) long lag screws.

Epoxy resin

The epoxy resin used to bond hex bolts was a general purpose epoxy produced by SystemThree Resin, Inc. The general purpose epoxy consisted of two parts which were mixed before being applied to the holes and hex bolts. Part A was a general resin, and Part B was a hardener. The minimum installation temperature was 1°C (35°F) with a recommended temperature of 16°C (61°F).

Temperature during installation was approximately 20°C (68°F). This epoxy resin had a compressive yield strength of 86 MPa (12.5 ksi) and a flexural modulus of elasticity of 2,413 MPa (350 ksi). The epoxy required 24 hr of curing after being applied before loading the stringer.

Drilling tools

Model TE 2 and TE 35 drilling tools manufactured by Hilti were used to drill the holes and to install the hex bolts and lag screws in the timber stringers. The TE 2 had an input power of 600 W and an output of 1200 rpm. Hilti drill TE 35 had an input power of 830 W and an output of 620 rpm. The TE 2 is shown in Figure 14 and the TE 35 is shown in Figure 15. The TE 35 was also used to attach the side plates using 76 mm (3 in.) lag screws. Holes were drilled using 13 mm (0.5 in.) diameter and 457 mm (18 in.) long drill bits manufactured by Irwin, Inc.



Figure 14. Hilti drill model TE 2 and drill bit.



Figure 15. Hilti drill model TE 35.

Timber specimens *

A total of sixteen timber stringers were tested. All of the timber stringers were stored in an uncontrolled, outdoor environment until testing. Chemical treatment was applied regularly to control insects and termites. To ensure that the temperature and moisture were not going to affect test results, specimens were moved indoor about 24 hr before testing. All of the testing materials were kept at ambient room conditions ($22 \pm 2^\circ\text{C}$) throughout the preparation and testing period. The moisture content was obtained from samples cut from stringers prior to testing. The moisture content was calculated according to ASTM 1999, as shown in equation 1:

$$\text{MoistureContent} = \frac{(\text{WetWeight} - \text{OvenDryWeight})}{\text{OvenDryWeight}} \times 100 \quad (1)$$

The average moisture content during testing was $11 \pm 1\%$. Damage in the timber stringers was detected visually and noted prior to testing.

Specimen C1

Stringer C1 was a control specimen. The stringer was in good condition except for several checks at the ends and along the length. Figure 16 shows several checks caused by unequal drying of the timber stringer. Checks were readily observed only on one side of the stringer. Specimen C1 did not have any deterioration at the tension zone or near the support points before testing.

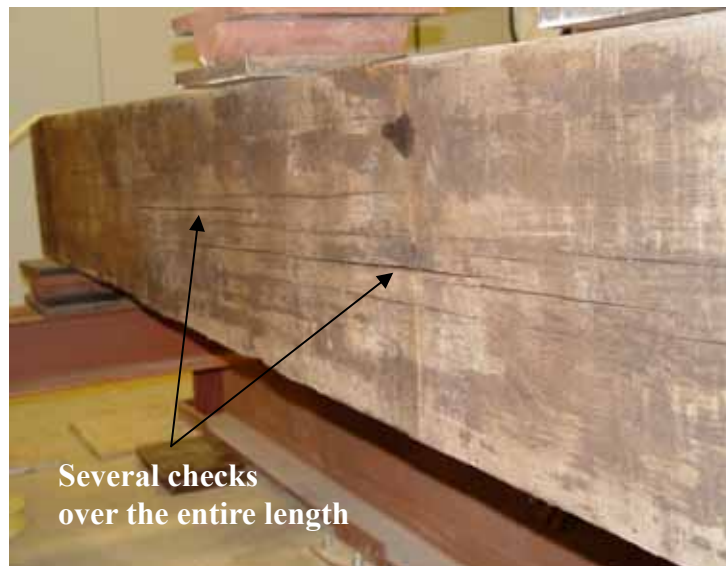


Figure 16. Checks along the length of specimen C1.

Specimen C2

Specimen C2 was in good condition with only several checks along the length and at the ends, as shown in Figure 17. The stringer did not have any other major damage prior to testing except for the aforementioned checks.



Figure 17. Checks at the end and along the length of specimen C2.

Specimen C3

Specimen C3 had several instances of checking and splitting, particularly at the ends close to the center of the cross section. The stringer had several knots at different locations, mostly close to the center of the cross section. A small tension splinter was observed at the midspan of the stringer. There were no other defects observed in the specimen C3.

Specimen C4

Specimen C4 was initially in good condition. There were no obvious signs of checking in specimen C4. The stringer had very slight surface cracks, but these cracks and checks were not as deep as the ones observed in specimens C1 and C2. The stringer had a wane that fell below one of the loading points, as shown in Figure 18. Since the damaged area was located in the compression zone, its effect on strength of the stringer was minimal.



Figure 18. Damaged area at the loading point of specimen C4.

Specimen C5

Specimen C5 had several knots along its length. The knots were located close to the center of the stringer, as well as in the tension zone near the midspan. The knots in the tension zone were expected to reduce the strength of the stringer. C5 also had several checks along its length; however, the checks were seen only on one side of the stringer, as in the case of specimen C1. There was a damaged area close to the center of the cross section at the end of the stringer, as shown in Figure 19. It was not expected that this damaged area would affect the strength of the specimen C5.

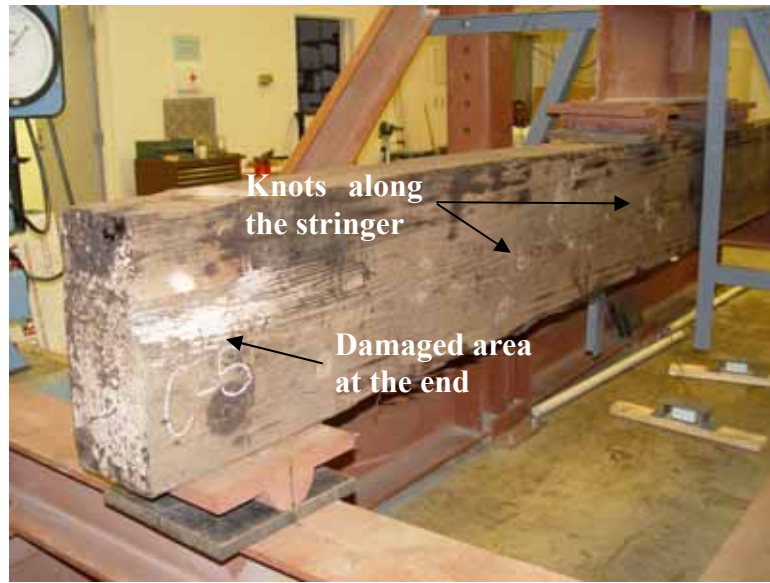


Figure 19. Damaged area close to the support and knots on specimen C5.

Specimen C6

Specimen C6 had severe end splits at the ends and along its length. Continuous splits were observed starting from the ends to the midspan of the stringer. These splits are typically caused by uneven drying of timber stringers. Splitting on the support face was close to the center of the cross section, where shear stress was at a maximum. The other support end had several splits on the cross section. The stringer also had several checks and other damage at the support edges, as shown in Figures 20 and 21.

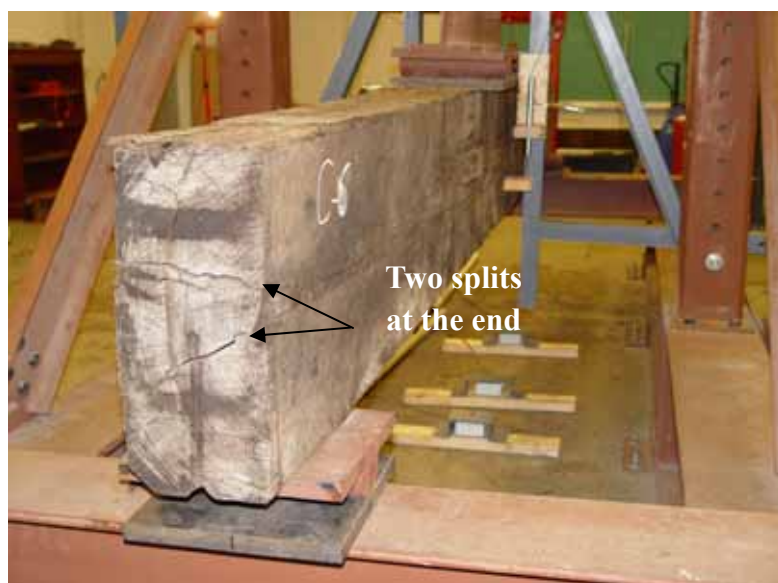


Figure 20. Splitting at the ends and along the length of specimen C6.



Figure 21. Splitting at the ends and along the length of specimen C6.

Specimen C7

Specimen C7 was in good condition except for a cross-grain tension crack at midspan, as shown in Figure 22. The stringer also had several checks along its length. There was no other major damage observed in the stringer before testing.

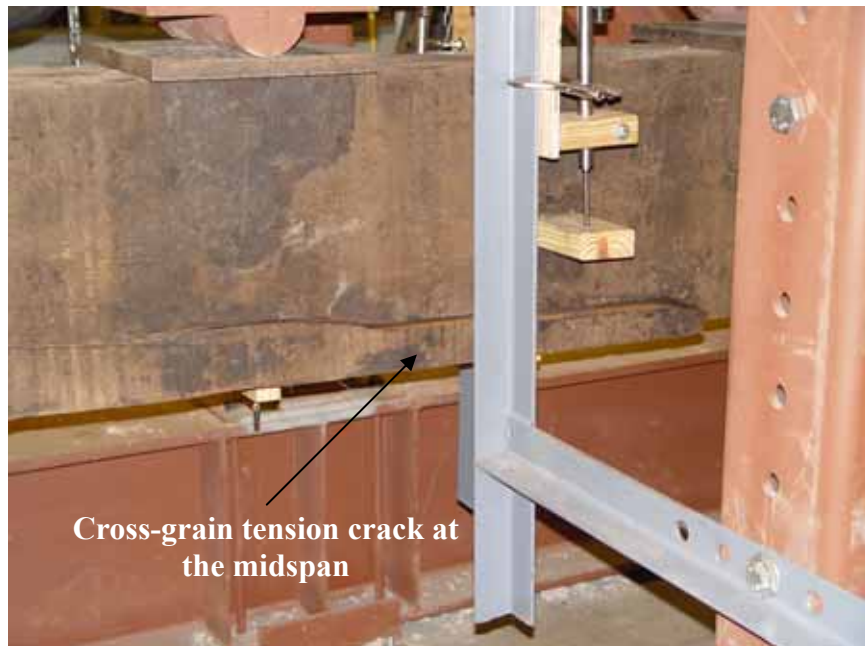


Figure 22. Cross-grain tension crack on specimen C7.

Specimen C8

Specimen C8 had several checks over its entire length. Horizontal splitting was observed from the support ends to the center of the stringer. The stringer also had knots located at different points along its length. It was discovered that the stringer had a colony of insects and ants living inside the horizontal cracks. Since the stringers were stored in an uncontrolled environment, chemical treatment manufactured by Terminate was applied to kill the insects prior to testing the stringer.

Specimen C9

Specimen C9 had several knots and small checks along its length. The knots at the midspan were expected to reduce the strength of the stringer. There was also a damaged area at the support end, as seen Figure 23.



Figure 23. Damaged area at the end of specimen C9.

Specimen C10

Specimen C10 had several heart checks observed along its length, as shown Figure 24. The heart checks were discontinuous and located close to the center of the stringer. Several shakes were also observed at the cross section of the support ends. C10 had several knots distributed close to the center along its length. The stringer did not show signs of decay in the tension zone and support points before testing.



Figure 24. Heart checks on specimen C10.

Specimen C11

Specimen C11 showed signs of deterioration at one end support. The cross section at the support point was rotted and had several shakes, as shown in Figure 25. After this stringer was repaired and tested, it was cut into small pieces to see if the rotting penetrated inside the stringer. Rotting was also observed at pieces cut at midspan. The stringer had checks along the length, and it had splitting at the other support end, as shown in Figure 26. The end split was only couple of inches long.

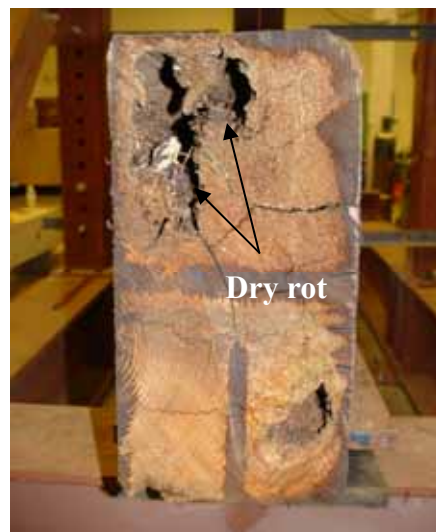


Figure 25. Rotting, shakes, and splits at the support end on specimen C11.



Figure 26. End splitting on specimen C11.

Specimen C12

Specimen C12 was generally in good condition, as shown in Figure 27. It had cracks along its length and several knots. When the tension zone of the stringer was inspected more closely, some signs of rotting were detected. Rot was apparent on the surface of the stringer, but did not penetrate to the interior of the member.



Figure 27. A view of specimen C12.

Specimen C13

Specimen C13 had a severe end split. The end split was close to the top of the cross section, and it was extended to the midspan, shown in Figure 28. The stringer also had small surface cracks and checks. The other support face exhibited signs of splitting along the cross section. The stringer did not have any other deterioration that might affect the strength except for end splits.



Figure 28. End splitting on specimen C13.

Specimen C14

Specimen C14 had several heart checks observed along its length, shown in Figure 29. Heart checks were discontinuous and located close to the center of the cross section. The stringer did not have any other major deterioration that might affect its strength except for the heart checks at the ends and along the length.

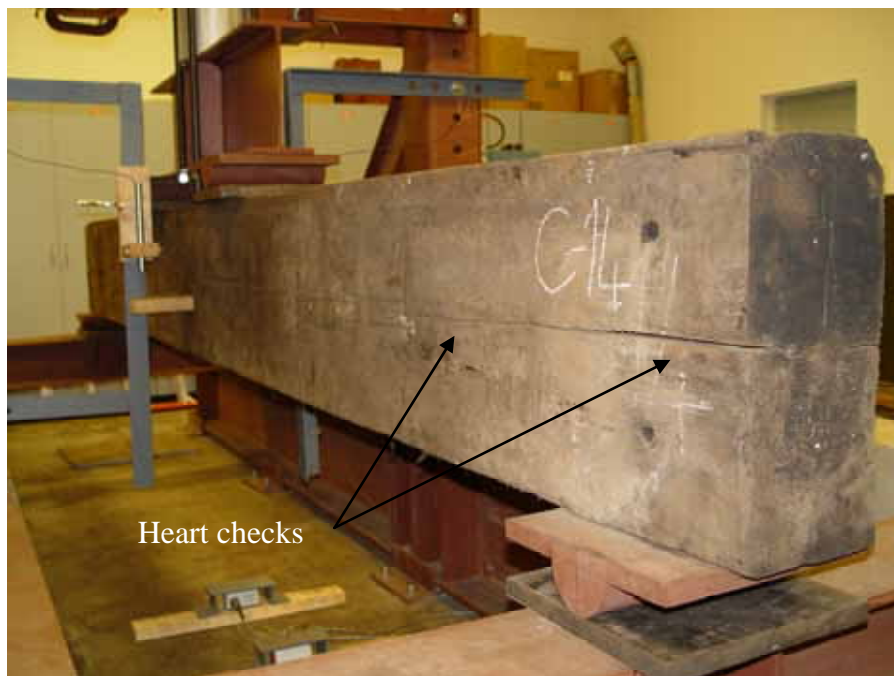


Figure 29. Heart checks on specimen C14.

Specimen C15

Specimen C15 had severe splitting at one end. Two separate splits were observed at the cross section along the length of the stringer, as shown in Figure 30. Several shakes were also observed on the support faces.



Figure 30. End splitting on specimen C15.

Specimen C16

Specimen C16 had signs of severe checking and splitting along its length. There was continuous checking from end to the midspan of the stringer. Initiation of splits was observed close to the center of the cross section where the in-service shear stress was at a maximum, as shown in Figure 31.



Figure 31. Initiation of end splitting on specimen C16.

Repair systems for stringers

Hex bolts, lag screws, plywood, and FRP side plates were used as repair systems to increase the shear strength of the split stringers. Hex bolts and screws were used in several configurations and spacings to strengthen and repair the timber stringers. AFPA mechanical connection concepts were utilized to determine the required number of hex bolts and lag screws needed to repair timber stringers (AFPA 1996). The distribution of shearing stresses in the transverse direction of a rectangular stringer is parabolic, as explained in Appendix A. The timber stringers were assumed to have a split at the center of the cross section over the entire length, since the shear stresses are at their maximum at the center of the cross section, as shown in Figure 32. The shear stresses are also zero at the top and bottom of the cross section. In other words, a stringer that has a lengthwise split at the neutral needed hex bolts or lag screws to transfer

the maximum stresses, as explained in Chapter 2, “Literature Review, Shear strength of wood beams, Effects of splits and checks and shear strength.” The function of the repair system was to carry the maximum shear stresses of the total cross section over the entire length. Details of the computations performed to determine the required number of hex and lag screws to repair the timber stringers are provided in Appendix B.

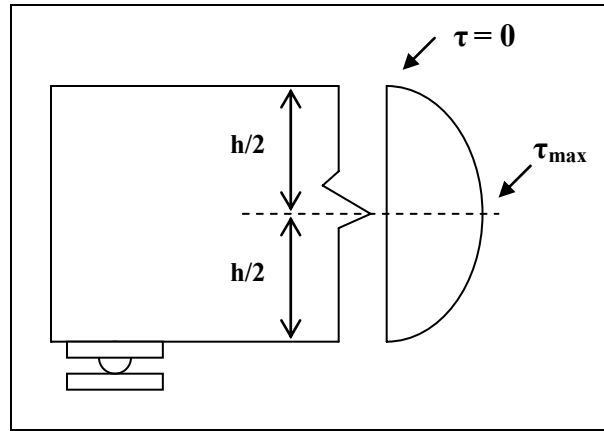


Figure 32. Shear stress distribution on a cross section of timber stringers.

Plywood and FRP plates were attached to the sides of the timber stringers using mechanical fasteners, in the same manner as a flitch beam. Similar concepts as explained above were utilized to determine the required number of lag screws needed to attach the plates to the sides of the stringers. Details of the computations used to determine the required number of lag screws to attach side plates are provided in Appendix C.

Number of hex bolts and lag screws

AFPA mechanical connection concepts were utilized to determine the required number of hex bolts and lag screws (AFPA 1996). A complete separation was assumed at the neutral plane, over the entire length of the stringers. The required number of hex bolts and lag screws were computed by modeling this system as a single shear connection, as shown in Figure 33.

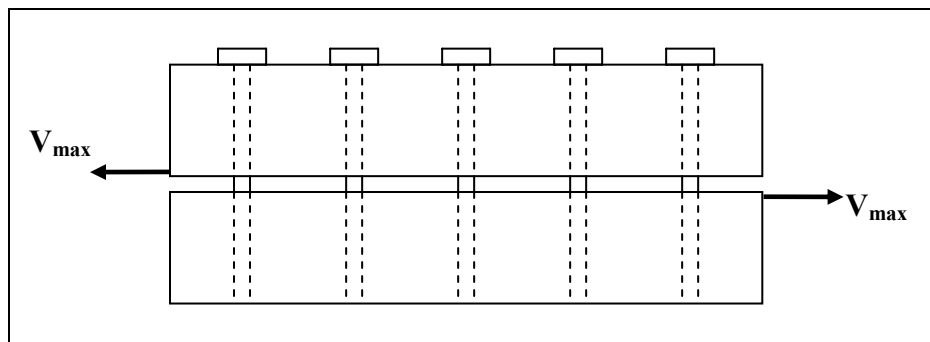


Figure 33. Single shear connection model for hex bolts and lag screws.

The purpose of the hex bolts and lag screws was to transfer the shear stresses along the length of the stringers. The reference lateral resistance of one hex bolt and lag screw was determined using Section 7.5 of AFPA (1996). Section 7.5 provides six different failure modes for hex bolts and three failure modes for lag screws for a single shear connection. Among the failure modes, the one which gave the smallest value controlled the capacity of the shear connection. The required number of hex bolts or lag screws was then determined by dividing the maximum shear force at the cross section by the capacity of a single bolt. Yield mode IV controlled the capacity of the single shear connections for both the hex bolts and lag screws. Yield mode IV exhibits two yield points in the hex bolts and lag screws near each shear plane. The lateral resistance of one hex bolt or lag screw was calculated as 13 kN (3 kips). The maximum shear capacity (V_{max}) of 191 mm by 406 mm (7.5 by 16 in) timber section was 150 kN (33.6 kips). The number of hex bolts or lag screws (N_f) was then computed by dividing the maximum shear capacity of the cross section by the capacity of a single hex bolt or lag screw. Details of the calculations are provided in Appendix B. The required number of hex bolts or lag screws along the entire length of the stringers was calculated to be 12. However, a total of 13 hex bolts or lag screws were used at a spacing of 305 mm (1 ft) to make field application simpler reducing possible errors while measuring the spacing. Since the splits were not present over the entire length of the stringers, 7 hex bolts or lag screws were also used in some experiments placed every 610 mm (2 ft) to compare the effectiveness of the different repair systems. Bolts at the loading points were inserted right next to steel plates to prevent applying any load on top of bolts.

Number of lag screws to attach side plates

AFPA mechanical connection concepts were utilized to find out the required number of lag screws needed to attach the side plates (AFPA

1996). A complete separation along the entire length of the stringers was assumed at the neutral plane as discussed in the previous section. The required number of lag screws was computed by modeling this system as a single shear connection, as shown in Figure 34.

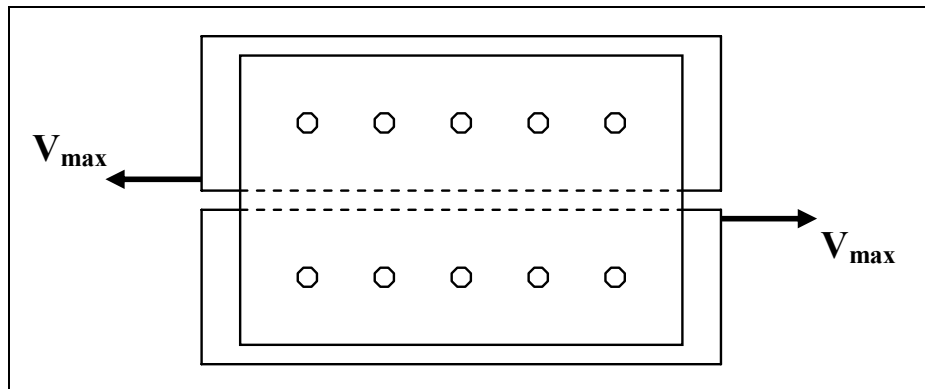


Figure 34. Single shear connection model for side plates attached using lag screws.

The purpose of the lag screws and side plates was to transfer the shear stresses along the length of the stringers. The bearing capacity of the side plates and timber stringer was assumed equal. Reference lateral resistance of one lag screw was determined using Section 7.5 of AFPA (1996).

Section 7.5 provides three failure modes for lag screws for a single shear connection. Among these failure modes, the one that yielded the smallest value controlled the capacity of the shear connection. Since separate side plates were used along the shear spans of timber stringers, the maximum shear force (V_{max}) on the cross section was divided by the number of plates to determine the force on each plate. Side plates were not used over the entire length of the timber stringers to prevent buckling problem at the midspan of the stringer. The required number of lag screws was then determined by dividing the shear force on each plate by the capacity of a single lag screw.

Yield mode I_s controlled the capacity of the single shear connections for side plates. Yield mode I_s was bearing at side member. The lateral resistance of one lag screw was calculated as 12.6 kN (2.84 kips). The shear force on each side plate was 37.5 kN (8.4 kips). The number of lag screws (N_f) needed to attach side plates was then computed by dividing the shear force on each plate by the capacity of a single lag screw. The required number of lag screws needed to attach each side plate was calculated to be 13. However, totals of 12 and 14 lag screws were used to attach the FRP and plywood side plates, respectively. Details of the calculations are

provided in Appendix C. Layout of the repair methods are presented in a subsequent section of this chapter.

Stringers repaired with hex bolts

Hex bolts with and without epoxy were used to repair the timber stringers. This section explains how the stringers were repaired using hex bolts.

Specimens C2-R and C3-R

Specimens C2-R and C3-R were repaired using hex bolts and epoxy. A total of seven hex bolts were used at every 610 mm (2 ft). Hex bolts were 13 mm (1/2 in.) in diameter and 406 mm (16 in.) in length. Holes were drilled from top to bottom by using 13 mm (1/2 in.) wood drill bit and a Hilti TE-2 drilling tool, as shown in Figure 35. An epoxy mixture was prepared and applied to the inside of the holes and to the surface of the bolts individually, as shown schematically in Figure 36. After the epoxy was

applied, the bolts were installed in the holes, as shown in Figure 37. The bolts were then allowed to cure for 24 hr before testing. A stringer ready for testing is shown in Figure 38. Figure 39 shows a schematic of the hex bolt layout for specimens C2-R and C3-R.



Figure 35. Holes being drilled with TE 2.

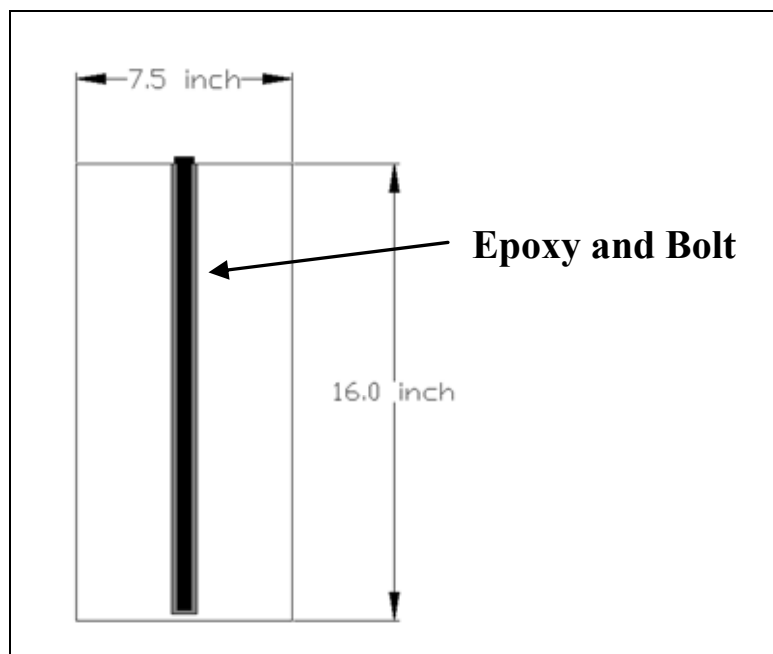


Figure 36. Schematic of cross section of specimens C2-R and C3-R.



Figure 37. Epoxy being applied to the hex bolts.



Figure 38. Specimen C3-R repaired using hex bolts and epoxy.

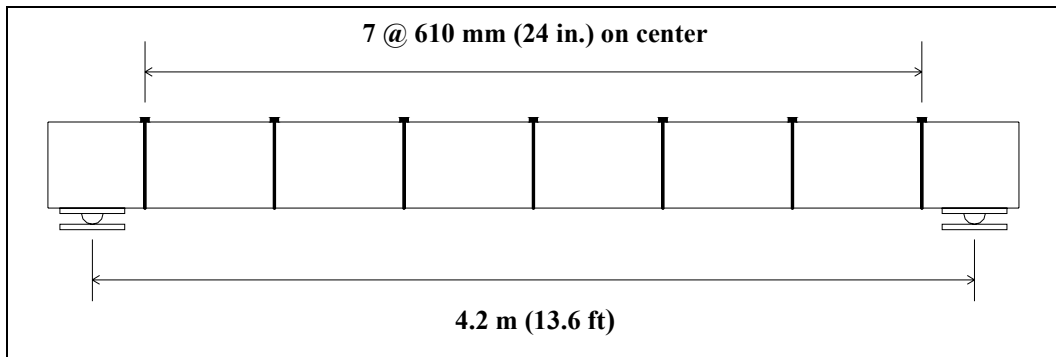


Figure 39. Schematic of hex bolt layout for specimens C2-R and C3-R.

Specimen C4-R

Specimen C4-R was repaired with hex bolts and epoxy, as were specimens C2-R and C3-R, but a spacing of 305 mm (1 ft) was used between bolts. Figure 40 shows a schematic representation of the repair method used for specimen C4-R. A total of 13 hex bolts were used. A picture of the stringer ready for testing is shown in Figure 41.

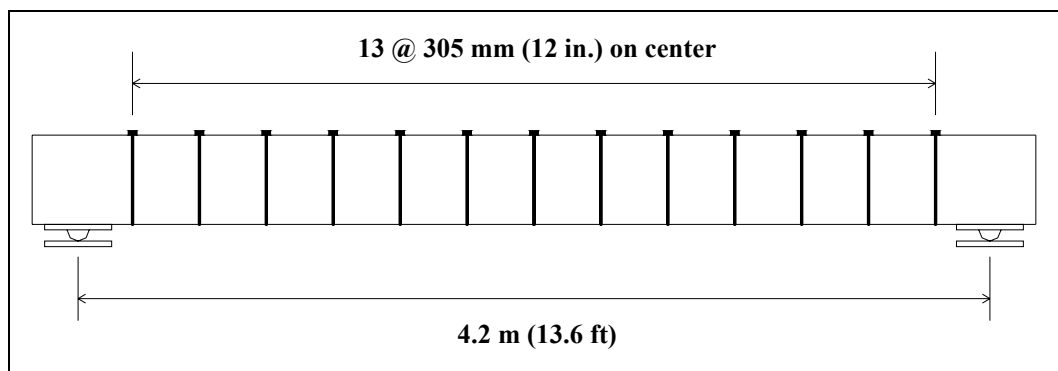


Figure 40. Schematic of hex bolt layout for specimen C4-R.



Figure 41. Specimen C4-R repaired with hex bolts.

Specimen C5-R

Specimen C5-R was repaired using a total of 13 hex bolts with steel plates and washers, as seen in Figures 42 and 43. The hex bolts were 508 mm (20 in.) long and 12.7 mm (1/2 in.) diameter and were spaced 305 mm (1 ft) on centers, as shown schematically in Figure 44. The steel plates were 102 mm (4 in.) square and 6.4 mm (1/4 in.) thick. The plates were used in addition to the bolts, and were located between the bolt head or nut and the timber stringer, both on top and underneath the stringer at each bolt. Since the hex bolts and steel plates were tightened into place with nuts, epoxy was not used. Steel washers were used both at the top and bottom between the bolt head or nut and the steel plate. The plates were

intended to introduce a compression force in the transverse direction to control several splinter and horizontal cracks which developed during testing of specimen C5.



Figure 42. Specimen C5-R repaired with hex bolts and steel plates from top view.



Figure 43. Specimen C5-R repaired with hex bolts and steel plates from underneath.

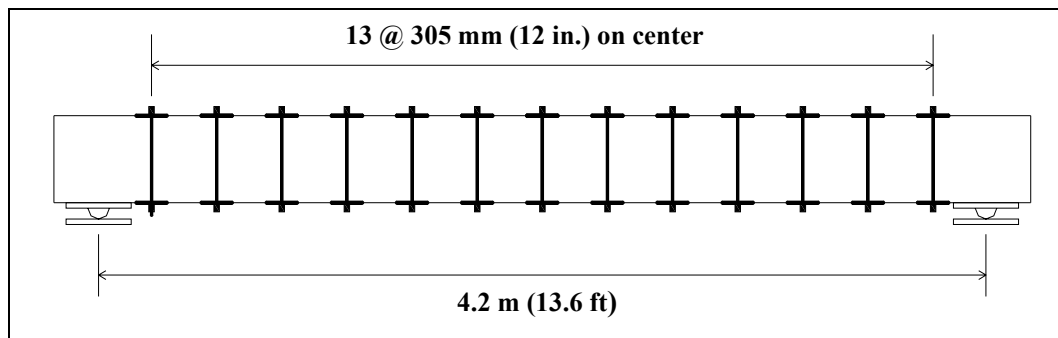


Figure 44. Schematic of hex bolt layout for specimen C5-R.

Stringers repaired with lag screws

Lag screws were used in different configurations and spaced every 610 mm (2 ft) and 305 mm (1 ft) on center to repair the timber stringers. This section explains how stringers were repaired using lag screws.

Specimen C6-R

Specimen C6-R was repaired with lag screws spaced every 305 mm (1 ft) on center, as shown schematically in Figure 45. The lag screws were 406 mm (16 in.) long and 13 mm (1/2 in.) in diameter. Holes were drilled in the transverse direction using the Hilti TE-2 drilling tool and a 13 mm (1/2 in.) wood drill bit. The 13 mm (1/2 in.) diameter lag screws were driven into the holes by the Hilti TE-35 drilling tool. Epoxy was not used with the lag screws.

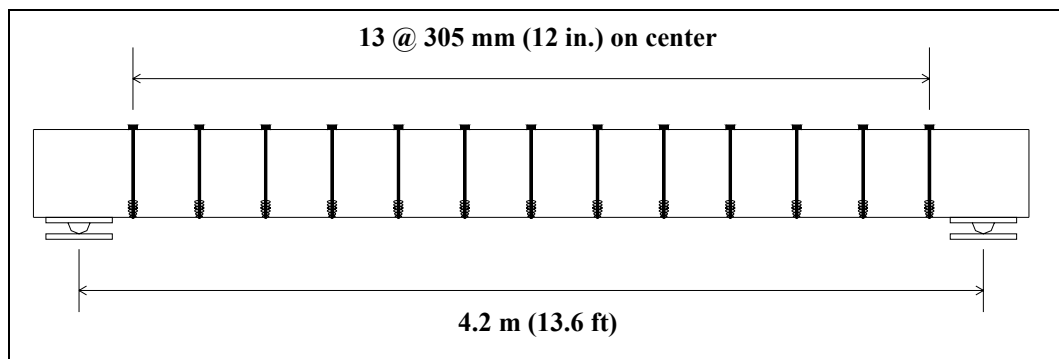


Figure 45. Schematic of lag screws layout for specimen C6-R.

Specimens C7-R and C10-R

Specimens C7-R and C10-R were repaired with lag screws. Specimen C10-R was repaired in the same fashion as specimen C7-R, but the 45° angle of the lag screws was installed in the opposite direction, as shown

schematically in Figures 46 and 47. A total of 10 lag screws were used to repair both timber stringers. The lag screws were 13 mm (1/2 in.) in diameter and 610 mm (24 in.) long. After marking points spaced at every 610 mm (2 ft) on the top of the stringer, guidelines at 45° to the transverse direction were drawn from the marked points to the bottom of the stringer. Holes making 45° angle with the transverse direction were then drilled along the guidelines using a 13 mm (1/2 in.) wood drill bit and the Hilti TE 2 drilling tool. Epoxy was not used with lag screws. The repaired stringer with lag screws is shown in Figure 48.

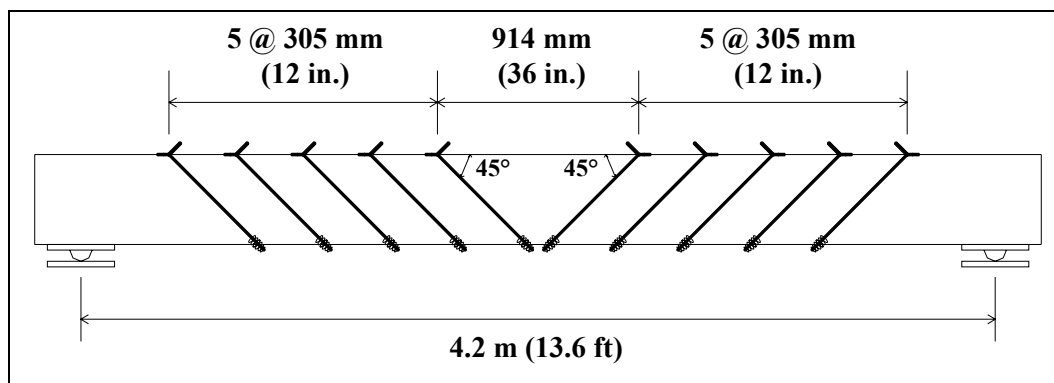


Figure 46. Schematic of lag screws layout for specimen C7-R.

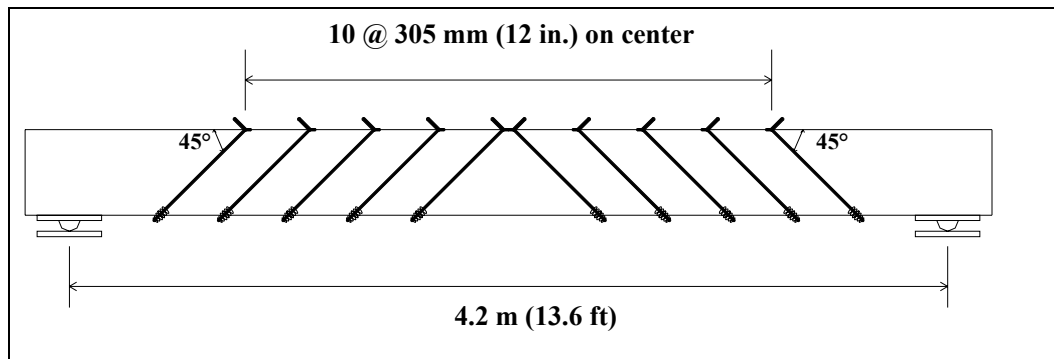


Figure 47. Schematic of lag screws layout for specimen C10-R.



Figure 48. Specimen C7-R repaired with lag screws.

Specimens C11-R and C15-R

Specimens C11-R and C15-R were repaired with 406 mm (16 in.) long lag screws similar to specimens C6-R. Figure 49 shows a schematic representation of the repairing method. Lag screws were placed at every 610 mm (2 ft) along the length of the stringer for a total of 13 lag screws.

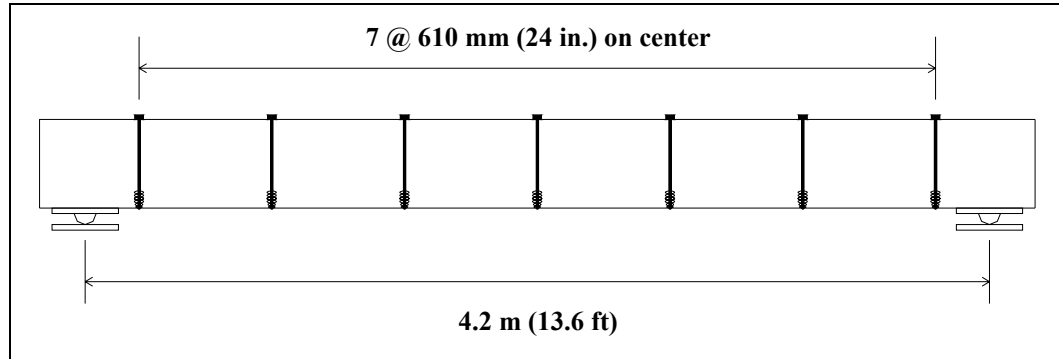


Figure 49. Schematic of lag screws layout for specimens C11-R and C15-R.

Stringer C13-R repaired with plywood side plates

Four plywood side plates were attached to the sides of stringer C13-R. The plywood was first cut into 406 mm by 2,057 mm (16 in. by 81 in.) plates. The plates were then duct taped to the sides of stringer C13, and 76 mm (3 in.) long lag screws were used to attach the side plates to the stringer.

using a TE 35 drill, as shown in Figures 50 and 51. Schematic of the plywood side plate layout is shown in Figure 52. A total of 14 lag screws were used to attach each plywood plate to the sides of the stringer. The plywood plates were not used over the entire length to prevent buckling in the midspan, as shown in Figure 53.



Figure 50. Lag screws being installed to specimen C13-R.



Figure 51. Lag screws being installed.

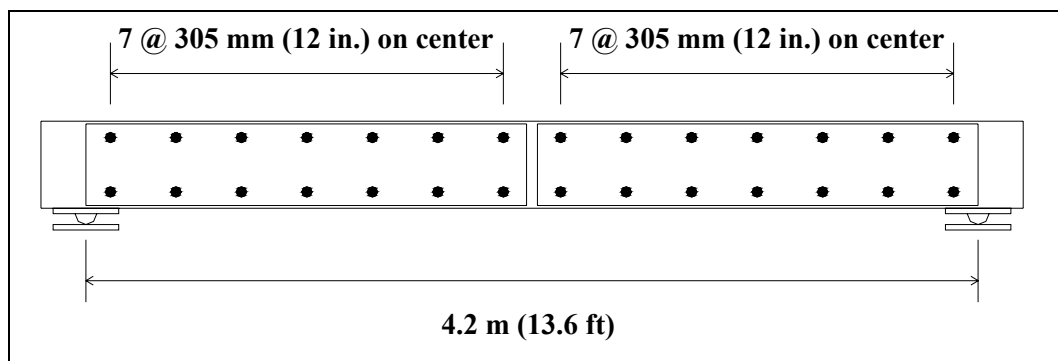


Figure 52. Schematic of plywood side plates for specimen C13-R.



Figure 53. Specimen C13-R repaired with plywood side plates.

Stringers repaired with FRP side plates or FRP strip

FRP plates were installed along the shear spans of the timber stringers to repair them in shear. FRP plates were attached to the sides of the stringers using mechanical fasteners. Two stringers were repaired with FRP side plates. One stringer was repaired using a FRP strip at the tension zone, since the stringer failed with cross-grain tension cracks at midspan.

Specimens C14-R and C16-R

Specimens C14-R and C16-R were repaired with four FRP plates attached to the sides of the stringers. The FRP plates were first cut into 406 mm by 1,829 mm (16 in. by 72 in.) plates, as shown in Figures 54.



Figure 54. FRP plates being cut to size.

The FRP plates were attached to sides of the timber stringers using a similar method to that used to attach the plywood plates. Lag screws were used with washers to attach the FRP side plates. The washers were used to protect the FRP plates from damage caused by the heads of the lag screws when tightened. A schematic of the FRP side plate layout is shown in Figure 55. A total of 12 lag screws were used to attach each FRP plate to the side of the stringer. FRP plates were used along the shear span, as shown in Figure 56, leaving a gap at the midspan. The FRP side plates used to repair stringer C14-R did not show any major damage after testing. Therefore, the same plates were used again to repair stringer C16-R.

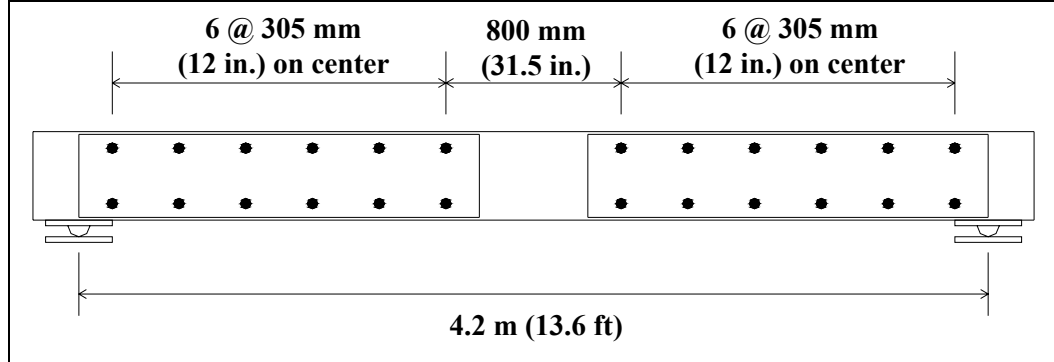


Figure 55. Schematic of FRP side plates for specimens C14-R and C16-R.



Figure 56. Specimen C14-R repaired with FRP plates.

Specimen C12-R

Specimen C12-R was repaired with lag screws and the FRP strip located at the tension zone. Lag screws were used to attach an FRP strip to the tension zone of the stringer. Lag screws were also used to attach the FRP plates as shear reinforcement in this method. Holes were drilled on the FRP strip at every 305 mm (1 ft) using Hilti TE-2 drill and 13 mm (1/2 in.) drill bit. FRP strip were then duct taped underneath the stringer. Holes in the timber were then drilled at 305 mm (1 ft) spacing. The holes were then drilled half way into the depth of the stringer with 13 mm (1/2 in.) diameter drill bit and other half way with a 9.5 mm (3/8 in.) diameter drill bit. After the holes were drilled into the stringer, the lag screws were installed using a Hilti TE-35. Figure 57 shows the repaired stringer with FRP strip attached with lag screws.



Figure 57. Stringer C12-R repaired at tension zone with FRP strip.

4 Testing Methods and Procedure

Stringer testing was carried out in the McDermott International, Inc. Materials Testing Laboratory of the Civil and Environmental Engineering Department, Tulane University. The equipment used and the testing methodology are presented in this section.

Testing frame

A self-reacting test frame was used in all of the tests. The tests were conducted according to ASTM D198 (1999). All stringers were tested on a span of 4.2 m (13.6 ft) with two equal loads applied symmetrically at a distance of 457 mm (18 in.) from the centerline, to create a constant moment region and two shear regions in the stringer. This required the fabrication of a spreader beam to split the applied load into two loads. The test setup is pictured schematically in Figure 58.

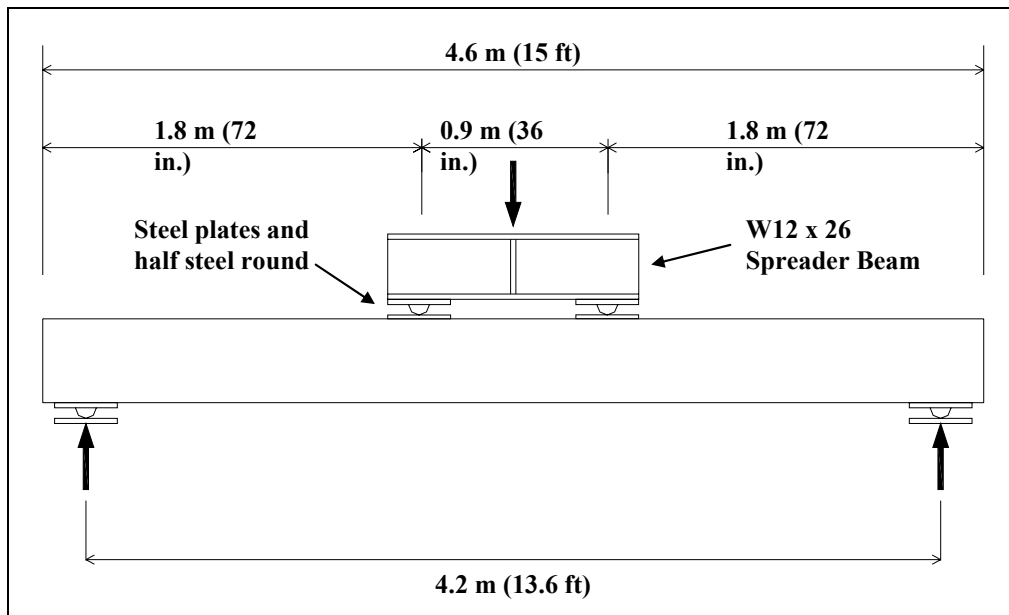


Figure 58. Configuration for the four-point bending test.

Half steel rounds, 102 mm (4 in.) in diameter, were used to allow free rotation points for load and reactions. The half steel rounds were attached to 25.4 mm (1 in.) thick steel plates measuring 305 mm by 305 mm (12 in. by 12 in.). Steel plates 305 mm by 305 mm (12 in. by 12 in.) were used to limit the compression stress perpendicular-to-grain at loading and

support points. Higher loads would have caused excessive compression at the loading points in the direction perpendicular to grain. The stringers had a cross section 191 mm (7.5 in.) wide and 406 mm (16 in.) deep, as shown in Figure 59. The typical configuration of the support plates is also shown in Figure 60.

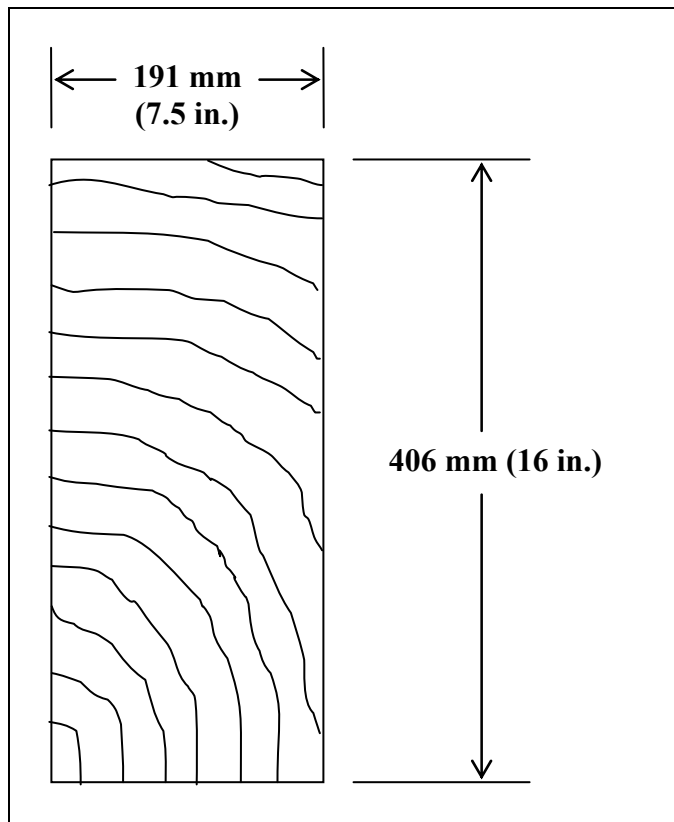


Figure 59. Typical cross section of timber stringers.

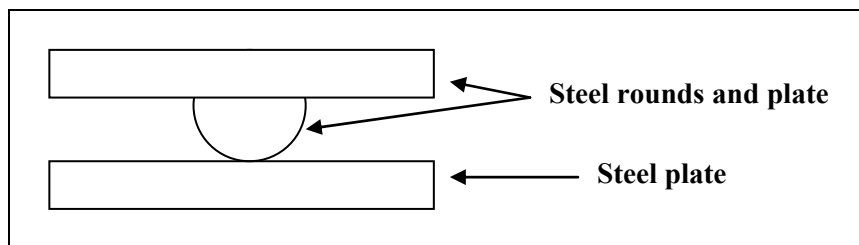


Figure 60. Typical configuration of the support plates.

Load application

A 445 kN (100 kips) capacity hydraulic ram or a 356 kN (80 kips) MTS actuator were used to apply the load to the stringers. The hydraulic ram had a maximum stroke of 152 mm (6 in.). Hydraulic pressure was supplied to the ram with an electric pump with a 69 MPa (10,000 psi) capacity. Two

needle valves were located in series on the hydraulic hose which helped to control the rate of loading. Five original timber stringers (C1, C2, C3, C4, and C5) and four repaired stringers (C2-R, C3-R, C4-R, and C5-R) were tested using the hydraulic ram. The load was increased at 22 kN (5 kips) increments. The remaining experiments (C6, C7, C8, C9, C10, C11, C12, C13, C14, C15, C16, C6-R, C7-R, C10-R, C11-R, C12-R, C13-R, C14-R, C15-R, C16-R) were performed with the 356 kN (80 kips) hydraulic MTS actuator controlled with a MTS Flextest GT controller. A monotonic static load was applied in displacement control at a rate of 1 mm/min (0.04 in./min.). The testing was continued beyond the peak load to observe the mode of failure and maximum deflection of the stringers.

Data acquisition for tests

Deflections were measured to examine the behavior of the stringers. Linear variable differential transformers (LVDTs) and string pots were placed at multiple positions of the test setup to monitor displacements. Figures 61 and 62 show the positions of the LVDTs and string pots on the test setup.

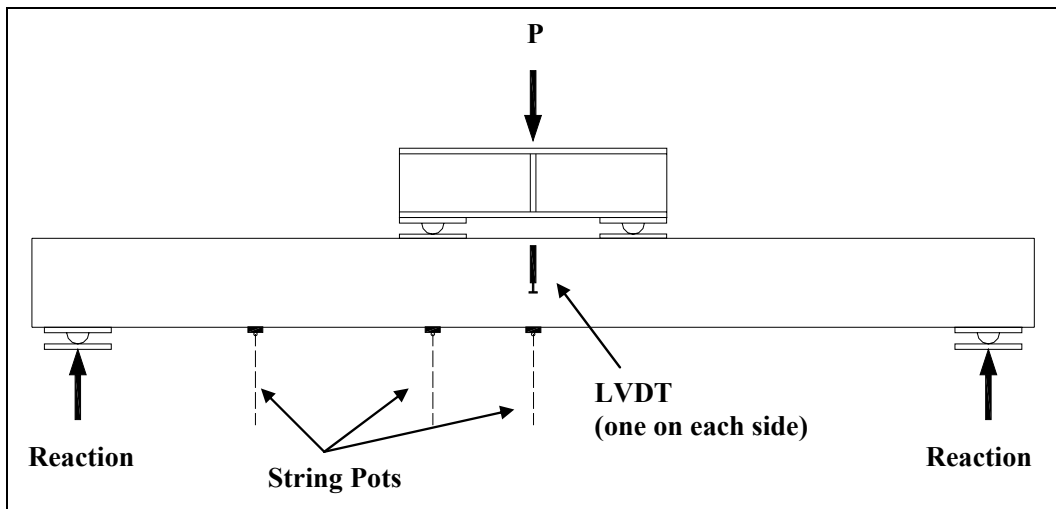


Figure 61. Placement of monitoring equipment on test specimens.



Figure 62. Monitoring equipment on timber stringers.

String pots consist of a wire cable on a coil attached to a tension spring in an enclosed housing. The tension spring maintains a constant tension on the wire cable. As the cable is drawn out or retracted, an electrical output signal specifying the amount of movement is sent to the data acquisition computer. The UniMeasure, Inc. P510-40-DS string pots were placed on the bottom of the stringers at the midspan, the loading point, and the middle of the shear span. Omega Technologies LD610 LVDTs with a stroke of 102 mm (4 in.) were mounted on the testing frame with the movable ends resting on blocks attached to the stringers on each side at the midspan. As the stringers deflected, the movable end extended, sending an electrical output signal directly related to the amount of the movement to the data acquisition system.

The load was monitored for the five original timber stringers (C1, C2, C3, C4 and C5) and the four repaired stringers (C2-R, C3-R, C4-R, and C5-R) with a 445 kN (100 kips) load cell, which was placed between the hydraulic ram and the spreader beam. The load cell was manufactured by AmCells Company and was calibrated prior to use. The stringers tested with the MTS actuator utilized a 356 kN (80 kips) load cell which was attached to the actuator. The load cell-hydraulic ram setup is shown in Figure 63, and the actuator is shown in Figure 64.



Figure 63. The load cell-hydraulic ram setup with spreader beam.



Figure 64. The MTS actuator and spreader beam.

Data were recorded by computerized data acquisition systems. A PCM12H data acquisition system was used for data collection for the experiments run with the hydraulic ram. The PCM12H has 8 channels and is manufactured by Super Logics, Inc. Data were collected for the rest of the experiments using the integrated 12 channel data acquisition functions of the MTS Flextest GT controller. MTS Basic TestWare software was used to carry out these experiments and to acquire data.

Loading application

The timber stringers without horizontal splits, but with checks along the length, were tested to failure in order to observe the failure type and unstrengthened postfailure capacity of the original stringer. Timber stringers with signs of checking were expected to fail in horizontal shear.

Repaired stringers were again loaded to failure, after repair techniques were applied. The effectiveness of the repairing technique was determined by comparing the unstrengthened postfailure capacity of original stringer to ultimate strength of repaired stringer. This idea is shown graphically in Figure 65. The average deflection measured by the LVDTs at midspan is used for all graphs in this study.

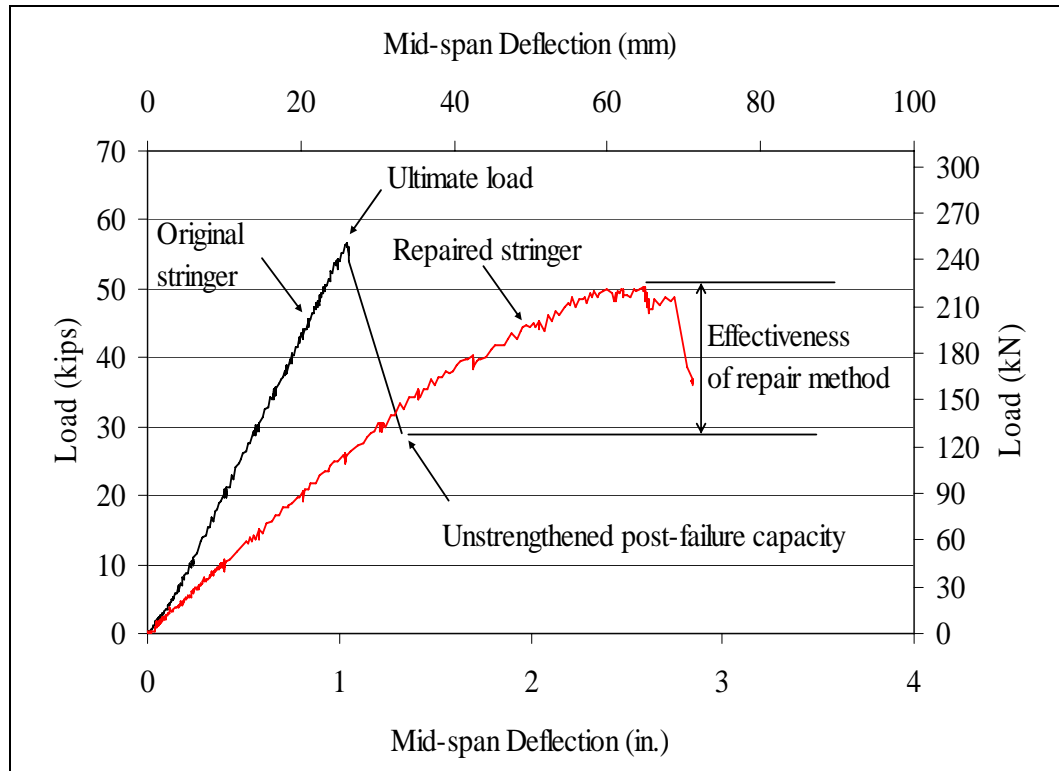


Figure 65. Effectiveness of a repair method.

For example, specimen C2 had checks over its entire length. When the stringer failed, load dropped to a certain level, which was called the unstrengthened postfailure capacity. It is this amount of load that the failed stringer is able to carry. After specimen C2-R was repaired, the repaired stringer was again loaded to failure. The repaired ultimate load was compared to the unstrengthened postfailure capacity of the original stringers to determine the effectiveness of repair method.

Timber stringers, which already showed horizontal splits, were tested to determine the postfailure capacity without obtaining ultimate load capacity. These stringers did not have the same stiffness as timber stringers which had only checks, because of the existing horizontal end splits. These stringers began to yield, after the load reached the unstrengthened postfailure capacity. The experiments were then terminated to prevent a tension crack from forming at the midspan due to excessive deformations.

5 Test Results and Discussion

The experimental results for original and repaired timber stringer tests are given in this chapter. Moment and shear diagrams, calculations of cross-section properties, and LRFD strength capacity sample calculations can be found in Appendix A. This LRFD strength capacity is plotted on each load-deflection curve.

A summary of the ultimate load, bending stresses and shear stress at the ultimate load, and unstrengthened postfailure capacity for each individual original timber stringer is given in Table 2. Deflections at the midspan are given in Table 3. Failure modes for the original stringers are in Table 4. The failure modes observed were horizontal shear, cross-grain, and simple tension.

Table 2. Ultimate loads, bending and shear stresses at the ultimate load and unstrengthened postfailure capacity of original timber stringers.

Original Timber Stringers	Ultimate Load		Bending Stress at the Ultimate Load [†]		Shear Stress at the Ultimate Load [†]		Unstrengthened Postfailure Capacity	
	kN	kips	MPa	ksi	MPa	ksi	kN	kips
C1	191	43	29.51	4.28	1.86	0.27	93	21
C2	254	57	39.16	5.68	2.52	0.36	129	29
C3	142	32	22	3.19	1.40	0.20	102	23
C4	222	50	34.34	4.98	2.17	0.31	89	20
C5	169	38	26.13	3.79	1.68	0.24	80	18
C6 ^{††}	-	-	-	-	-	-	53	12
C7	227	51	35.03	5.08	2.24	0.32	89	20
C8	9	2	1.38	0.20	0.07	0.01	0.9	0.2
C9	56	12.5	8.62	1.25	0.56	0.08	13	3
C10	285	64	44	6.38	2.79	0.40	98	22
C11 ^{††}	-	-	-	-	-	-	71	16
C12	196	44	30.20	4.38	1.96	0.28	129	29
C13 ^{††}	-	-	-	-	-	-	125	28
C14	231	52	35.72	5.18	2.31	0.33	102	23
C15 ^{††}	-	-	-	-	-	-	93	21
C16 ^{††}	-	-	-	-	-	-	67	15

[†] Calculated from the experimental ultimate load.
^{††} These stringers already had horizontal splitting.

Table 3. Deflections at ultimate moment for original timber stringers.

Original Timber Stringers	Ultimate Moment		Deflection at Moment Load	
	kN-m	k-ft	mm	in.
C1	154.71	114.38	27	1.06
C2	205.74	151.62	26	1.04
C3	115.02	85.12	36	1.40
C4	179.82	133	46	1.80
C5	136.89	101.08	54	2.12
C6	42.93	31.92	75	2.94
C7	183.87	135.66	33	1.28
C8	7.29	5.32	6	0.24
C9	45.36	33.25	7	0.29
C10	230.85	170.24	26	1.03
C11	57.51	42.56	48	1.90
C12	158.76	117.04	27	1.08
C13	101.25	74.48	38	1.53
C14	187.11	138.32	24	0.94
C15	75.33	55.86	46	1.81
C16	54.27	39.9	48	1.90

Table 4. Failure modes of original timber stringers.

Original Timber Stringers	Failure Modes
C1	Horizontal shear
C2	Horizontal shear
C3	Horizontal shear
C4	Cross-grain tension
C5	Simple tension
C6	End Splitting before testing
C7	Horizontal shear
C8	Tension failure caused by a knot
C9	Tension failure caused by a knot
C10	Horizontal shear
C11	End Splitting before testing
C12	Cross-grain tension

Original Timber Stringers	Failure Modes
C13	End Splitting before testing
C14	Horizontal Shear
C15	End Splitting before testing
C16	End Splitting before testing

The ultimate load at failure varied from 9 kN (2 kips) to 285 kN (64 kips) among the original timber stringers. The maximum ultimate load was 285 kN (64 kips) for stringer C10. Stringer C10 failed in horizontal shear at the ultimate load, and then the load dropped to 98 kN (22 kips), which was the unstrengthened postfailure capacity. The minimum ultimate load was 9 kN (2 kips) for stringer C8. A tension crack initiated by a knot reduced the ultimate load of stringer C8. The six timber stringers (C1, C2, C3, C7, C10, and C14) which showed signs of checking prior to testing failed in horizontal shear at the ultimate load. Stringer C5 developed tension and horizontal cracks at the ultimate load. Cross grain tension failure was observed in stringers C4 and C12. The ultimate load of stringers C8 and C9 was low because of the presence of knots. Stringers C6, C11, C13, C14, and C15 contained end splitting prior to testing. Sliding on the support face was observed as the load increased to failure for these stringers, as shown schematically in Figure 66.

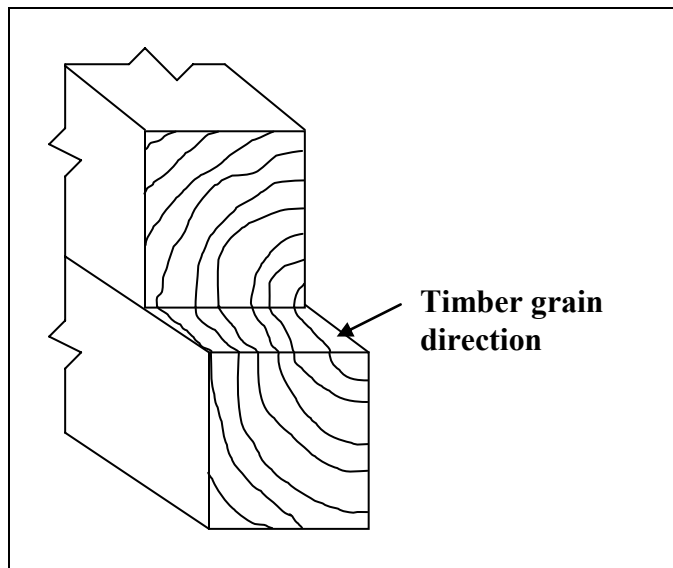


Figure 66. Schematic of idealized sliding on support face.

A summary of the repaired ultimate load, bending and shear stresses at the repaired ultimate load for each individual repaired timber stringer,

and effectiveness of repair methods are provided in Table 5. Midspan deflections at repaired ultimate moment are given in Table 6. The failure modes are indicated in Table 7. The maximum ultimate load was 222 kN (50 kips) for stringer C2-R. The minimum ultimate load was 62 kN (14 kips) for stringer C6-R. The repaired timber stringers typically failed in simple tension. Of the 13 repaired stringers, 9 failed in simple tension, 2 failed in horizontal shear and 1 failed in compression.

Table 5. Repaired ultimate load, bending and shear stresses at the repaired ultimate load, and effectiveness of repair methods.

Repaired Timber Stringers	Repaired Ultimate Load		Increase over Unstrengthened Post-Failure Capacity (%)	Bending Stress at the Ultimate Load [†]		Shear Stress at the Ultimate Load [†]	
	kN	kips		MPa	ksi	MPa	ksi
C2-R	222	50	72.4	34.34	4.98	2.14	0.31
C3-R	133	30	30.4	20.62	2.99	1.31	0.19
C4-R	121	27	35	18.55	2.69	1.17	0.17
C5-R	121	27	50	18.55	2.69	1.17	0.17
C6-R	62	14	16.7	9.58	1.39	0.62	0.09
C7-R	138	31	55	21.31	3.09	1.31	0.19
C10-R	196	44	100	30.20	4.38	1.93	0.28
C11-R	76	17	6.3	10.96	1.59	0.69	0.10
C12-R	151	34	17.2	23.37	3.39	1.45	0.21
C13-R	142	32	14.3	22	3.19	1.38	0.20
C14-R	196	44	91	30.20	4.38	1.93	0.28
C15-R	98	22	4.8	15.10	2.19	0.97	0.14
C16-R	120	27	80	18.55	2.69	1.17	0.17

[†] Calculated from the repaired experimental ultimate load

Table 6. Deflections at ultimate moment for repaired timber stringers.

Repaired Timber Stringers	Repaired Ultimate Moment		Deflection at Repaired Ultimate Moment	
	kN-m	k-ft	mm	in.
C2-R	179.82	133	66	2.60
C3-R	107.73	79.8	5	2.00
C4-R	98.01	71.82	67	2.62
C5-R	98.01	71.82	49	1.93
C6-R	50.22	37.24	90	3.56
C7-R	111.78	82.46	45	1.77
C10-R	158.76	117.04	58	2.30
C11-R	61.56	45.22	52	2.05
C12-R	122.31	90.44	42	1.66
C13-R	115.02	85.12	50	1.95
C14-R	158.76	117.04	74	2.92
C15-R	49.98	58.52	50	1.96
C16-R	97.2	71.82	80	3.13

Table 7. Failure modes of repaired timber stringers.

Repaired Timber Stringers	Failure Modes
C2-R	Simple Tension
C3-R	Horizontal shear
C4-R	Cross-grain tension
C5-R	Simple Tension
C6-R	Simple Tension
C7-R	Simple Tension
C10-R	Simple Tension
C11-R	Simple Tension
C12-R	Horizontal shear
C13-R	Simple Tension
C14-R	Compression
C15-R	Simple Tension
C16-R	Simple Tension

Test results of original stringers

This section presents the results of the original timber stringer tests. The ultimate load at failure varied between 9 kN (2 kips) to 285 kN (64 kips) for the original timber stringers. The maximum ultimate load was 285 kN (64 kips) for stringer C10. The minimum ultimate load was 9 kN (2 kips) for stringer C8, which failed in tension caused by a knot located at the tension zone. Deflections at midspan were measured as an average of the 2 LVDTs.

Specimen C1

This first stringer was tested as a control specimen without repair. The load-deflection curve of stringer C1 was relatively linear until the failure, as shown in Figure 67. The maximum midspan load resisted by the stringer was 191 kN (43 kips) at a displacement of 27 mm (1.06 in.). As the load reached 178 kN (40 kips), cracking noises were heard. The stringer suddenly failed in shear, parallel to grain, and the load dropped to 93 kN (21 kips) which was the unstrengthened postfailure capacity. Horizontal sliding was observed at the support faces following the horizontal shear failure, as seen in Figure 68.

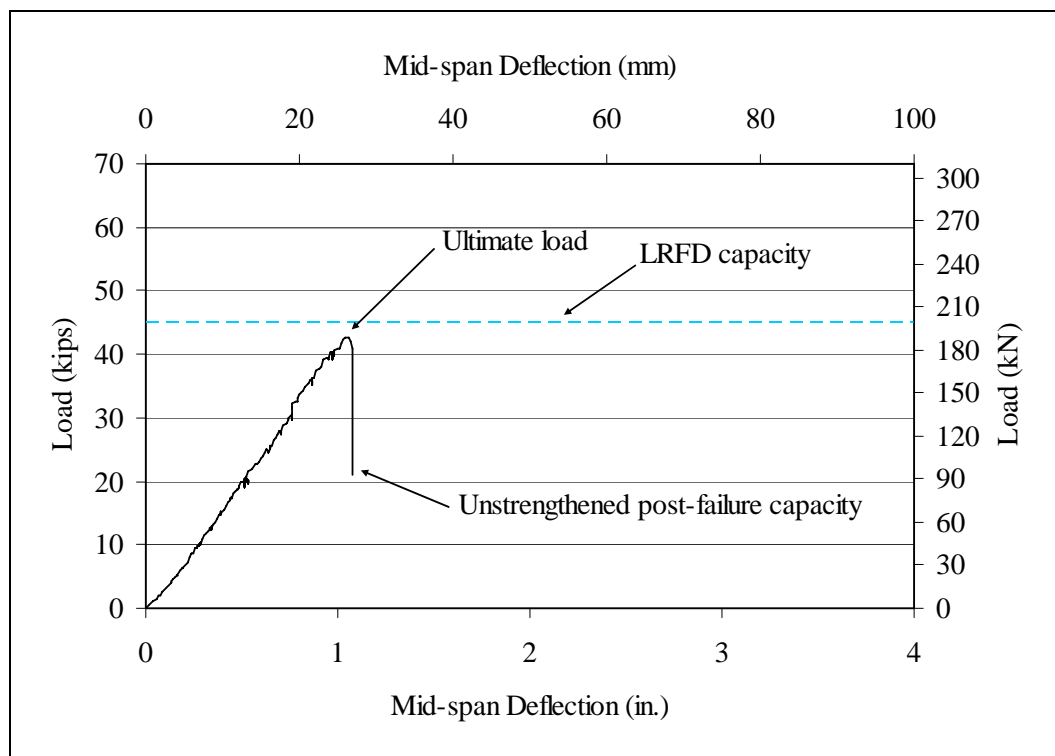


Figure 67. Load-deflection curve for stringer C1.



Figure 68. Horizontal sliding on support face after shear failure of stringer C1.

Specimen C2

The load-deflection behavior for stringer C2 was linear up to the ultimate load, as seen in the load-deflection curve in Figure 69. The stringer failed in horizontal shear. The ultimate load was 254 kN (57 kips) at a displacement of 26 mm (1.02 in.). Following the horizontal shear failure, the load dropped to 129 kN (29 kips) which was the unstrengthened postfailure capacity. Horizontal sliding was only observed at one support face. Horizontal cracks at failure were close to the center of the cross section.

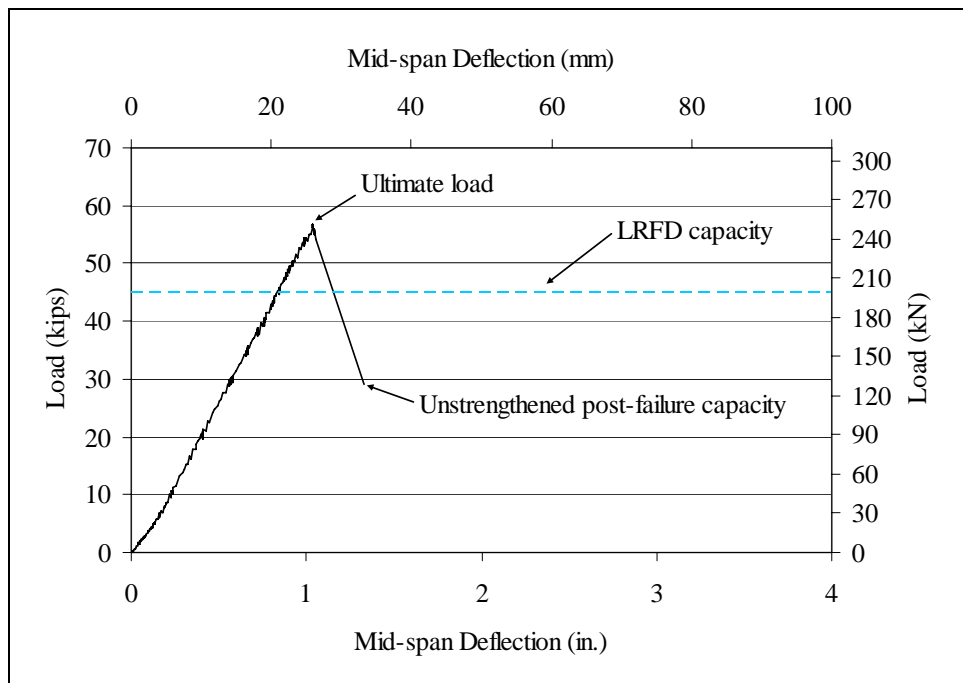


Figure 69. Load-deflection curve for stringer C2.

Specimen C3

The load-deflection relationship for stringer C3 was linear until the timber cracked in the tension zone at a load of 98 kN (22 kips), as seen in the load-deflection curve in Figure 70. The supported load dropped to 76 kN (17 kips) after tensile cracking. The stringer then gained a load capacity up to 138 kN (31 kips) where crushing occurred, and then the timber cracked again in tension at the midspan. A close-up of the second tension failure is shown in Figure 71. The stringer then continued to gain load until, the stringer failed in horizontal shear. This was the ultimate load of 142 kN (32 kips), and a midspan deflection was 36 mm (1.40 in.). After the horizontal shear failure, the unstrengthened postfailure capacity was 102 kN (23 kips).

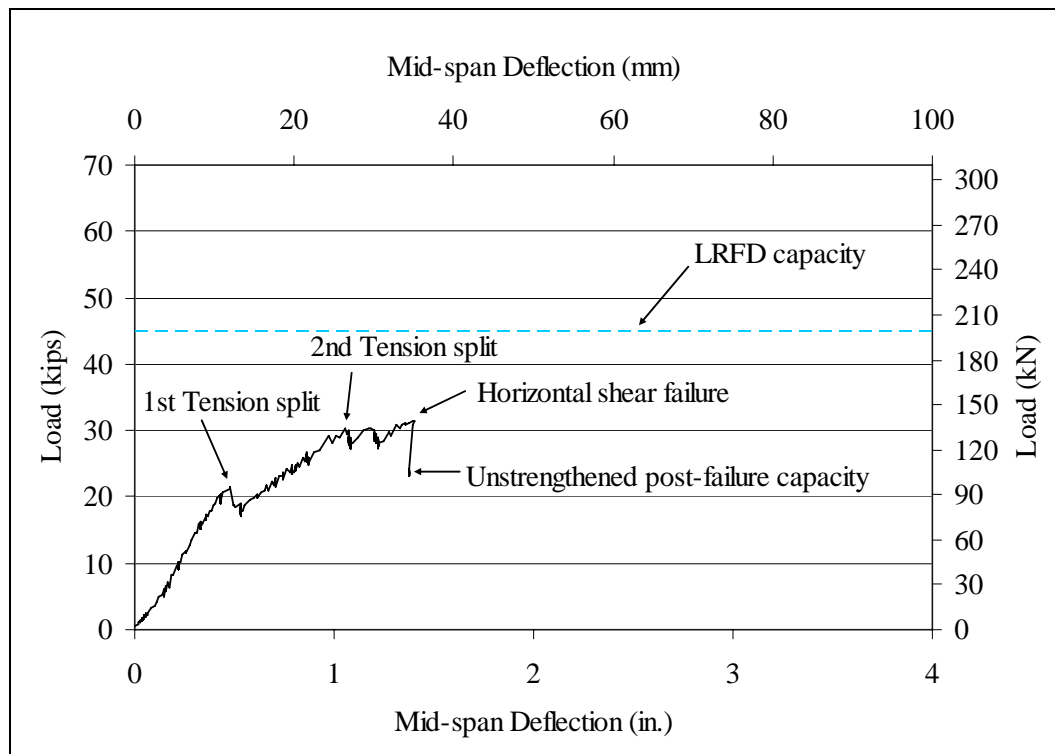


Figure 70. Load-deflection curve for stringer C3.



Figure 71. Splinter at the midspan on stringer C3.

Specimen C4

The initial slope of load-deflection curve for stringer C4, shown in Figure 72, was linear until the timber cracked in the tension zone at 182 kN (41 kips) causing a drop in the supported load to 173 kN (39 kips). The stringer underwent additional deflection with increasing load carrying capacity until the ultimate load was reached at 222 kN (50 kips). Several tension cracks and splinters were observed at the ultimate load. The ultimate load at failure was 222 kN (50 kips), and the midspan deflection was 46 mm (1.80 in.). The stringer had cross-grain tension failure at this ultimate load, and then the load dropped to 187 kN (42 kips). The failure split is shown in Figure 73. With a decreased stiffness, the load capacity again increased to 200 kN (45 kips) where the stringer had sudden horizontal shear failure, causing a drop in the supported load to 89 kN (20 kips). This was the unstrengthened postfailure capacity. The experiment was terminated after the horizontal shear failure. The horizontal shear crack was not directly across the width of the cross section, as shown in Figure 74.

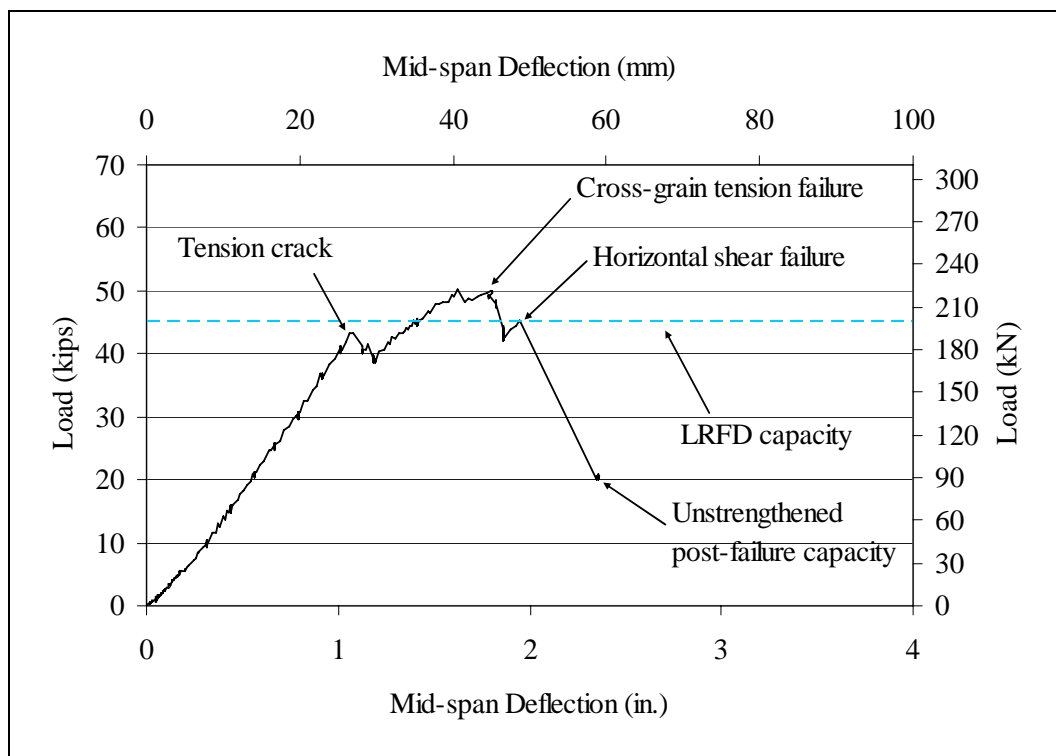


Figure 72. Load-deflection curve for stringer C4.



Figure 73. Cross-grain tension failure at 222 kN (50 kips) on stringer C4.

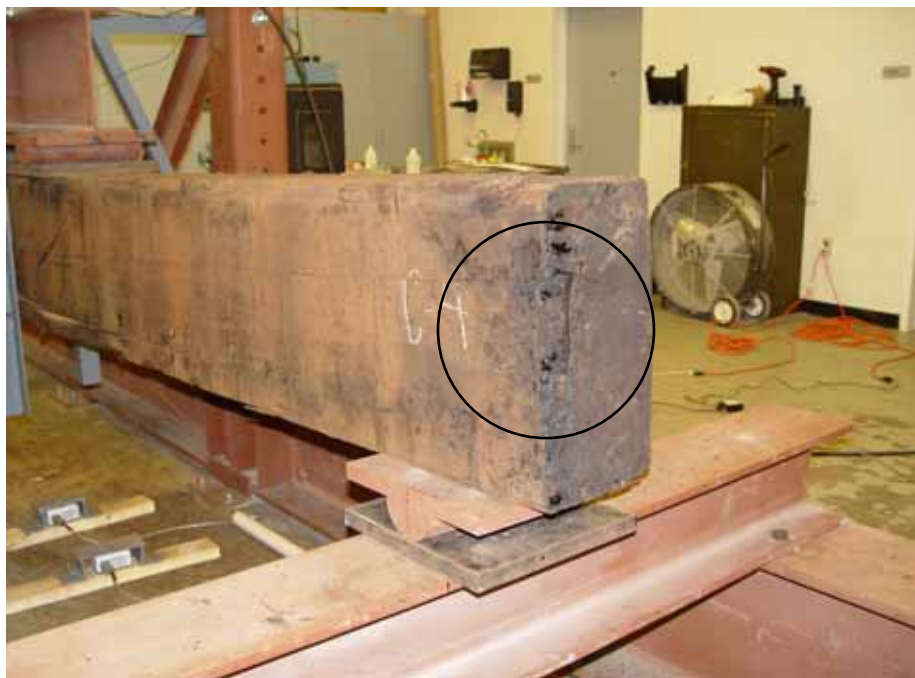


Figure 74. Horizontal shear failure on stringer C4.

Specimen C5

The initial slope of the load-deflection curve for stringer C5 is shown in Figure 75. The curve was linear until the timber cracked horizontally at 151 kN (34 kips), causing a drop in the supported load to 111 kN (25 kips). With the decreased stiffness, the stringer carried additional load while undergoing additional deflection until the ultimate load was reached and the stringer failed in simple tension. The failure pattern of stringer C5 is shown in Figure 76. The ultimate load was reached at 169 kN (38 kips) and at a deflection of 54 mm (2.12 in.). The unstrengthened postfailure capacity was 80 kN (18 kips).

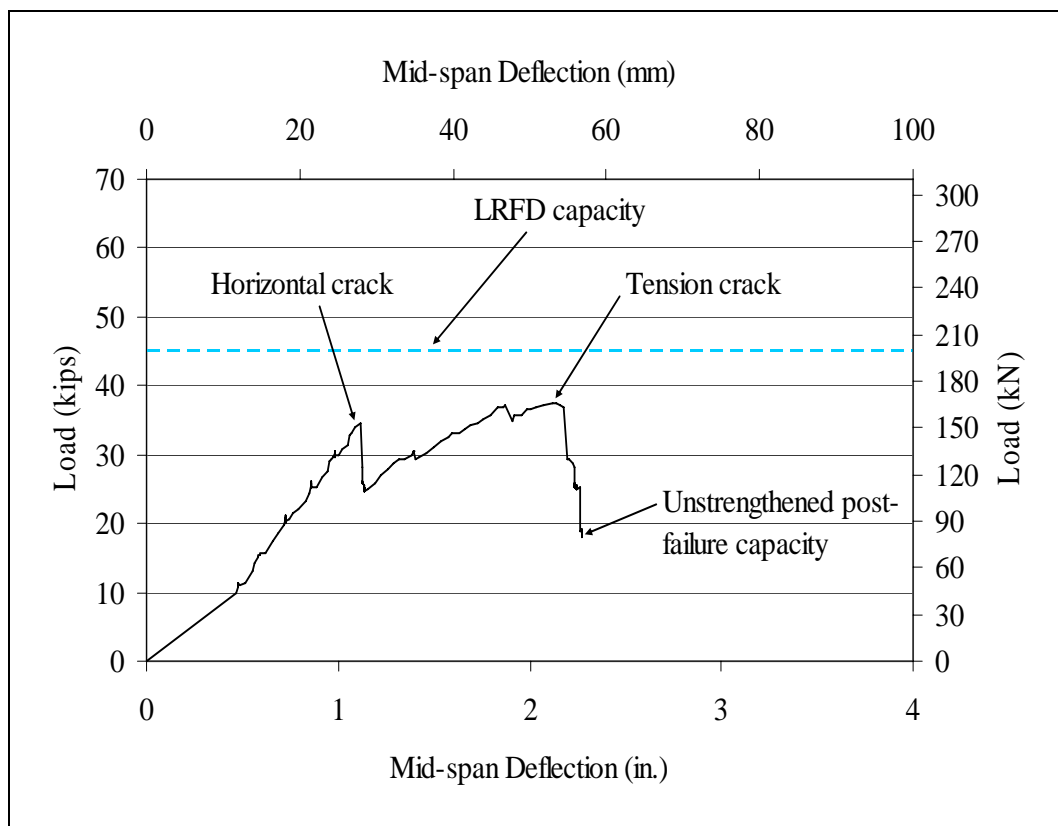


Figure 75. Load-deflection curve for stringer C5.



Figure 76. Horizontal and tension cracks at failure for stringer C5.

Specimen C6

Horizontal sliding was observed at the support faces as the load increased, since stringer C6 had horizontal end splits prior to testing. The initial slope of the load-deflection curve for stringer C6, as shown in Figure 77, was linear until the timber cracked in tension at a load of 53 kN (12 kips). The stiffness in this portion was due to the sliding friction between the two sides of the horizontal splits. A tension crack formed at failure and is shown in Figure 78. At the ultimate load, the stringer reached the unstrengthened postfailure capacity, and then underwent additional deflection without any increase in load. The experiment was terminated when the postfailure capacity was reached.

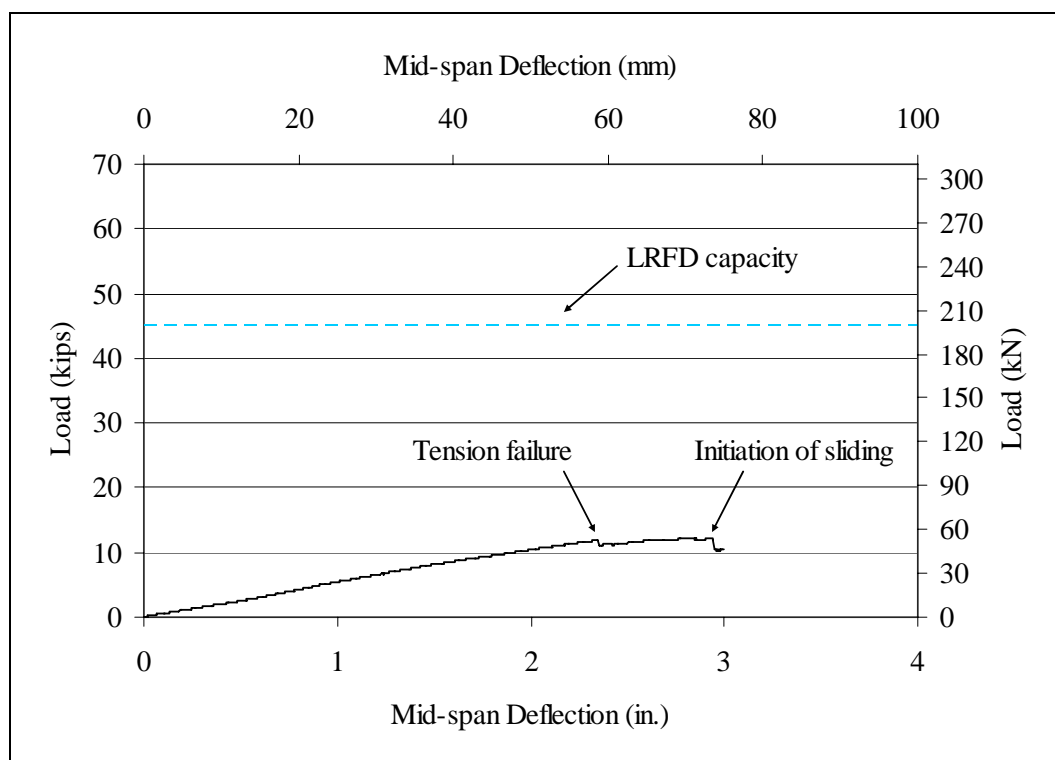


Figure 77. Load-deflection curve for stringer C6.



Figure 78. Tension crack at failure for stringer C6.

Specimen C7

The initial slope of the load-deflection curve for stringer C7 is shown in Figure 79. It was linear until the timber cracked in tension at 222 kN (50 kips), causing a small drop in the load capacity to 214 kN (48 kips). As the load increased to failure, the stringer failed in horizontal shear, as shown in Figure 80. The ultimate load at failure was 227 kN (51 kips) at a displacement of 33 mm (1.29 in.). The unstrengthened postfailure capacity was 89 kN (20 kips).

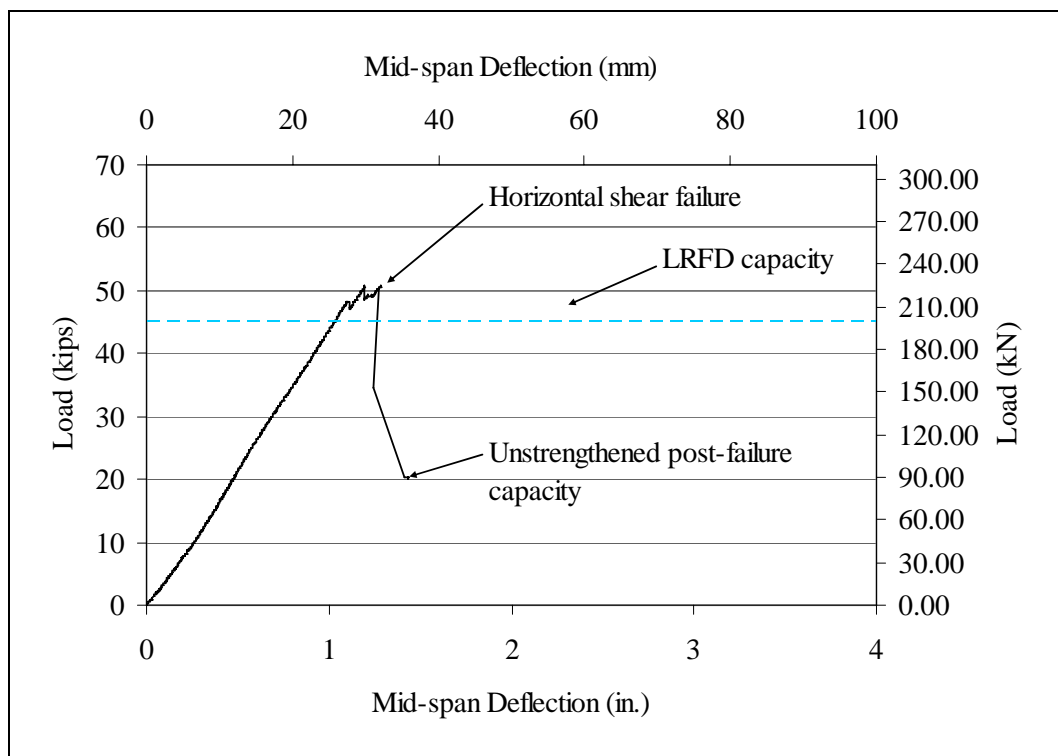


Figure 79. Load-deflection curve for stringer C7.



Figure 80. Horizontal shear failure and tension crack on stringer C7.

Specimen C8

Failure was caused in stringer C8 by a tension crack initiated by a knot. The ultimate load at failure was 9 kN (2 kips), and the midspan deflection was 6 mm (0.24 in.), as shown in Figure 81. As it was explained in Chapter 2, “Literature review, Structural behavior of timber, Natural defects in wood,” the ultimate strength of the stringer was reduced due to the presence of knots. These knots are shown in Figure 82.

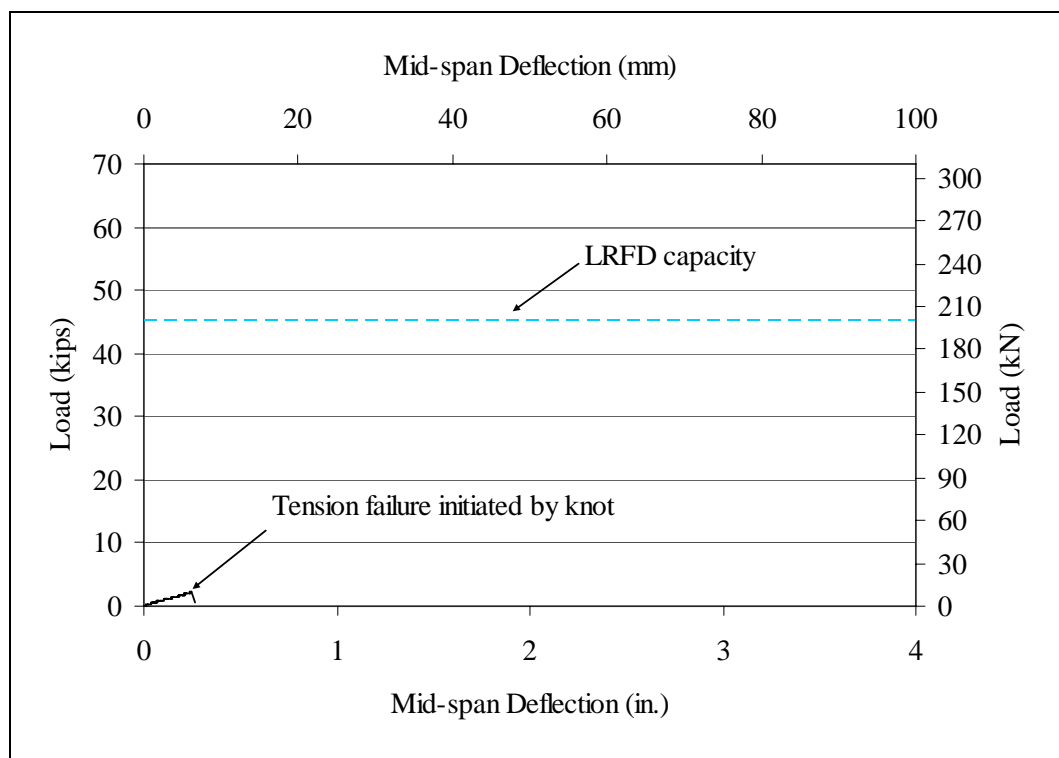


Figure 81. Load-deflection curve for stringer C8.

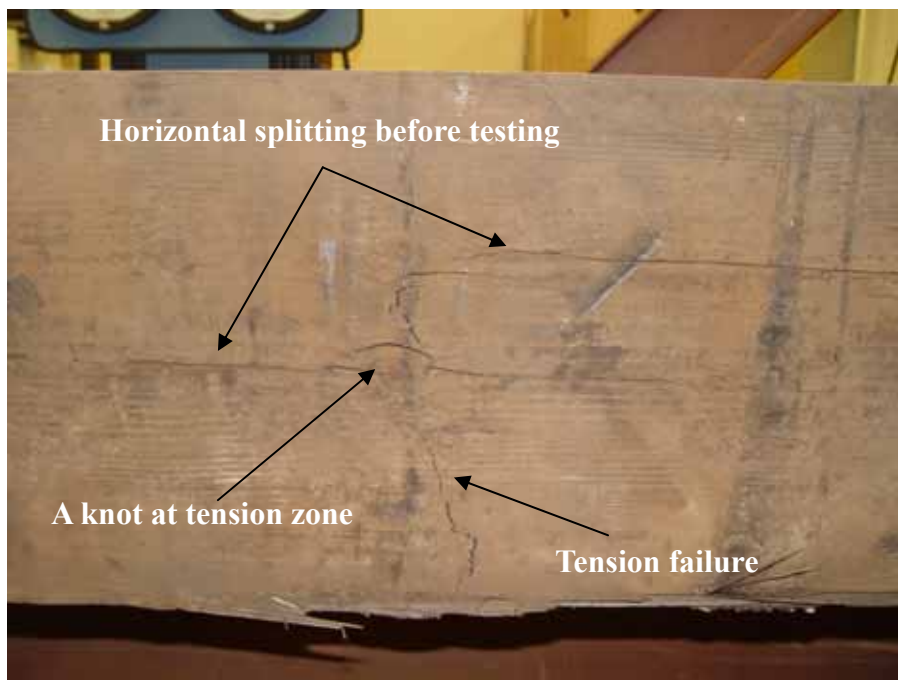


Figure 82. Tension failure initiated by a knot on stringer C8.

Specimen C9

The load-deflection curve for stringer C9, shown in Figure 83, was linear until the stringer suffered a tension crack initiated by a knot under the loading point, as seen in Figure 84. The tension crack propagated upward into the compression zone, and as a result caused the stringer to fail at a relatively lower strength. The ultimate load was 56 kN (12.5 kips) at a deflection of 7 mm (0.29 in.).

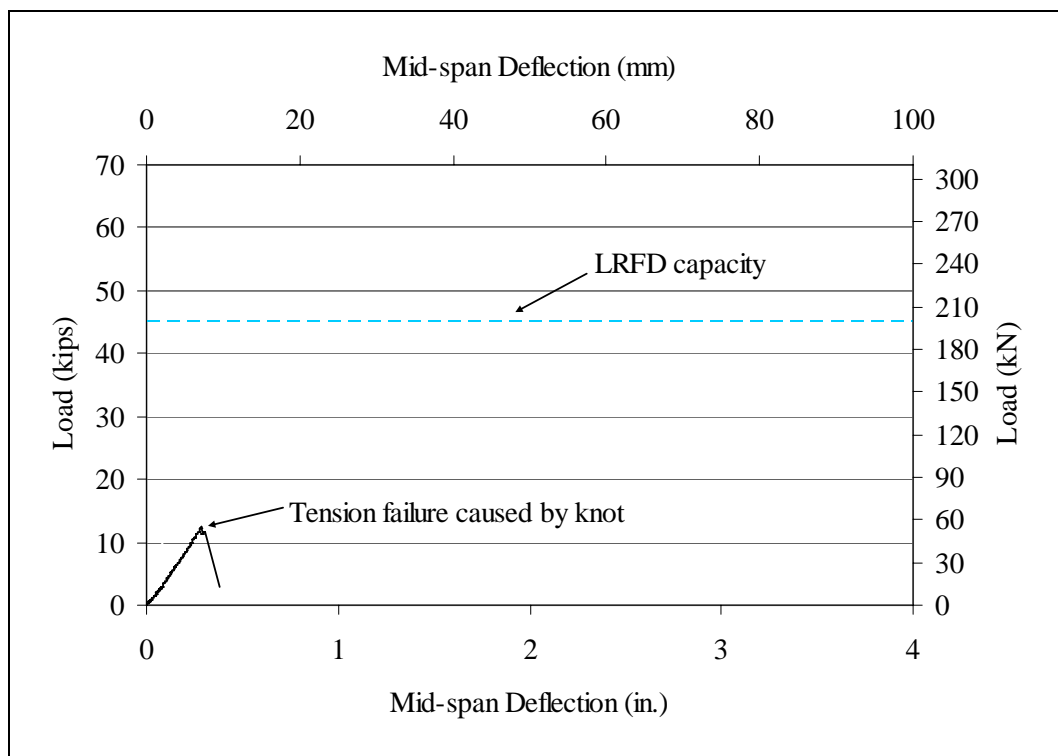


Figure 83. Load-deflection curve for stringer C9.

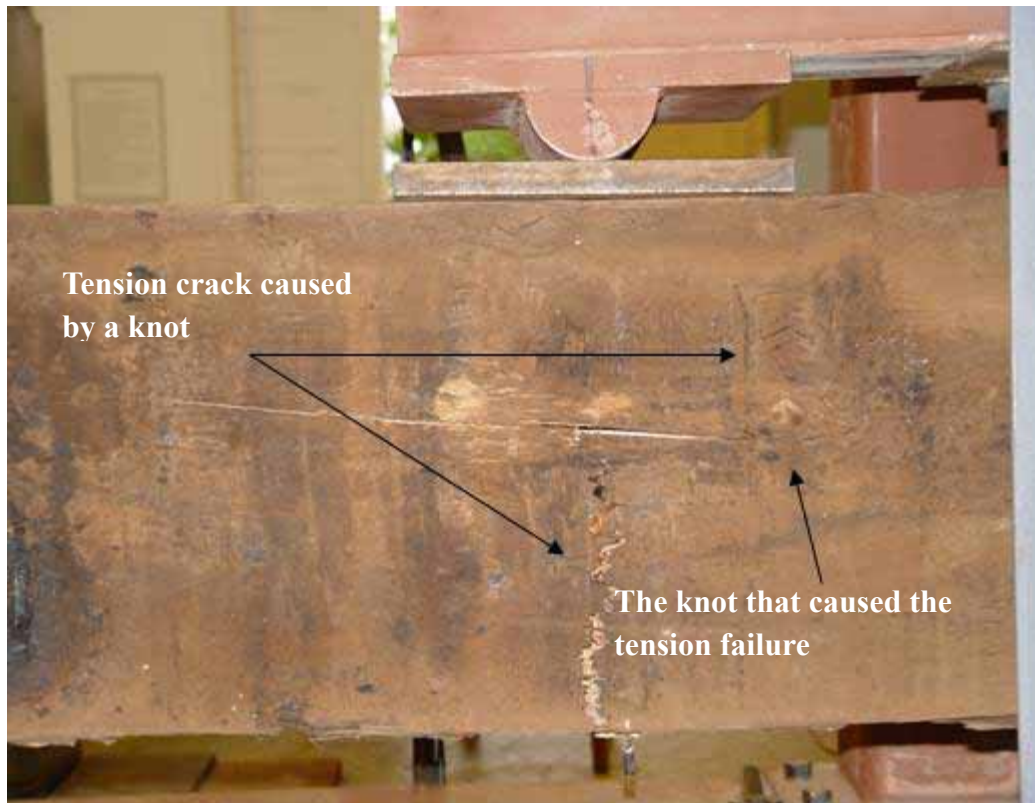


Figure 84. Tension failure caused by a knot on stringer C9.

Specimen C10

The stringer behaved linearly up until it reached the ultimate load, as seen in load-deflection curve shown in Figure 85. Stringer C10 failed in horizontal shear, and horizontal sliding was observed at the support face. The ultimate load at failure was 285 kN (64 kips) at a displacement of 26 mm (1.03 in.). The unstrengthened postfailure capacity was 98 kN (22 kips).

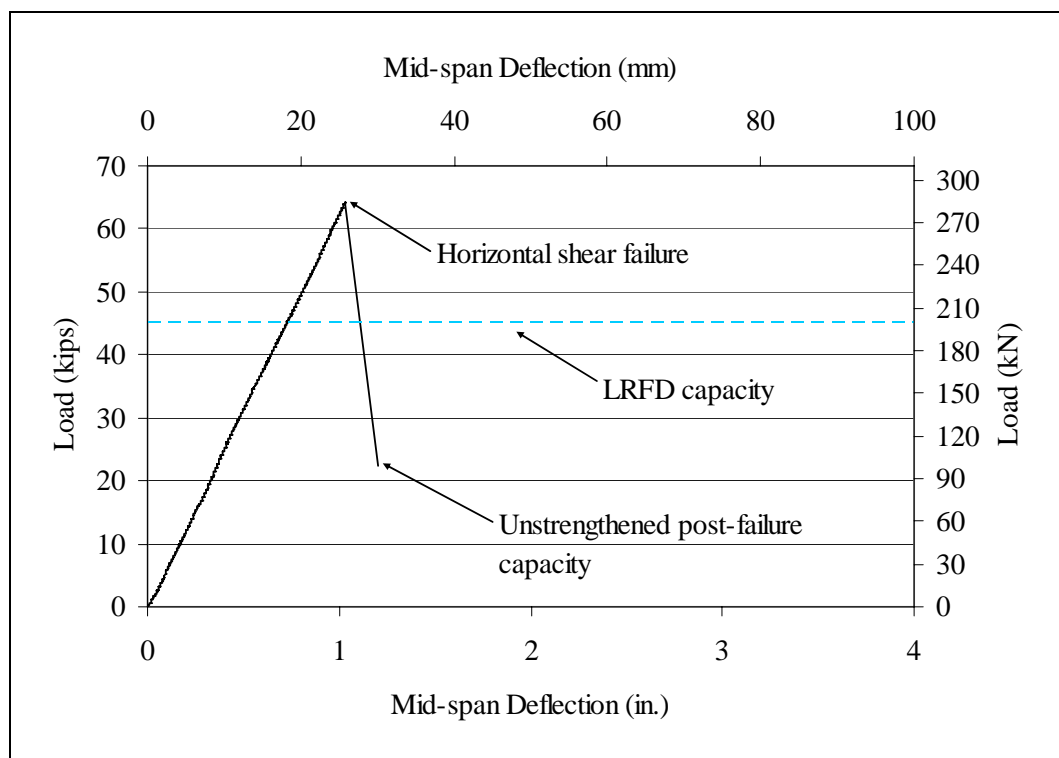


Figure 85. Load-deflection curve for stringer C10.

Specimen C11

Horizontal sliding was observed at the support faces of stringer C11 as the load increased. There were existing horizontal end splitting before testing. The initial portion of the load-deflection curve, shown in Figure 86, was linear until the timber cracked again in horizontal shear at 67 kN (15 kips), causing a drop in the supported load to 58 kN (13 kips). The stringer underwent additional deflection with the increased load carrying capacity until postfailure capacity was reached. This large deflection was caused by the two pieces sliding over one another. Several horizontal cracks were observed as a result of excessive deformation. The unstrengthened

postfailure capacity was 76 kN (17 kips) at a deflection of 48 mm (1.90 in.). The experiment was terminated at the postfailure capacity.

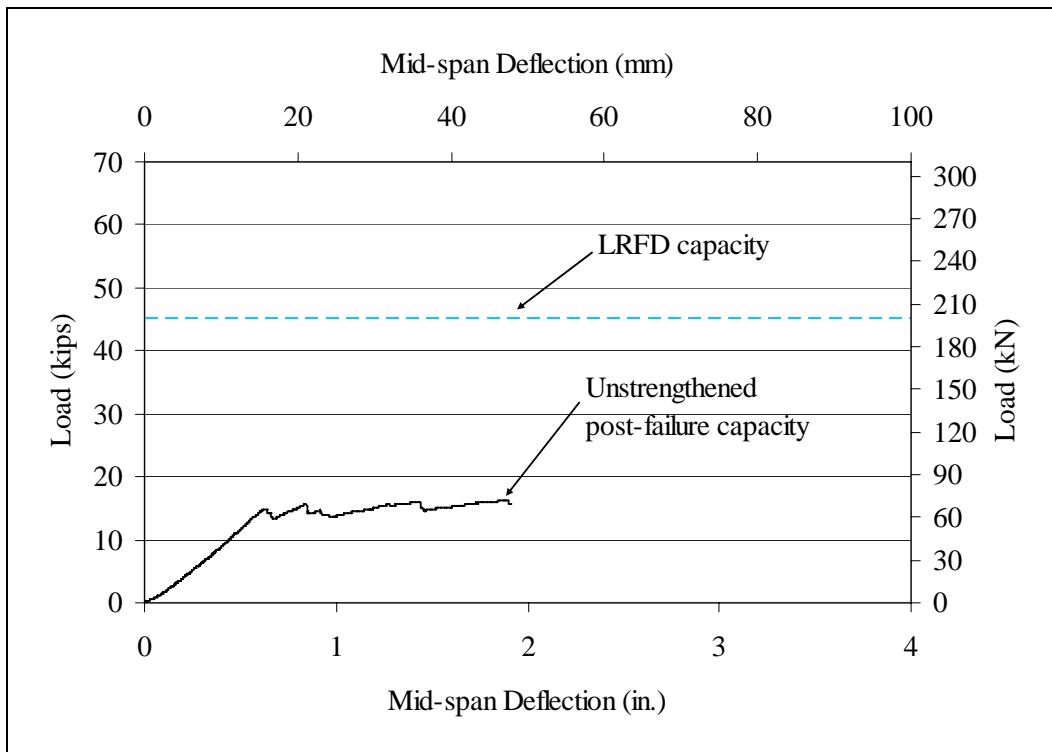


Figure 86. Load-deflection curve for stringer C11.

Specimen C12

The initial slope of the load-deflection curve for stringer C12, shown in Figure 87, was linear until the stringer cracked in the tension zone causing the capacity to drop. The stringer had a cross-grain tension failure, as shown in Figure 88. The ultimate load resisted by the stringer was 196 kN (44 kips) at a displacement of 27 mm (1.07 in.). After the tension failure, the unstrengthened postfailure capacity was 129 kN (29 kips).

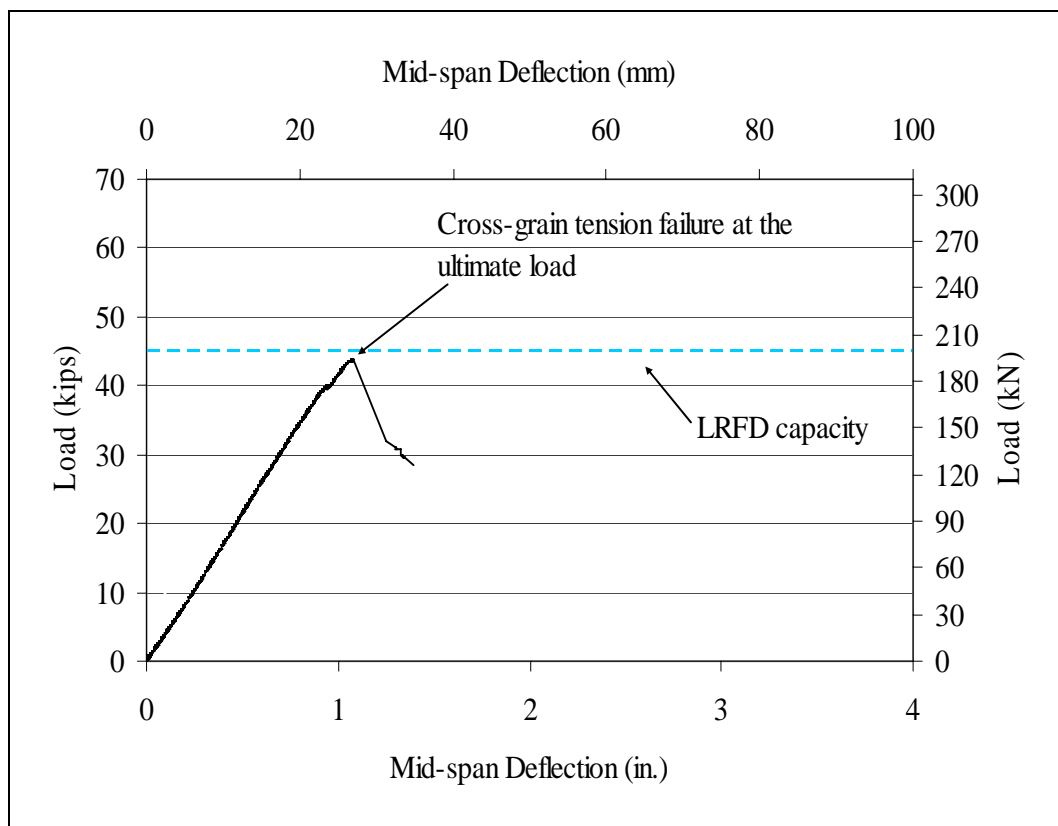


Figure 87. Load-deflection curve for stringer C12.



Figure 88. Cross-grain tension failure on stringer C12.

Specimen C13

Stringer C13 had end splitting prior to testing. The stringer showed horizontal sliding on the support face as the load increased. The load-deflection curve of the stringer, shown in Figure 89, was linear until the stringer reached the unstrengthened postfailure capacity of 125 kN (28 kips) at a deflection of 39 mm (1.53 in.). With a decreased stiffness, the load increased further. The stringer underwent additional deflection while developing tension cracks.

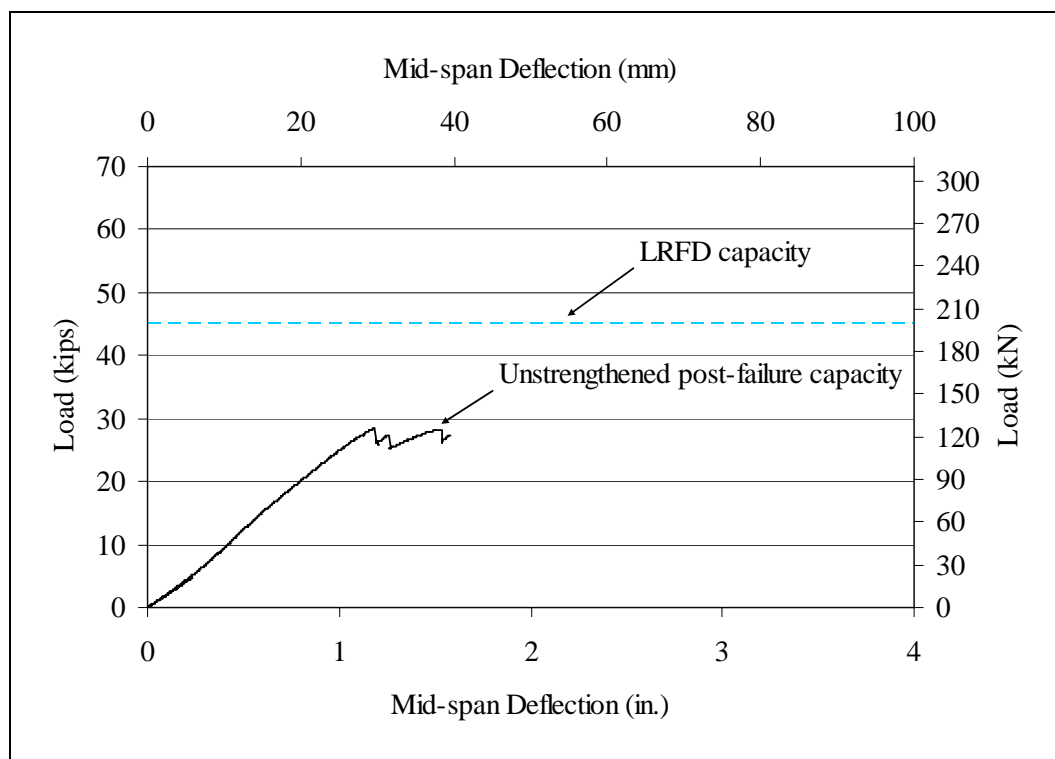


Figure 89. Load-deflection curve for stringer C13.

Specimen C14

Stringer C14 had signs of heart checks prior to testing. The stringer behaved linearly until it reached its ultimate load capacity, as seen in the load-deflection curve shown in Figure 90. The stringer failed in horizontal shear. The ultimate load was 231 kN (52 kips) at a displacement of 24 mm (0.94 in.). The unstrengthened postfailure capacity was 102 kN (23 kips). Horizontal sliding was observed on the cross section after the horizontal shear failure, as shown in Figure 91. Horizontal splitting occurred at the center of the cross section where shear stresses reached their maximum value.

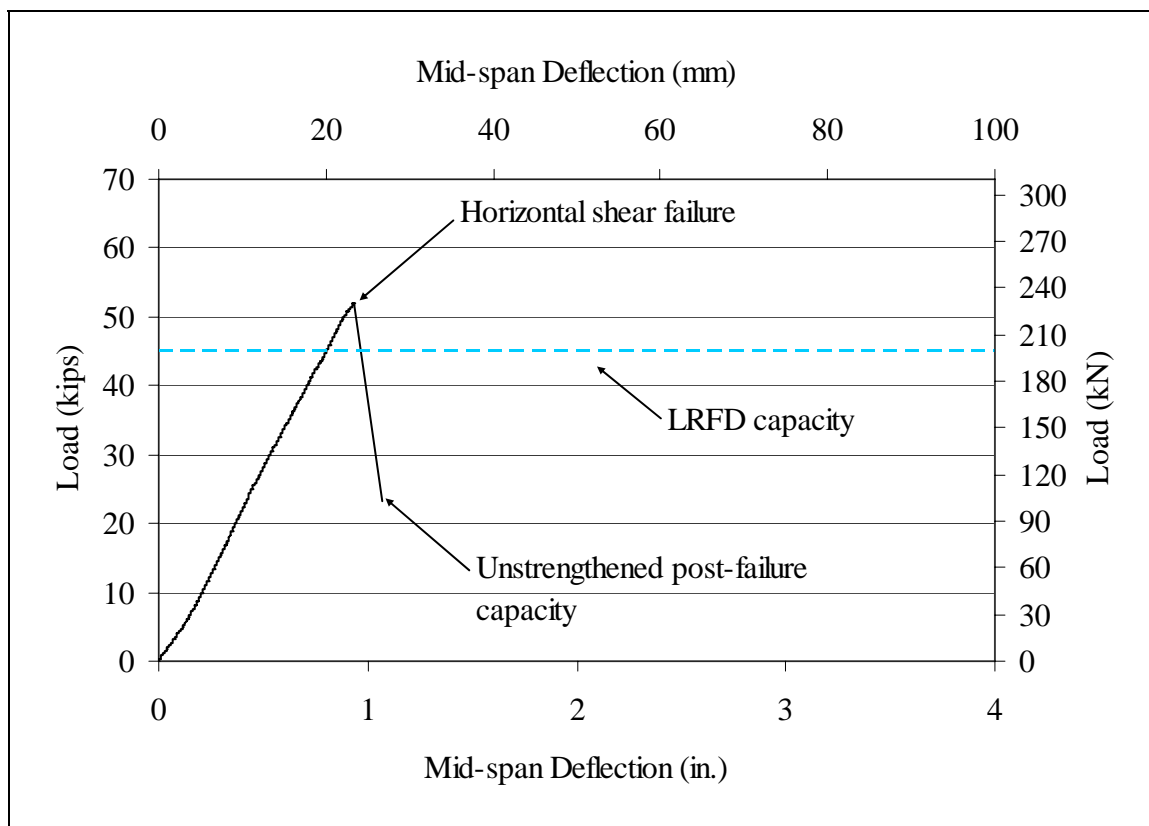


Figure 90. Load-deflection curve for stringer C14.



Figure 91. Horizontal shear failure on stringer C14.

Specimen C15

Horizontal sliding was observed at the support faces of stringer C15 as the load increased due to horizontal end splitting. The initial slope of the load-deflection curve for stringer C15, shown in Figure 92, was linear until the timber cracked in the tension zone at a load of 89 kN (20 kips). This caused a small drop in the supported load to 85 kN (19 kips). The stringer then underwent additional deflection of 13 mm (0.5 in.) with increasing load. Several additional horizontal cracks were formed because of the excessive deformation in the stringer. The unstrengthened postfailure capacity was 93 kN (21 kips). The experiment was terminated at the postfailure capacity in order to prevent the formation of additional tension cracks.

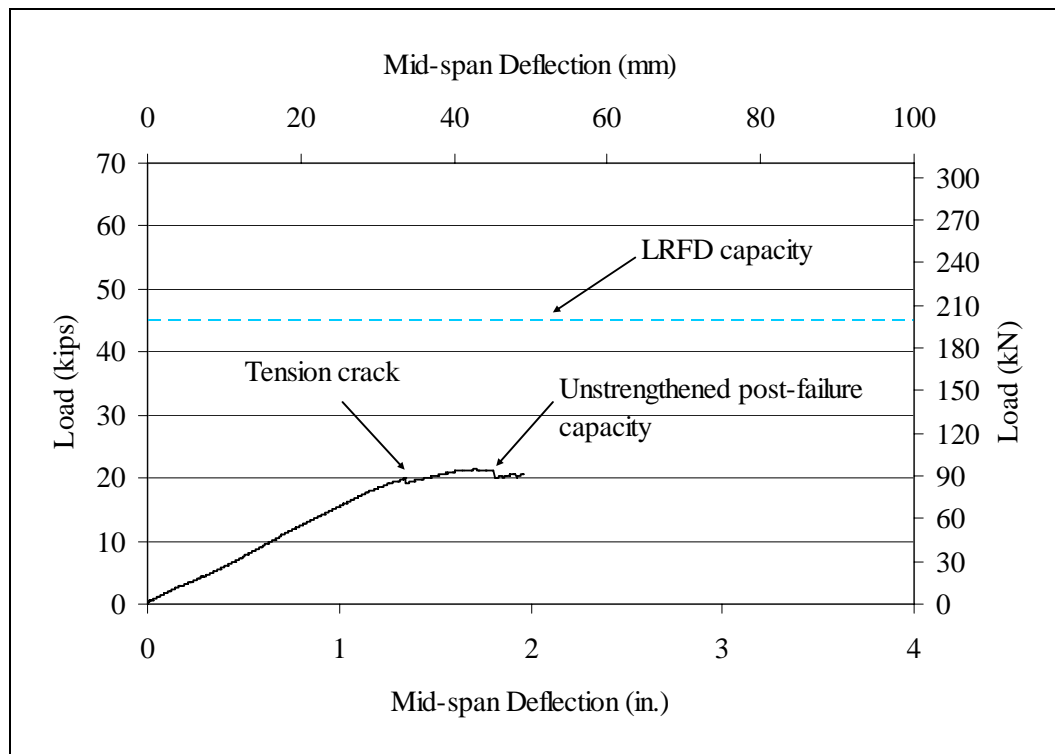


Figure 92. Load-deflection curve for stringer C15.

Specimen C16

Stringer C16 exhibited end splitting prior to testing. The stringer behaved linearly until the unstrengthened postfailure capacity, as seen in the load-deflection curve given in Figure 93. Horizontal sliding on the support face was observed as the load increased throughout the test. The unstrengthened postfailure capacity was 67 kN (15 kips). The experiment was

terminated to prevent the formation of tension cracks after the postfailure capacity was reached.

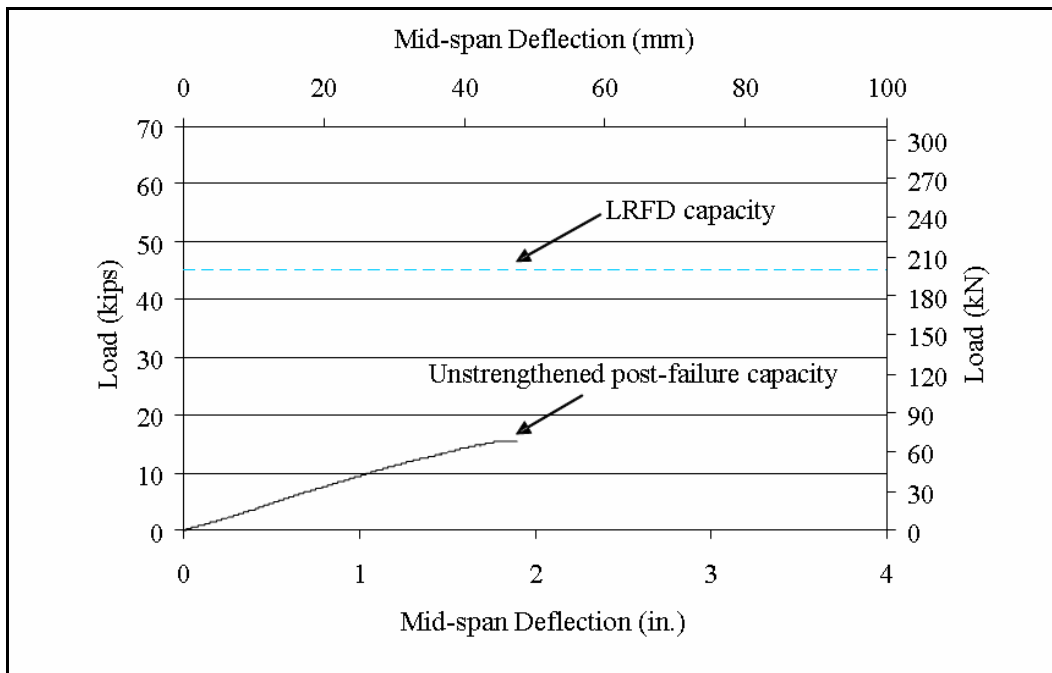


Figure 93. Load-deflection curve for stringer C16.

Discussion of original timber stringers

The shear strength of timber stringers that have been in service for a considerable period of time is a concern because these members are likely to have experienced strength loss as a result of checking, splitting, and deterioration. Timber stringers that were tested to determine their unstrengthened postfailure capacity also provided data to assess the remaining strength of timber stringers which have been in-service for many decades.

All timber stringers were inspected prior to testing to identify signs of checking or horizontal splitting caused by swelling and shrinkage from uneven drying or from repeated wet/dry moisture cycles. Stringers C1 and C5 had severe and deep checking only on one side. As discussed in Chapter 2, “Literature review, Timber bridge maintenance, Repairs,” this revealed that these stringers were in service as outer members in a timber bridge. Severe end splitting was also observed in timber stringers C6, C13, C15, and C16. Stringer C7 had tension cracks and splinters and stringer C11 showed deteriorations at an end support.

The ultimate strength distribution for the original stringers without end splitting before testing was shown in Figure 94. The ultimate strength values obtained from these stringers ranged from 142 kN (32 kips) for the weakest stringer C3 to 285 kN (64 kips) for the strongest stringer C10. An average ultimate load was 180 kN (40.5 kips) for original timber stringers. The variation was expected because these stringers have been in service for decades and were exposed to severe weather conditions. Based on the limited number specimens, it is appropriate to determine trends rather than concentrating on specific values such as the average.

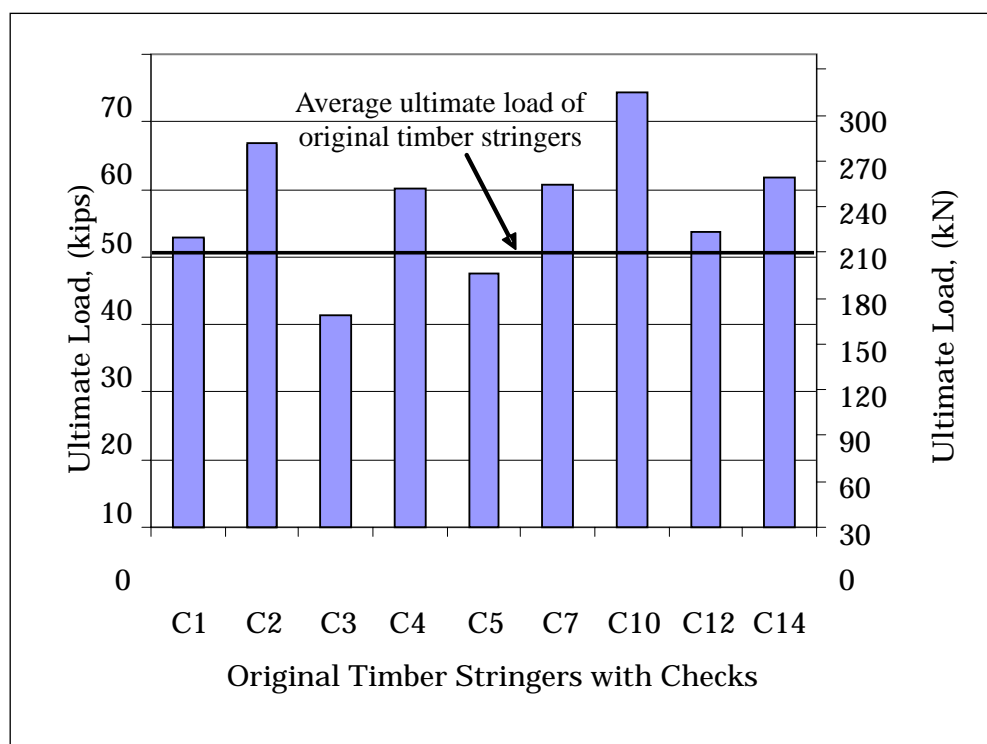


Figure 94. Distribution of ultimate load for original stringers without end splitting.

Bending stresses at the ultimate load ranged between 22 MPa (3.19 ksi) and 44 MPa (6.38 ksi) for the stringers with several checks along their lengths. The average for bending stress at ultimate load was 33 MPa (4.77 ksi). The LRFD reference bending strength value for dense select structural southern pine was 30.7 MPa (4.45 ksi) (AFPA 1996). Horizontal shear stress at ultimate load ranged between 1.40 MPa (0.20 ksi) and 2.79 MPa (0.40 ksi) for the stringers with several checks along their lengths. The average horizontal shear strength for tested timber stringers with checks was 2.08 MPa (0.30 ksi). LRFD reference shear strength value for dense select structural southern pine was 2.21 MPa (0.32 ksi) (AFPA 1996). The timber stringers test results are summarized in Table 8. Bend-

ing and shear stresses were compared to the LRFD reference strength values for dense select structural southern pine in Table 9 (AFPA 1996).

Table 8. Maximum, minimum, and average bending and shear stresses at ultimate load for original timber stringers with checks.

Original Timber Stringers with Checks	Bending Stress at Ultimate Load						Shear Stress at Ultimate Load					
	Maximum		Minimum		Average		Maximum		Minimum		Average	
	MPa	ksi	MPa	ksi	MPa	ksi	MPa	ksi	MPa	ksi	MPa	ksi
	44	6.38	22	3.19	33	4.77	2.79	0.40	1.40	0.20	2.08	0.30

Table 9. Comparison of bending and shear stresses to LRFD (AFPA 1996) reference strength values for dense select structural southern pine.

Original Timber Stringers with Checks	Bending Stress		Shear Stress		LRFD Bending		LRFD Shear		Bending Stress		Shear Stress	
	MPa	ksi	MPa	ksi	MPa	ksi	MPa	ksi	LRFD	LRFD	LRFD	LRFD
C1	29.51	4.28	1.86	0.27					0.96		0.84	
C2	39.16	5.68	2.52	0.36					1.28		1.13	
C3	22	3.19	1.40	0.20					0.72		0.63	
C4	34.34	4.98	2.17	0.31					1.12		0.97	
C5	26.13	3.79	1.68	0.24					0.85		0.75	
C7	35.03	5.08	2.24	0.32					1.14		1	
C10	44	6.38	2.79	0.40					1.43		1.25	
C12	30.20	4.38	1.96	0.28					0.98		0.88	
C14	35.72	5.18	2.31	0.33					1.16		1.03	
								Average	1.07		0.94	

The bending stresses at unstrengthened postfailure load ranged between 8.27 MPa (1.20 ksi) and 19.24 MPa (2.79 ksi) for the original stringers with end splitting. An average value for the bending strength of these stringers was 12.64 MPa (1.83 ksi), which was less than one-third of the LRFD reference bending strength value of 30.7 MPa (4.45 ksi) for dense select structural southern pine (AFPA 1996). The horizontal shear stress at unstrengthened postfailure load ranged between 1.26 MPa (0.18 ksi) and 0.56 MPa (0.08 ksi) for the stringers with several checks along their lengths. The average shear stress at unstrengthened postfailure load was 0.80 MPa (0.12 ksi), which was below the LRFD reference shear strength value of 2.21 MPa (0.32 ksi) for dense select structural southern pine (AFPA 1996). This indicated that the end splitting reduced the actual val-

ues below the design values, as would be expected. These stringers should be replaced or retrofitted with appropriate repair methods. Tables 10 and 11 summarized the test results for original timber stringers with end splitting.

Table 10. Comparison of bending and shear stresses of timber stringers with end splitting to LRFD (AFPA 1996) reference strength values for dense select structural southern pine.

Original Timber Stringers with End Splitting	Bending Stress at Unstrengthened Post-failure Load		Shear Stress at Unstrengthened Post-failure Load		LRFD Bending		LRFD Shear		Bending Stress LRFD		Shear Stress LRFD	
	MPa	ksi	MPa	ksi	MPa	ksi	MPa	ksi				
C6	8.27	1.20	0.56	0.08	30.7	4.45	2.21	0.32	0.27		0.25	
C11	10.96	1.59	0.70	0.10					0.36		0.31	
C13	19.24	2.79	1.26	0.18					0.63		0.56	
C15	14.41	2.09	0.91	0.13					0.47		0.41	
C16	10.27	1.49	0.63	0.09					0.34		0.28	
							Average		0.41		0.36	

Table 11. Maximum, minimum, and average bending and shear stresses at ultimate load for original timber stringers with end splitting.

Original Timber stringers with end splitting	Bending Stress						Shear Stress					
	Maximum		Minimum		Average		Maximum		Minimum		Average	
	MPa	ksi	MPa	ksi	MPa	ksi	MPa	ksi	MPa	ksi	MPa	ksi
	19.24	2.79	8.27	1.20	12.64	1.83	1.26	0.18	0.56	0.08	0.80	0.12

For the original timber stringers with checks, an average of 1.07 was obtained when bending stress values at ultimate load was divided by the design values. The average for shear stresses was 0.94. These numbers show the design values are close to the experimental values. End splits reduced the bending and shear stress values at ultimate load by almost one-third of the design values, as seen in Table 11.

Original timber stringers showed different types of failure modes such as horizontal shear, simple tension and cross-grain tension, as defined by ASTM D143 (1999). Stringers which exhibited only signs of checking failed in shear parallel to grain. Of the 16 original timber stringers, 6 stringers (C1, C2, C3, C7, C10, and C14) with several checks along their lengths failed in horizontal shear parallel-to-grain direction. These failures were

sudden. The load-deflection curves for these stringers were linear up to the ultimate load, after which the load dropped to the unstrengthened post-failure capacity. New checks, especially heart checks, created a plane of weakness in parallel-to-grain direction which caused horizontal shear failures in stringers C1, C2, C3, C7, C10, and C14.

Horizontal shear failure occurred near the center of the cross section where the shear stresses were at a maximum. Timber stringers C10 and C14, both with heart checks, were the best example for this type of failure. As expected, these stringers developed shear failure parallel to grain along the heart checks. Stringers C10 and C14 then began to act like two separate beams, one sliding on top of the other. This supported the assumptions in Chapter 3, “Experimental program, Repair systems for stringers,” which were used to determine the required number of hex bolts or lag screws. Full longitudinal separation was assumed along the length of the stringers in the previous calculations. Splitting was not over the entire lengths of the stringer used in the experiments. A smaller number of hex bolts or lag screws were also feasible to repair timber stringers.

Timber stringers with signs of tension cracks typically failed in flexure; stringers C4, C5, and C12 had tension cracks and failed in flexure. These flexural cracks reduced the effectiveness of the repair methods utilized in this study, by an average of 34%, which were aimed at shear repair. Stringers C4 and C12 had cross-grain tension failure. Timber stringer C5 had horizontal shear and simple tension cracks as it was loaded to failure. These stringers (C4, C5, and C12) had local drops in load capacity caused by tension cracks. For example, the load-deflection curve of stringer C5 was not linear until it reached ultimate load. Horizontal local cracks occurred during the loading, but the stringer continued to gain load carrying capacity until it failed in simple tension.

Another factor which reduced the load capacity of the timber stringers was the presence of knots. Timber stringers C8 and C9 developed tension cracks due to knots that were oriented vertically from the bottom to top of the stringers. These stringers had an 82% lower load capacity than the stringers with checks, as seen in Table 12. As expected, the natural defects decrease the strength and durability of timber members. The discontinuities introduced by the knots in stringers C8 and C9 reduced the ultimate strength by 95% and 70%, respectively. The attempted repair methods proved to be unfeasible for these two stringers.

Table 12. Timber stringers which failed due to presence of knots.

Original Timber Stringers with Knots	Ultimate Load		Average Ultimate Load for Timber Stringers with Checks	
	kN	kips	kN	kips
C8	9	2	180.14	40.5
C9	56	12.5		

End splitting reduced both the flexural and the shear strength of stringers C6, C11, C13, C15, and C16 by an average of 20.30 MPa (2.94 ksi) and 1.24 MPa (0.18 ksi), to almost one-third of the strength of the other tested stringers without end splitting. The load-deflection behavior of these stringers was linear until they reached the unstrengthened postfailure capacity. After the postfailure capacity was reached, they underwent significant deflection without further increase in their load carrying capacity. Horizontal sliding was also observed at the support faces indicating a loss of shear performance in these timber stringers. The loss of stiffness in these stringers is related to the loss of shear performance.

Test results of repaired stringers

This section reviews the experimental results for the repaired stringers. The repaired ultimate load capacity of the repaired timber stringers was compared with the unstrengthened postfailure capacity of original stringers to determine the effectiveness of the repair methods, as shown in Figure 95. The use of hex bolts, lag screws, and FRP side plates increased the unstrengthened postfailure capacity of the repaired timber stringers. None of the repair methods was adequate to restore the load capacity of the repaired stringers to the original unsplit member strength, as seen in Figure 96. Increase in strength over unstrengthened postfailure capacity was 100% for stringer C10-R. The minimum percent strength increase over unstrengthened postfailure capacity was 4.8% for stringer C15-R.

Repair methods also changed the mode of failure from horizontal shear to simple tension. The repaired timber stringers tended to fail in simple tension. Of the 13 repaired stringers, 9 failed in simple tension, 2 failed in horizontal shear, and 1 failed in compression. Stringers C3-R and C12-R had horizontal shear cracks at failure. Stringer C14-R showed cracks in compression zone at the ultimate load.

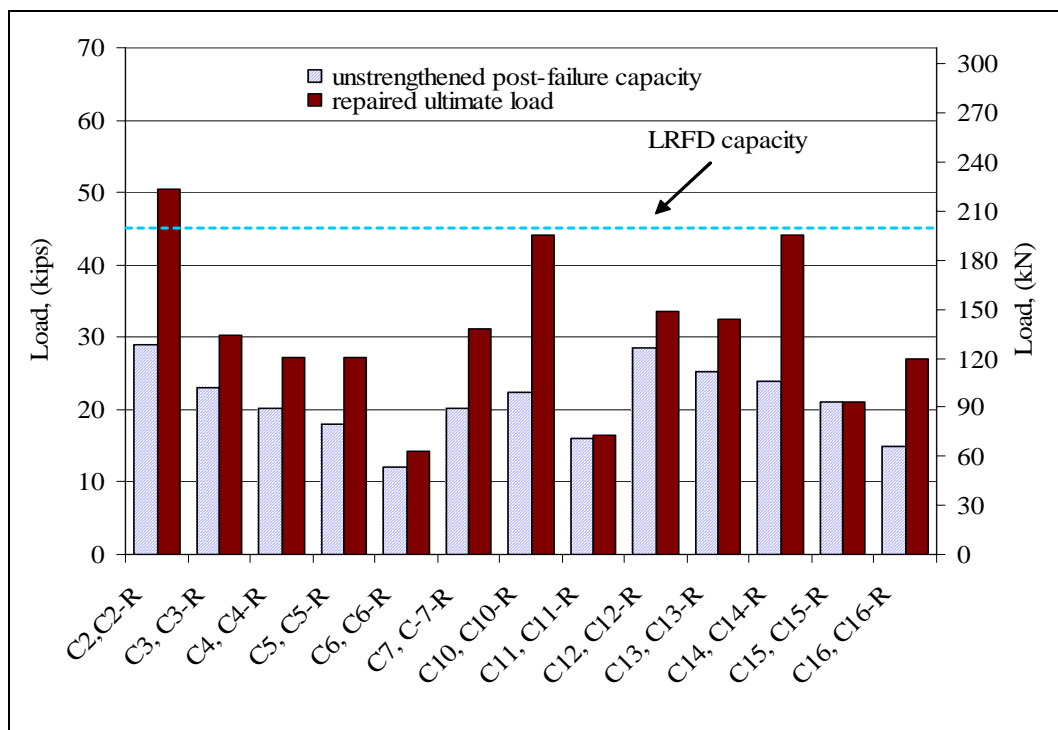


Figure 95. Unstrengthened postfailure capacity and repaired ultimate load capacities.

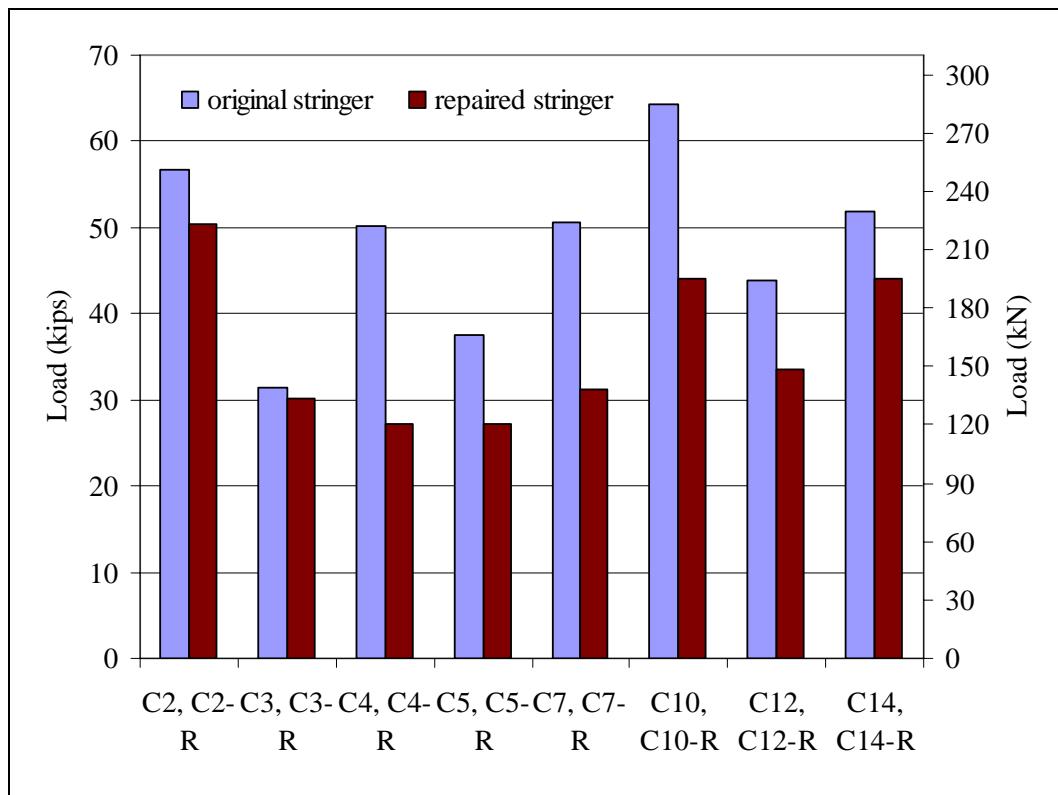


Figure 96. Ultimate load of original and repaired stringers without end split before testing.

Stringers repaired with hex bolts

This section presents the test results of the stringers repaired with hex bolts. Hex bolts with epoxy were used to repair stringers C2-R and C3-R at every 610 mm (24 in.). Stringers C4-R and C5-R were repaired at every 305 mm (12 in.).

Specimens C2-R and C3-R

The load-deflection curve for stringer C2-R, shown in Figure 97, was linear until the stringer C2-R cracked in the tension zone which caused a drop in its load capacity. Cracking noise was heard and horizontal sliding was observed at the support face as the load increased to failure. Stringer C2-R had tension cracks and tension splinters at the midspan at the repaired ultimate load, as shown in Figure 98. The repaired ultimate load was 222 kN (50 kips) at a displacement of 66 mm (2.6 in.).

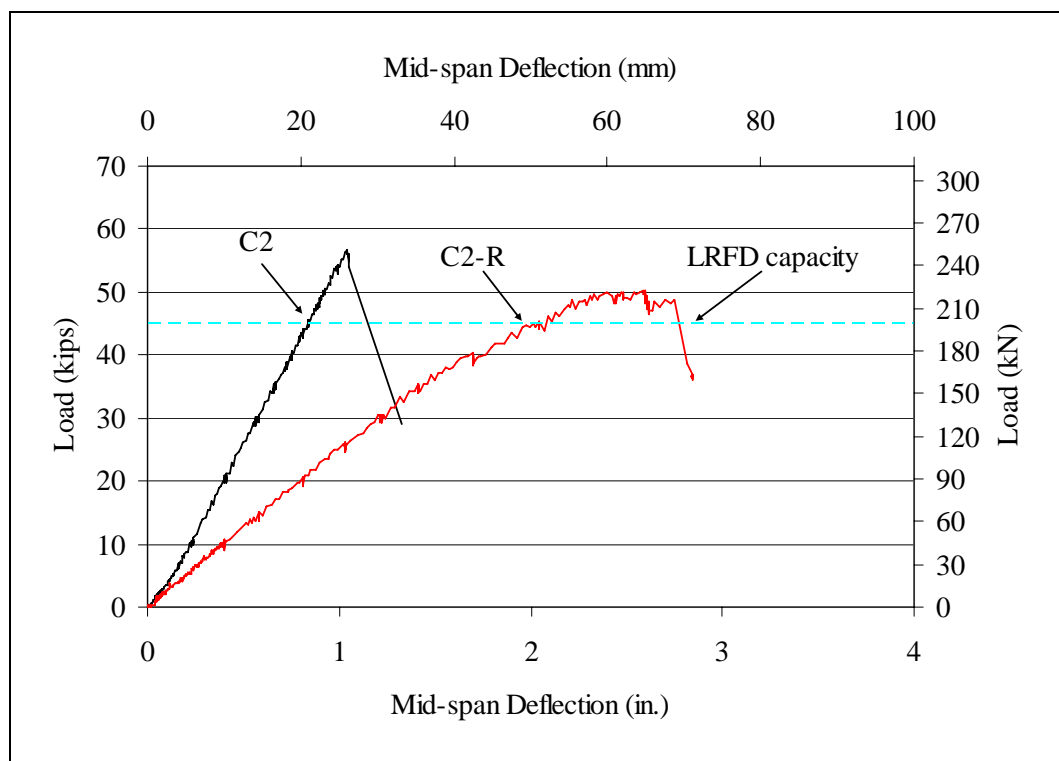


Figure 97. Load-deflection curves for stringers C2 and C2-R.



Figure 98. Tension cracks at the failure on stringer C2-R.

Stringer C3-R behaved linearly until it reached the repaired ultimate load, as seen in the load-deflection curve shown in Figure 99. The stringer failed in horizontal shear, which caused a drop in its load capacity. Horizontal sliding was observed at the support faces, as the load increased to failure. The repaired ultimate load was 133 kN (30 kips) at a displacement of 51 mm (2 in.).

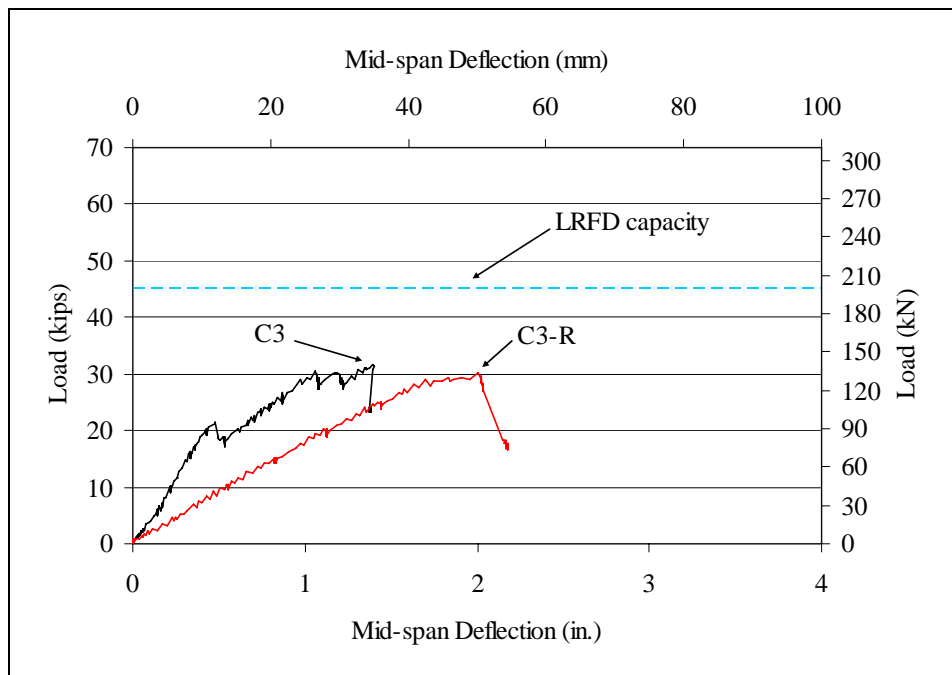


Figure 99. Load-deflection curves for stringers C3 and C3-R.

The increase in the repaired ultimate load over the unstrengthened postfailure capacity was 72.4 and 30.4% for repaired stringers C2-R and C3-R, respectively. These stringers were repaired using hex bolts at every 610 mm (2 ft) with epoxy. The epoxy used on the surface of the hex bolts improved the load transfer between the timber and the hex bolts. Since stringers C2 and C3 developed horizontal shear cracks prior to the repair, the repair method was effective. The original and repaired ultimate loads were 254 kN (57 kips) and 222 kN (50 kips) for stringers C2 and C2-R, respectively. This represents 88% recovery of ultimate load for stringer C2-R, and the increase in the unstrengthened postfailure capacity was 72.4%. The repair method was effective because the initial failure of stringer C2 was only in horizontal shear and; therefore, effectiveness of the shear repair method was maximized for stringer C2-R.

The original and repaired ultimate loads were 142 kN (32 kips) and 133 kN (30 kips) for stringers C3 and C3-R, respectively. Stringer C3-R with hex bolts and epoxy recovered 94% of ultimate load of stringer C3. Effectiveness of stringer C3-R was lower than stringer C2-R because of the tension cracks that developed during testing of stringer C3, as explained in Chapter 5, “Test results and discussion, Test results of original stringers, Specimen C3.” Two tension cracks occurred in stringer C3 as the load increased to failure to 93 kN (21 kips) and 133 kN (30 kips). At failure, a horizontal shear crack was visible in this stringer. Using hex bolts with epoxy did not restore the stiffness of stringers C2-R and C3-R to their original unsplit stiffness.

Specimen C4-R

The load-deflection curve for stringer C4-R, shown in Figure 100, was linear until the stringer cracked in the tension zone. Cracking noise was heard and horizontal sliding was observed at the support face as the load increased to failure. The stringer had cross-grain tension cracks and tension splinters near the midspan at failure, as shown in Figure 101. The repaired ultimate load was 120 kN (27 kips) at a displacement of 67 mm (2.63 in.).

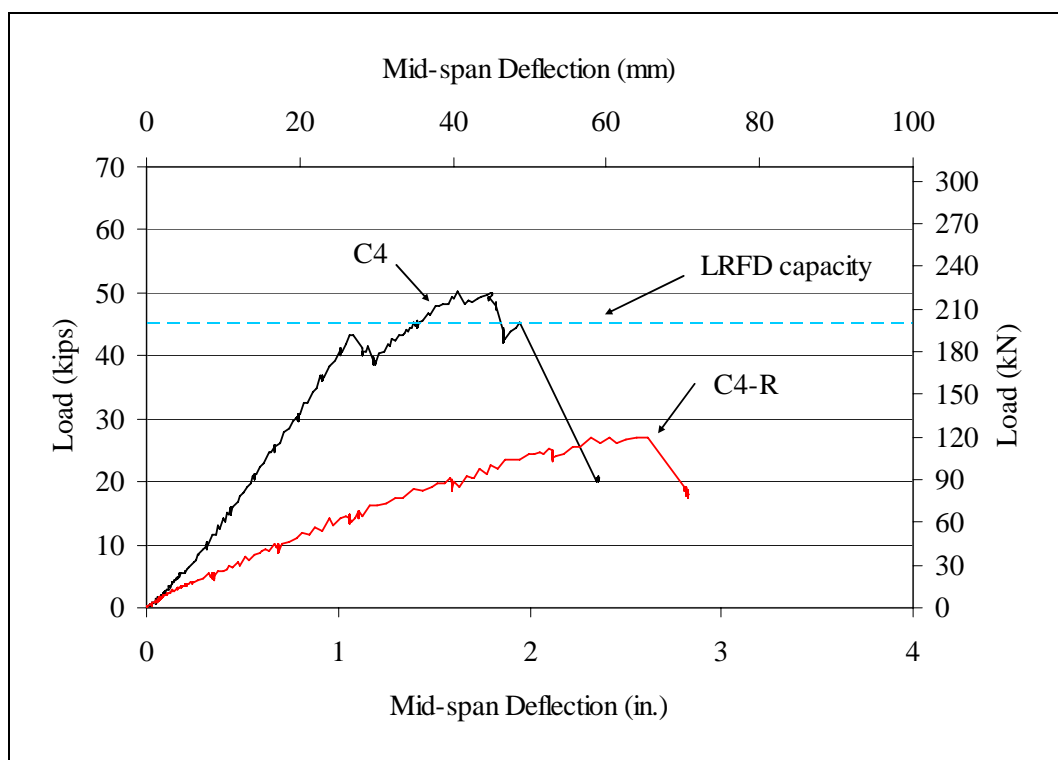


Figure 100. Load-deflection curves for stringers C4 and C4-R.



Figure 101. Cross-grain tension failure and tension splinters at the midspan on stringer C4-R.

The increase in the repaired ultimate load over the unstrengthened post-failure capacity was 35% for repaired stringer C4-R. This value was near the percent increase observed for timber stringer C3-R which was 30.4%. Stringer C4-R was repaired with hex bolts and epoxy at every 305 mm (1 ft). Decreasing the spacing from 605 mm (2 ft) to 305 mm (1 ft) did not significantly improve the repaired ultimate load of the timber stringers. The original and repaired ultimate loads were 222 kN (50 kips) and 121 kN (27 kips) for stringers C4 and C4-R, respectively. This represents 54% recovery in the ultimate load capacity of stringer C4-R. The increase in the unstrengthened postfailure capacity and recovery of the ultimate load was low because of the cross-grain tension cracks that developed in stringer C4 and affected the repair method as compared to the repaired stringer C2-R. Cross-grain tension failure in stringer C4 reduced the recovery of the repair ultimate load on the stringer C4-R, although the unstrengthened postfailure capacity increased by 35% from 89 kN (20 kips) to 121 kN (27 kips). Recovery of the ultimate load with respect to stringer C4 was low for stringer C4-R, and the stiffness of stringer C4-R was not enhanced compared with stringer C4.

Specimen C5-R

The load-deflection curve for stringer C5-R, shown in Figure 102, was linear until the stringer cracked in the tension zone at the midspan. The repaired ultimate load was 120 kN (27 kips) at a displacement of 49 mm (1.93 in.). Horizontal sliding was observed at the support face during this period of deflection.

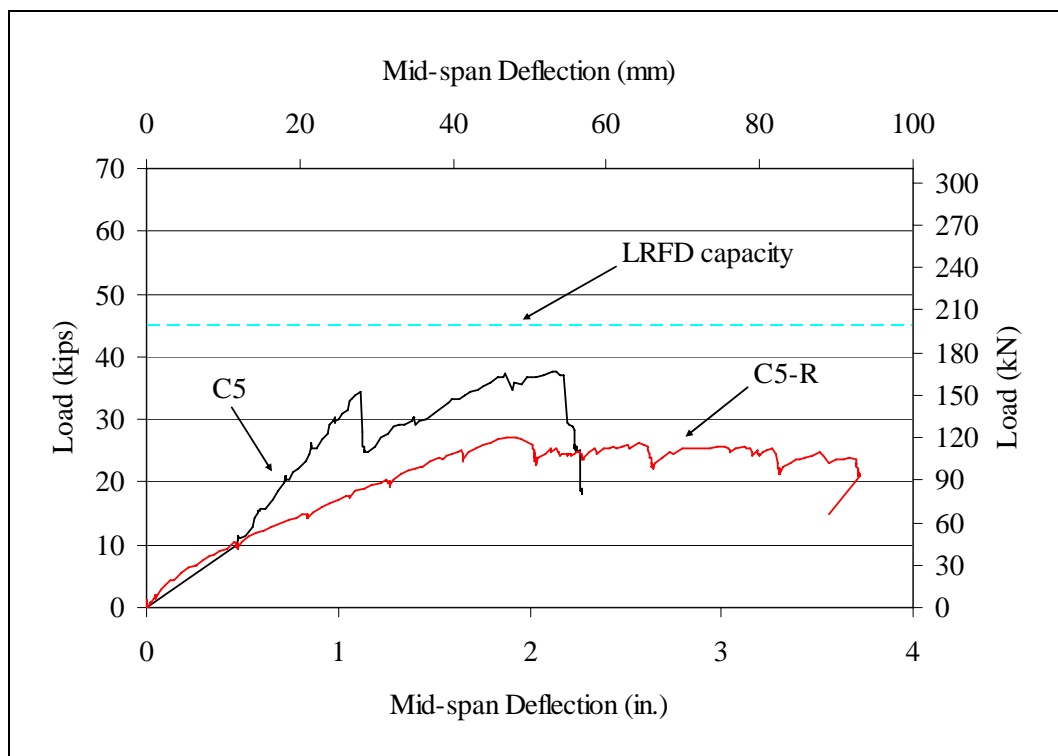


Figure 102. Load-deflection curves for stringers C5 and C5-R.

The increase in the repaired ultimate load over the unstrengthened postfailure capacity was 50% for the repaired stringer C5-R. This increase was greater than that observed in timber stringers C3-R and C4-R and lower than for stringer C2-R. Timber stringer C5 developed horizontal and tension cracks as explained in Chapter 5, “Test results and discussion, Test results of original stringers, Specimen C5.” Stringer C5 was repaired using hex bolts with steel plates. A compression force in the transverse direction was applied using the steel plates at the top and bottom of the stringer which increased the stiffness at the beginning of load-deflection curve until the load reached 45 kN (10 kips). Above 45 kN (10 kips), stiffness of stringer C5-R was again lower than that of stringer C5. The original and repaired ultimate loads were 169 kN (38 kips) and 121 kN (27 kips) for stringers C5 and C5-R, respectively. This was 71% recovery in the ultimate load of stringer C5-R with respect to stringer C5.

Stringers repaired with lag screws

This section presents the test results for the stringers repaired with lag screws. Lag screws were used in several configurations at every 610 mm (2 ft) and 305 mm (1 ft) to repair the timber stringers.

Specimen C6-R

The load-deflection curve for stringer C6-R, shown in Figure 103, was linear until the stringer cracked in the tension zone. Several tension cracks and tension splinters near the midspan were visible, which were caused by excessive deformation. The repaired ultimate load carried by the stringer was 62 kN (14 kips) at a displacement of 90 mm (3.56 in.). As the load increased to failure, horizontal sliding occurred at the support faces. A lag screw spacing of 305 mm (1 ft) was used for stringer C6-R, which resulted in a strength increase over the unstrengthened postfailure capacity of 16.7%. This was a lower increase than the timber stringers repaired with hex bolts and lag screws because of the preexisting end splitting on timber stringer C6. The tension cracks that developed in the tension zone of stringer C6 affected the repair method, as discussed in Chapter 5, “Test results and discussion, Test results of original stringers, Specimen C6.” There was no increase in the slope of the load-deflection curve of timber stringer C6-R. As for stringer C5-R, steel plates could have been utilized on stringer C6-R to apply compressive pressure to close the end splitting gap and to increase the stiffness of split timber stringers.

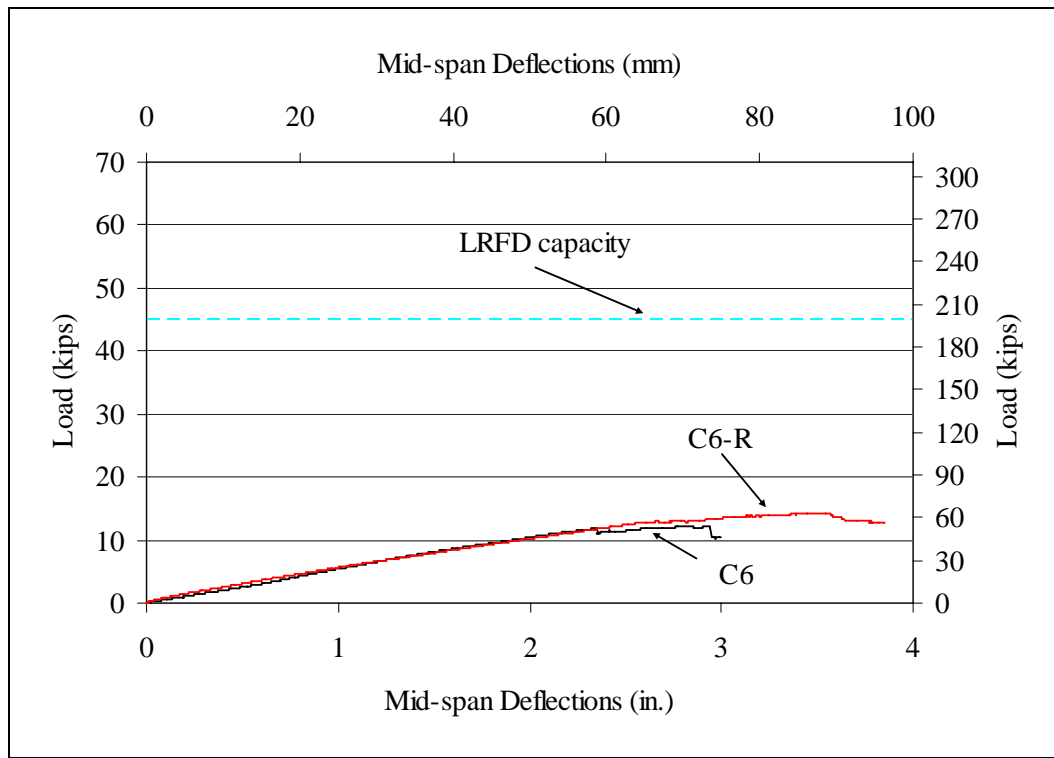


Figure 103. Load-deflection curves for stringers C6 and C6-R.

Specimens C7-R and C10-R

The load-deflection curve for stringer C7-R, seen in Figure 104, was linear until the stringer failed in the tension zone with several tension splinters, which caused a drop in the supported load. The repaired ultimate load at the failure was 138 kN (31 kips) at a displacement of 45 mm (1.77 in.). Horizontal sliding occurred at the support faces as the load approached failure. Stringer C10-R behaved linearly until it reached the ultimate load, as seen in the load-deflection curve shown in Figure 105. As the load increased to failure, horizontal sliding occurred at the support face. The repaired ultimate load resisted by the stringer was 196 kN (44 kips) at a displacement of 51 mm (2.02 in.). The stringer failed in simple tension at 187 kN (42 kips) at a displacement of 58 mm (2.3 in.).

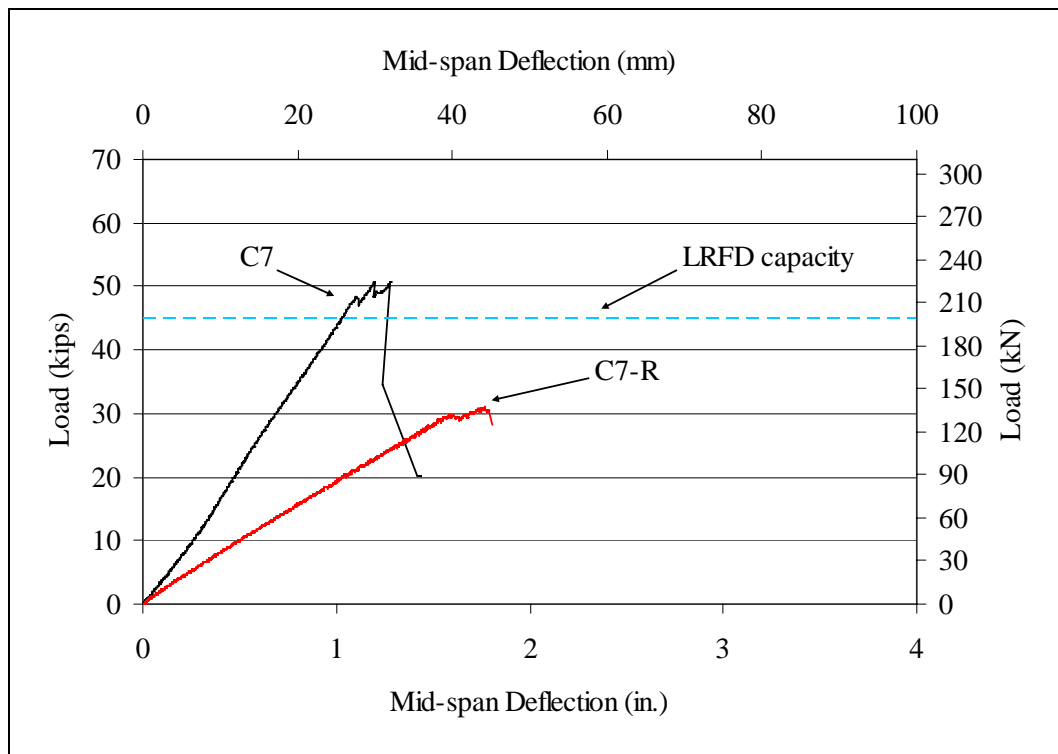


Figure 104. Load-deflection curves for stringers C7 and C7-R.

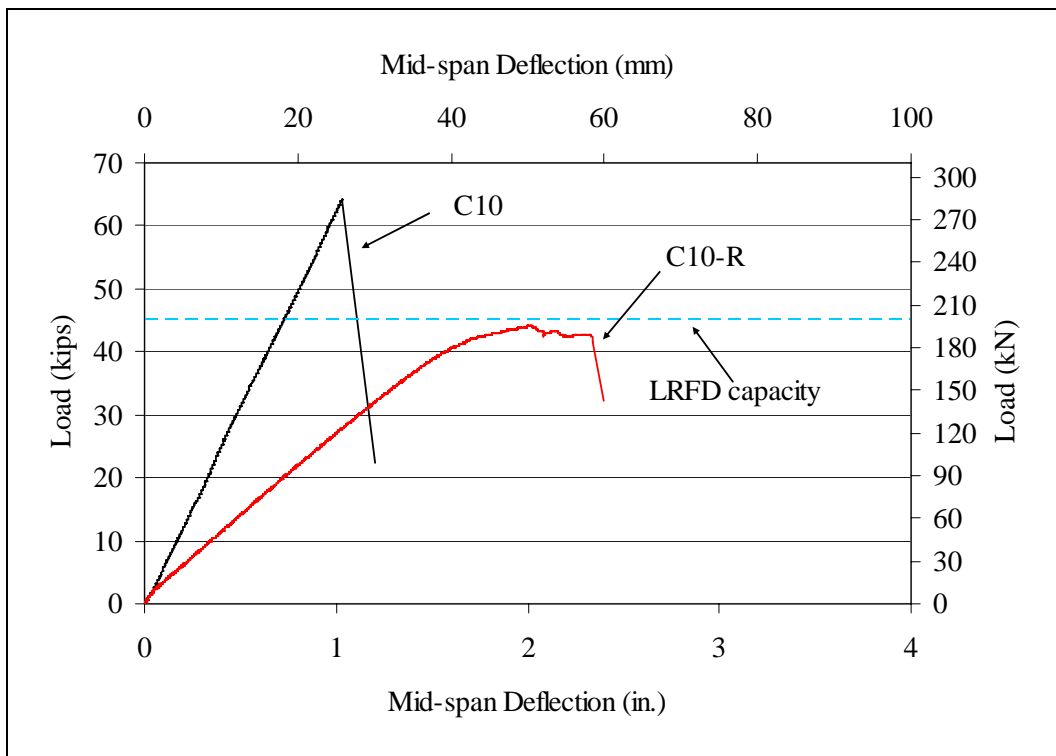


Figure 105. Load-deflection curves for stringers C10 and C10-R.

The increase in the repaired ultimate load over the unstrengthened postfailure capacity was 55% and 100% for stringers C7-R and C10-R, respectively. These stringers were repaired using lag screws making a 45° angle with the transverse direction. Stringers C7 and C10 developed horizontal shear cracks before the repair which made the repair scheme effective. The original and repaired ultimate loads were 227 kN (51 kips) and 138 kN (31 kips) for stringers C7 and C7-R, respectively. This represents a 61% recovery for stringer C7-R, although the increase in unstrengthened postfailure capacity was 55%. The lag screws layout used in stringer C10-R; therefore, produced a more effective repair than the layout used in stringer C7-R.

The original and repaired ultimate loads were 285 kN (64 kips) and 196 kN (44 kips) for stringers C10 and C10-R, respectively. Stringer C10-R recovered 69% of the ultimate load of stringer C10. Using lag screws did not restore the stiffness of stringers C7-R and C10-R to their original unsplit stiffness. Stringers C7-R and C10-R developed tension cracks at failure.

Specimens C11-R and C15-R

Stringer C11-R behaved linearly up to the repaired ultimate load, as seen in the load-deflection curve shown in Figure 106. The stringer developed tension cracks near the midspan at the repaired ultimate load. The repaired ultimate load carried by the stringer was 71 kN (16 kips) at a displacement of 52 mm (2.05 in.). Horizontal sliding occurred at the support faces as the load approached failure.

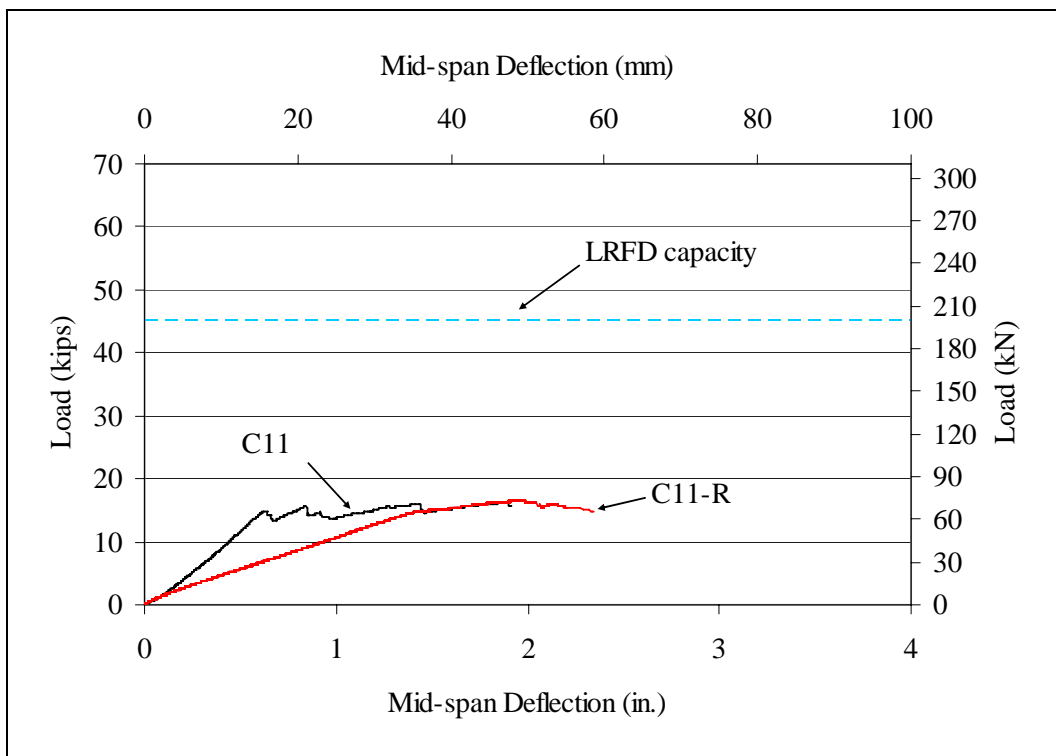


Figure 106. Load-deflection curves for stringers C11 and C11-R.

Stringer C15-R behaved linearly until it reached a load of 93 kN (21 kips), as seen in the load-deflection curve shown in Figure 107. The stringer then cracked in the tension zone causing a small drop in the supported load. The stringer then gained load capacity up to 98 kN (22 kips) where crushing started and the timber cracked again in tension. The stringer failed in tension and developed several cracks and tension splinters at the midspan. The repaired ultimate load was 98 kN (22 kips) at a displacement of 50 mm (1.96 in.).

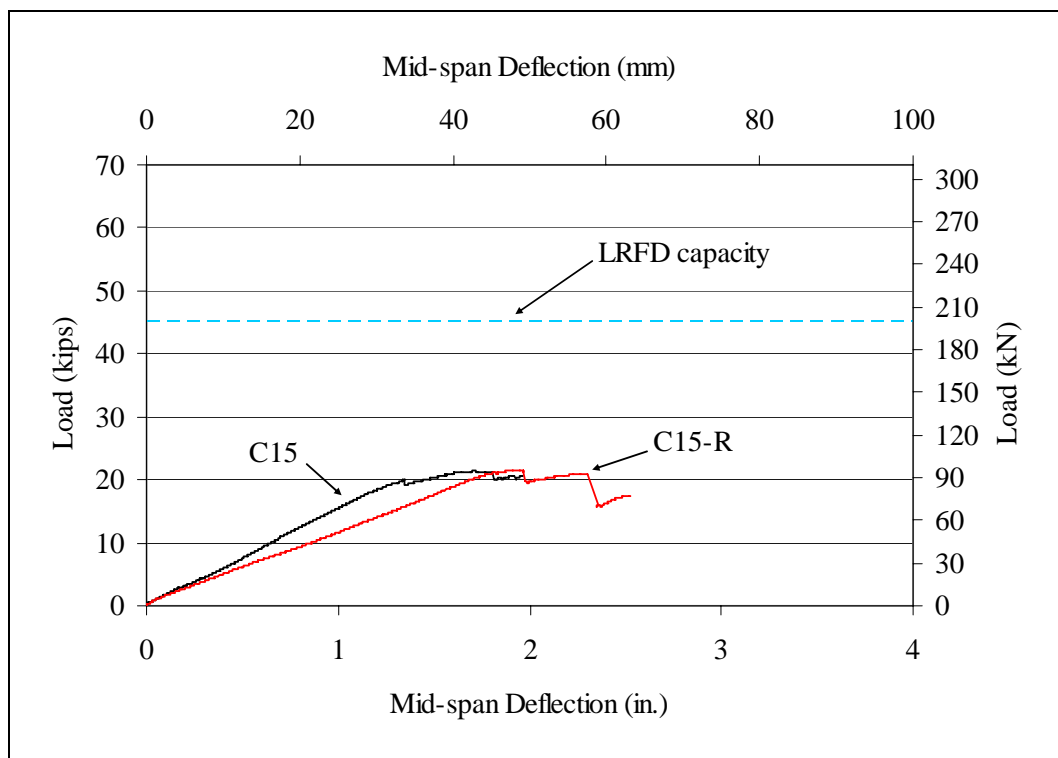


Figure 107. Load-deflection curves for stringers C15 and C15-R.

A lag screw spacing of 610 mm (2 ft) was used to repair stringers C11-R and C15-R. The increase in the repaired ultimate load over the unstrengthened postfailure capacity was 6.3% and 4.8%, which were the lowest values among all of the repaired timber stringers. Stringer C11 was severely deteriorated at one end support before testing, as explained in Chapter 3, “Repair systems for stringers, Timber specimens, Specimen C11,” which caused this lower percent increase in strength for the repaired stringer C11-R. These stringers also had lower stiffness than the original stringers with end split.

Specimen C13-R repaired with plywood side plates

Stringer C13-R behaved linearly until it reached its repaired ultimate load, as seen in the load-deflection curve shown in Figure 108. As the load approached failure, buckling and horizontal cracks occurred in one of the side repair plates, as seen in Figure 109. There was no other damage observed in the plywood side plates. The stringers then failed in the tension zone causing a drop in the supported load. The repaired ultimate load was 142 kN (32 kips) at a displacement of 50 mm (1.95 in.). Tension cracks and splinters occurred at the midspan at failure. Following the test, the plywood side plates were removed and inspected for additional

damage. There was bearing damage at the holes where they were attached and horizontal cracks along the length of the plates.

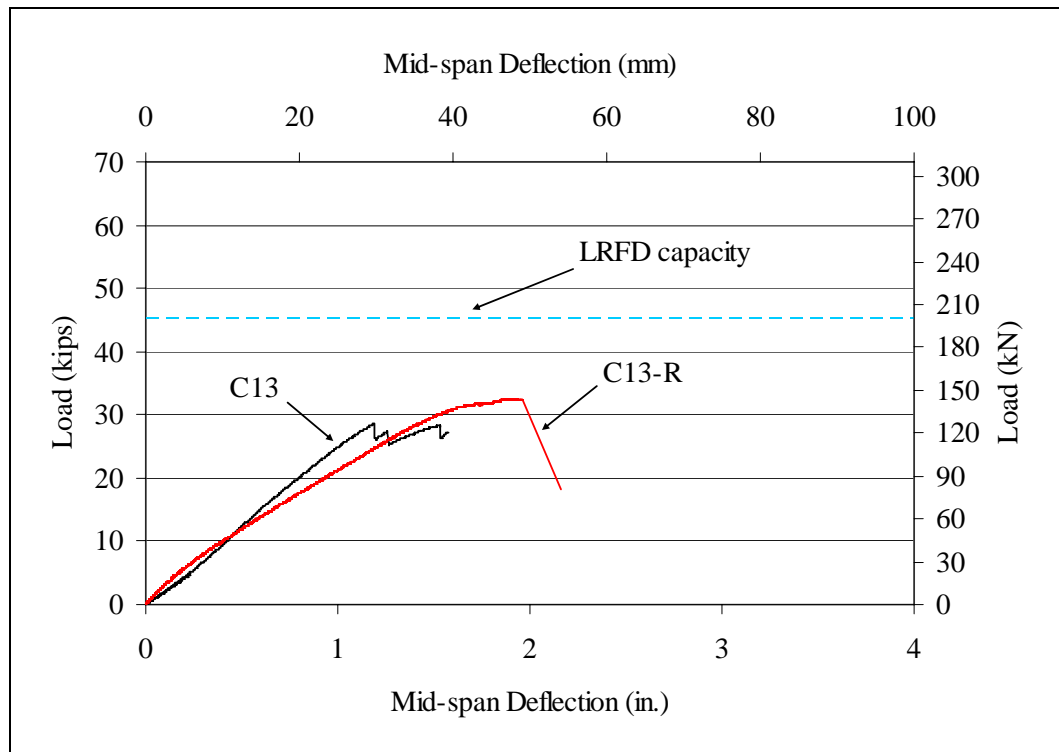


Figure 108. Load-deflection curves for stringers C13 and C13-R.



Figure 109. Buckling of the side plate on stringer C13-R.

Plywood side plates were used to repair stringer C13-R which had severe end splitting prior to testing. The increase in the repaired ultimate load over the unstrengthened postfailure capacity of the stringer was 14.3%, which was higher than the stringers repaired with lag screws. The stiffness of the repaired stringer was higher than that of stringer C13 up to a load of 45 kN (10 kips), as shown in Figure 108. The plywood plates developed bearing damage at the holes where they were attached, horizontal cracks along the length of the plywood plates, and several horizontal surface cracks along their lengths.

Stringers repaired with FRP side plates or FRP strip

FRP plates were used along the shear spans to repair the timber stringers in shear. They were attached to the sides of the stringers using mechanical fasteners. Two stringers were repaired with FRP side plates. One stringer was repaired with a side plate and an FRP strip at the tension zone since the stringer had cross-grain tension cracks at the midspan.

Specimens C14-R and C16-R

The load-deflection curve for stringer C14-R, shown in Figure 110, was linear until the stringer reached a load of 182 kN (41 kips). As the load approached ultimate failure load, horizontal sliding occurred at the support face. The repaired ultimate load was 196 kN (44 kips) at a displacement of 57 mm (2.24 in.). The stringer underwent a deflection of 23 mm (0.9 in.) without any increase in load capacity after the stringer reached the repaired ultimate load. The stringer developed tension cracks and compression failure at a load of 187 kN (42 kips) and a displacement of 74 mm (2.92 in.) causing a drop in the load capacity. The compression failure is shown in Figure 111. The experiment was terminated at this point due to excessive deformation. The side plates had minor bearing damage at the holes where they were attached, as seen in Figure 112.

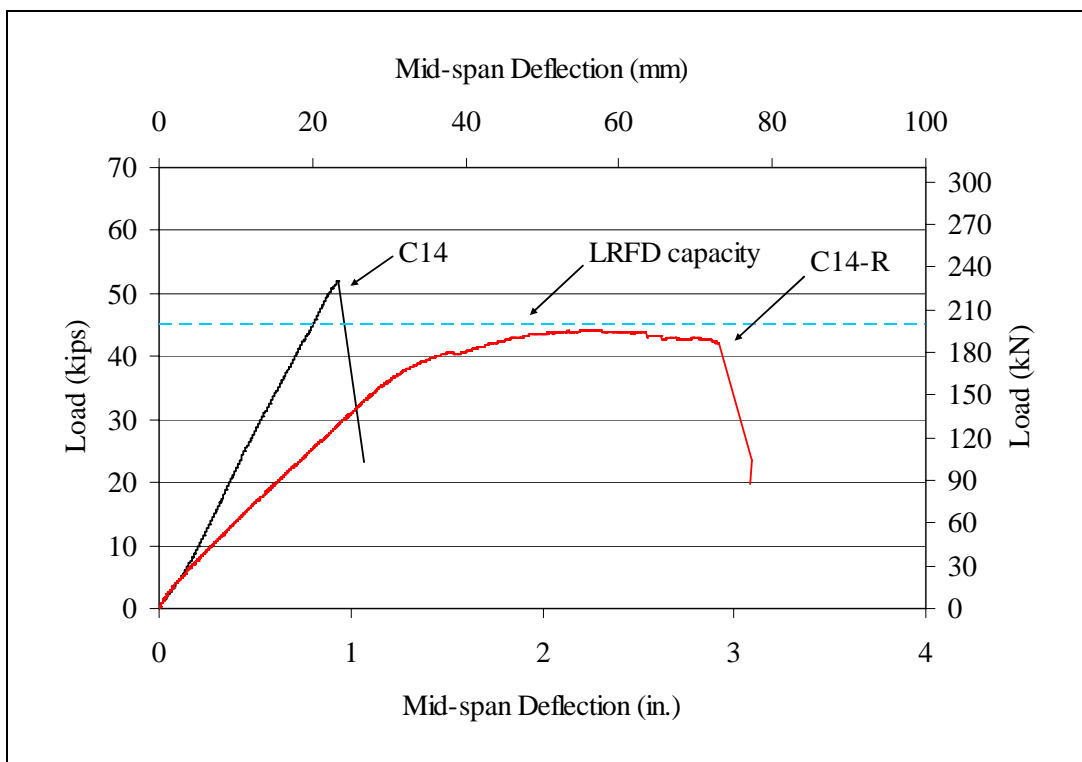


Figure 110. Load-deflection curves for stringers C14 and C14-R.



Figure 111. Compression failures due to excessive deformations on stringer C14-R.



Figure 112. Minor bearing damages at the holes on FRP plates.

The load-deflection curve for stringer C16-R, shown in Figure 113, was up to a load of 111 kN (25 kips). The stringer developed tension cracks and splinters within the tension zone at failure. The repaired ultimate load was 120 kN (27 kips) at a displacement of 80 mm (3.15 in.). Horizontal sliding occurred at the support faces as the load approached failure. There was no visible damage on the FRP side plates, except for minor local buckling problems.

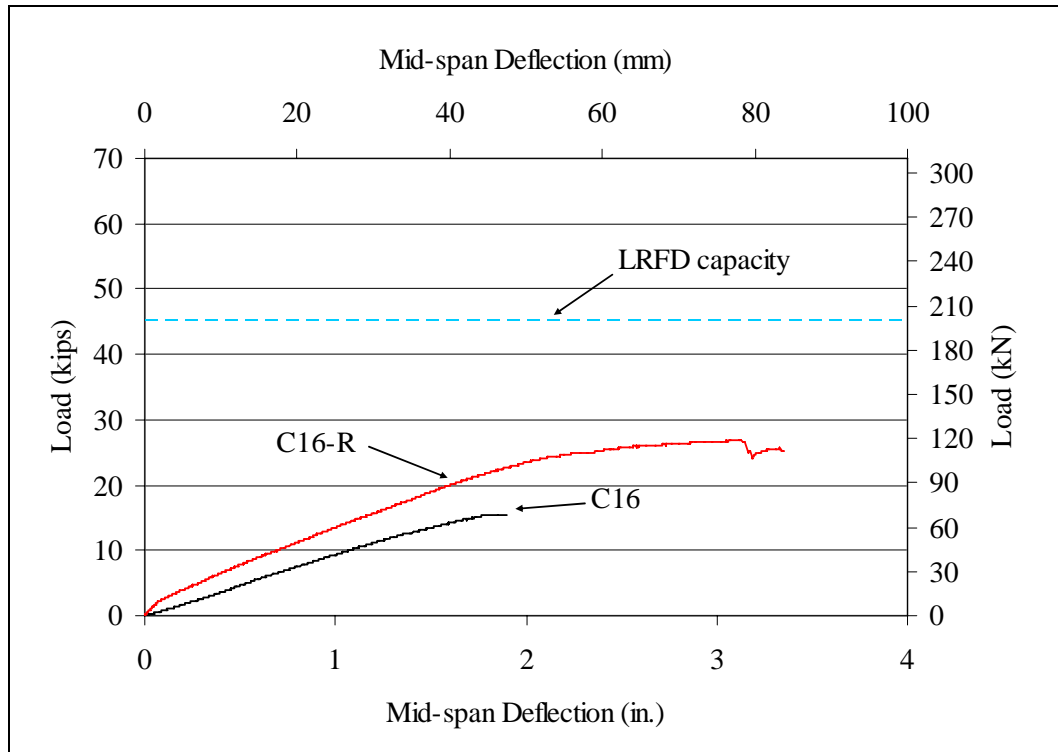


Figure 113. Load-deflection curves for stringers C16 and C16-R.

Timber stringer C14-R was repaired using FRP side plates. The increase in the repaired ultimate load over the unstrengthened postfailure capacity was 91%. This repair method was more effective. It yielded 18.6% higher strength than stringer C2-R repaired with hex bolts, but 9% lower strength than stringer C10-R repaired with lag screws. Stringer C14 developed a horizontal shear crack at failure, as explained in Chapter 5, “Test results and discussion, Test results of original stringers, Specimen C14.” Stiffness of the repaired stringer C14-R, shown in Figure 110, was also below the stiffness of stringer C14, as the other repaired stringers.

Timber stringer C16-R had existing end splitting before testing, and it was repaired using FRP side plates. The increase in the repaired ultimate load over the unstrengthened postfailure capacity was 80%, and a higher stiffness was provided by the repair, as shown in Figure 113. The FRP plates provided higher increase in the repaired ultimate load and stiffness. Therefore, it was feasible to use FRP side plates to enhance the load behavior of the timber stringers with end splitting when compared with repairing with hex bolts or lag screws. The FRP side plates also did not develop major damage except minor bearing damage where lag screws were installed.

Specimen C12-R

The load-deflection curve for stringer C12-R, shown in Figure 111, was linear until a small drop occurred in the load carrying capacity at 147 kN (33 kips). There were no visible cracks at this point. The load increased further until the stringer failed in horizontal shear, causing a drop in the load carrying capacity. The repaired ultimate load was 151 kN (34 kips) at a displacement of 42 mm (1.66 in.).

Stringer C12-R had an FRP strip attached to the tension zone using lag screws. Flexural reinforcement was used along with the lag screws because stringer C12 developed a cross-grain tension failure. The increase in the repaired ultimate load over the unstrengthened postfailure capacity for the repaired stringer was 17.2%. The original and repaired ultimate loads were 196 kN (44 kips) and 151 kN (34 kips) for stringers C12 and C12-R, respectively. This represents a 77% recovery in the ultimate load of stringer C12-R. The stiffness of the timber stringer was lower than that of stringer C12-R, as seen Figure 114. The repaired stringer had a horizontal

shear crack at failure. However, the horizontal shear failure was not entirely across the width of the cross section, as shown in Figure 115.

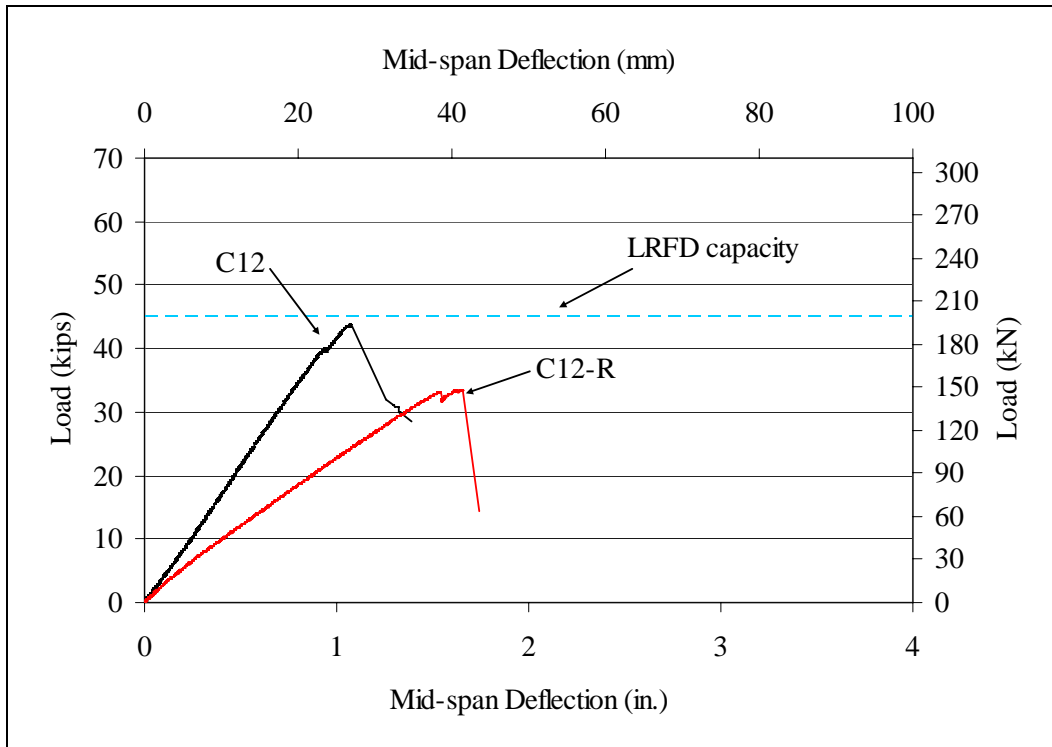


Figure 114. Load-deflection curves for stringers C12 and C12-R.



Figure 115. Horizontal shear crack after the failure of stringer C12-R.

Overall discussion

Timber stringers which had signs of checking tended to fail in shear in the parallel-to-grain direction. These horizontal shear failures were very sudden and horizontal sliding occurred at the support faces. The average horizontal shear strength for the tested timber stringers with checks was 2.08 MPa (0.30 ksi). The LRFD manual reference shear strength value for dense select structural southern pine was 2.21 MPa (0.32 ksi), which is close to that observed value in the tests (AFPA 1996). The bending stress for stringers with checks was 7% higher than the bending design values provided in the LRFD manual (AFPA 1996). The average bending stress for stringers with checks at ultimate load was 33 MPa (4.78 ksi). LRFD reference bending strength value for dense select structural southern pine is 30.7 MPa (4.45 ksi) (AFPA 1996). Local tension cracks caused small irregularities in the load-deflection behavior shortly before the failure of the stringers in horizontal shear.

End splitting reduced the experimental shear and bending strength values 64% and 59% below the design values, respectively. These stringers should be replaced or retrofitted with an appropriate repair method, FRP or plywood side plates. The average bending strength of these stringers was 12.64 MPa (1.83 ksi), which was less than one-third of the LRFD reference bending strength value of 30.7 MPa (4.45 ksi) for dense select structural southern pine (AFPA 1996). Horizontal shear stress at the unstrengthened postfailure load ranged between 1.26 MPa (0.18 ksi) and 0.56 MPa (0.08 ksi) for stringers with end splits. The average shear stress at the unstrengthened postfailure load was 0.80 MPa (0.12 ksi) which was also below the LRFD reference shear strength value of 2.21 MPa (0.32 ksi) for dense select structural southern pine by 64 percent (AFPA 1996).

The test results showed that using hex bolts, lag screws, and FRP side plates are effective methods for increasing the shear capacity of the split timber stringers. However, the repaired timber stringers had lower stiffness than the unsplit stringer stiffness. Timber stringers in-service for decades should be inspected prior to applying repair methods because types and magnitude of existing damage greatly impacts the effectiveness of the repair method, such as seen in the tests on timber stringers with end splitting (C6, C8, C9, C11, C13, C16).

Repair methods for stringers with end splitting should close the end splitting gap by applying transverse pressure or by utilizing adhesives. It is

important to consider existing cracks, checks, splits, and knots in the selection of a repair method. Hex bolts and lag screws, therefore, were not good options to increase the strength and stiffness for stringers with end splitting. The average increase in the repaired ultimate load over the unstrengthened postfailure capacity was 9.3% when lag screws were used. It was 14.3% when plywood side plates were used. FRP side plates, however, provided 80% increase in the unstrengthened postfailure capacity of split stringer because of the higher stiffness of the side plates. FRP side plates prevented horizontal sliding and increased the stiffness of stringers with end splits. There was no visible damage on FRP plates, except for minor bearing damage where the lag screws were inserted.

Hex bolts installed with epoxy at every 610 mm (2 ft) provided 51.4% average increase in the repaired ultimate load over unstrengthened postfailure capacity. The increase in strength over the unstrengthened postfailure capacity was only 35% when the hex bolts were spaced at every 305 mm (1 ft). Increasing the number of hex bolts did not improve the effectiveness. Steel plates with the same 610 mm (2 ft) spacing provided a 50% increase in the repaired ultimate load capacity over the unstrengthened postfailure capacity. The increase in the repaired ultimate load over the unstrengthened postfailure capacity was 55% for lag screws used with an angle of 135° in counter-clockwise direction from timber grain. The increase in the repaired ultimate load over the unstrengthened postfailure capacity was 100% for lag screws installed at an angle of 45° in counter-clockwise direction from timber grain. Lag screws with a 45° angle resisted the sliding of the top layer, whereas lag screws in a stringer with a 135° did not resist as much horizontal sliding because of the closer angle to the sliding plane and grain direction. FRP side plates were effective in repairing timber stringers. The increase in the repaired ultimate load over the unstrengthened postfailure capacity was 91%.

Repair methods tested in this study provided satisfactory results. However, in situ application of side plates to sides of the timber members presents problems. The close spacing of the timber stringers in many bridge applications prevents access to the sides of the stringers. Only the outer face of the outer members would be readily accessible, while the interior members would only be reachable by removing the outer stringers. The in situ application of reinforced side plates is, therefore, not very feasible. Hex bolts with epoxy or lag screws can be applied without removal of the stringers from service, as only the lower or upper surface

must be accessed for insertion of the reinforcement. Ties will dictate spacing if the bolts or lag screws are inserted from the top. Using hex bolts or lag screws for shear repair reduces the amount of work required in the field. It has been shown in this study that the application of hex bolts with epoxy and lag screws can overcome horizontal shear damage, and this approach should be further developed to determine the ultimate potential as an in-service repair approach for timber transportation infrastructure.

6 Summary and Conclusions

The majority of timber bridges in the United States are nearing the end of their service life. Most timber bridges exhibit several types of damage, which occurs mostly in structural elements such as timber stringers. The most commonly encountered damage type in timber bridge stringers is horizontal splits. This splitting is caused by shear stresses, and it severely impacts the flexural capacity of the timber stringers. This study examined the feasibility of repairing timber stringers that show signs of horizontal splitting along the length of the member. It was proven that the methods examined in this study are feasible to repair timber stringers.

Summary of study

Within the scope of this study, timber stringer damage types were reviewed with particular attention to horizontal splits along the span. The reasons contributing to these types of failure were studied. Timber stringers that were recently in service were examined to understand effects of type of damage on the effectiveness of repair methods.

Hex bolts, lag screws, and plywood and FRP side plates were used as repair methods. Calculations to predict the number of fasteners assumed a lengthwise separation along the neutral axis.

Timber stringers were subjected to four-point bending to experimentally evaluate the proposed repair methods. Fifteen stringers were repaired with different methods with few repeats. Hex bolts and lag screws were installed in several configurations and spacings to repair the timber stringers. Plywood and FRP plates were attached to the sides of the timber stringers using lag screws.

Timber stringers that did not have horizontal splits but had checks along the length were tested to shear failure to determine unstrengthened post-failure capacity. The repair methods were then applied. Timber stringers that already had horizontal splits were tested to find the unstrengthened postfailure capacity. All of the stringers were tested to failure, after installation of a repair method, to determine the effectiveness of the method. The effectiveness of a repair method was determined by

comparing the unstrengthened postfailure capacity of original stringer to ultimate strength of repaired stringer.

Conclusions

This study showed that hex bolts, lag screws, and plywood and FRP side plates can be effective in increasing the shear capacity of split timber stringers. Based on the limited number of specimens, it is appropriate to determine trends rather than concentrating on specific values. The specific findings of this study are as follows:

1. Timber stringers that exhibited signs of checking tended to fail in shear in the parallel-to-grain direction. Failure was sudden, and horizontal sliding occurred later on the support face.
2. Horizontal shear strength of timber stringers with checks was within 6% of the LRFD reference shear strength value for dense select structural southern pine (AFPA 1996).
3. Bending stresses for timber stringers with checks were within 7% of the LRFD reference bending strength value for dense select structural southern pine (AFPA 1996).
4. Shear and bending strength values for timber stringers with end splitting were less than one-third of the LRFD reference strength values for dense select structural southern pine (AFPA 1996). An average value for the bending strength of these stringers was 12.64 MPa (1.83 ksi), which was less than one-third of the LRFD reference bending strength value of 30.7 MPa (4.45 ksi) for dense select structural southern pine (AFPA 1996). The average shear stress at unstrengthened postfailure load was 0.80 MPa (0.12 ksi), which was also below the LRFD reference shear strength value of 2.21 MPa (0.32 ksi) for dense select structural southern pine (AFPA 1996).
5. All but one of the repaired timber stringers had lower stiffness than the unsplit stringer stiffness.
6. It is important to consider the amount and extent of the existing cracks, checks, splits, and knots in the selection of a repair method.
7. Lag screws and plywood side plates were not good options for improving either strength or stiffness of stringers with end splitting. The average increase in the repaired ultimate load over the unstrengthened postfailure load was one-tenth.
8. FRP side plates provided a four-fifths increase in the unstrengthened postfailure capacity of timber stringers with end splits.
9. Using a larger number of hex bolts did not improve the effectiveness of the repair method over using the calculated number of bolts. Hex bolts with

epoxy placed at every 610 mm (2 ft) provided an increase in the repaired ultimate load of an additional one-half over the unstrengthened postfailure capacity. The repaired ultimate load was increased only an additional one-third of the unstrengthened postfailure capacity with the hex bolts spaced at every 305 mm (1 ft). Steel plates with the same spacing, however, provided an increase of one-half over the unstrengthened postfailure capacity.

10. Lag screws installed at a 45° angle with timber grain direction are more effective than lag screws installed vertically. The repaired ultimate load was increased only an additional one-half of the unstrengthened postfailure capacity with the lag screws installed at an angle of 135° in counter-clockwise direction from timber grain. The repaired ultimate load was double the unstrengthened postfailure capacity with the lag screws installed at an angle of 45° in counter-clockwise direction to the timber grain direction.
11. FRP plates attached to the sides of timber stringers were effective in repairing the timber stringers. The repaired ultimate load was increased by 90% over the unstrengthened postfailure capacity.

It is feasible to use hex bolts, lag screws, and plywood and FRP side plates to repair timber bridge stringers in shear. Timber stringers with checks along their lengths can be repaired by utilizing any of these methods. Stringers with severe end splitting, however, should be repaired with FRP side plates.

Recommendations for future studies

In order to achieve full understanding of the structural behavior of repaired timber stringers, further work is recommended in the following areas:

1. Extensively investigate use of hex bolts with epoxy and lag screws in timber stringers as shear reinforcement.
2. Investigate attaching FRP side plates with lag screws and adhesives.
3. Develop higher order mathematical models for shear repair for timber stringers.
4. Evaluate the behavior of repaired timber stringers under cyclic and dynamic loading.
5. Develop techniques for both shear and flexural strengthening of timber stringers.
6. Conduct a cost study of the different effective repair methods.

References

AFPA. 1996. *Standard for load and resistance factor design (LRFD) for engineered wood construction*. Washington, DC: The American Forest and Paper Association and ASCE.

ASTM D 143. 1999. *Standard methods of testing small clear specimens of timber*. West Conshohocken, PA: American Society for Testing and Materials.

ASTM D 198. 1999. *Standard test methods of static test of lumber in structural sizes*. West Conshohocken, PA: American Society for Testing and Materials.

Avent, R. R. 1985. Decay, weathering and epoxy repair of timber. *Journal of Structural Engineering* 111(2):328-342.

Avent, R. R. 1986. Design criteria for epoxy repair of timber structures. *Journal of Structural Engineering* 112(2):222-240.

Biblis, E. J. 1965. Analysis of wood-fiberglass composite beams within and beyond the elastic region. *Forest Product Journal* 15(2):81-88.

Bodig, J., and Jayne, B. A. 1982. *Mechanics of wood and wood composites*. New York: Van Nostrand Reinhold Company, Inc.

Bohannan, B. 1962. Prestressed wood members. *Forest Products Journal* 12(12):596-602.

Bulleit, W. M., Sandberg, L. B., and Woods, G. J. 1989. Steel-reinforced glued laminated timber. *Journal of Structural Engineering* 115(2):433-444.

Chamarthy, R., and GangaRao, H. 2003. Composite repair wrapping of used wooden railroad crossties with composite fabrics. *SAMPE Journal* 39(3):25-33.

Chen, Y., and Balaguru, P. N. 2002. Fiber reinforced polymers (FRP) for strengthening timber beams. In *Proceedings, 47th international SAMPE Symposium and Exhibition, 12-16 May*, 47:680-690.

Code, C. J. 1963. Anti-Splitting Devices. *Railway Track and Structures* 10:32-34.

Cofer, W. F., Proctor, F. D., and McLean, D. I. 1997. Prediction of the shear strength of wood beams using finite element analysis. In *Proceeding, American Society of Mechanical Engineers* 77:69-78. Evanston, IL.

Coleman, G. E., and Hurst, H. T. 1974. Timber structures reinforced with light gage steel. *Forest Product Journal* 24(7):45-53.

Davalos, J. F., Zipfel, M. G., and Qiao, P. 1999. Feasibility Study of Prototype GFRP-Reinforced Wood Railroad Crosstie. *Journal of Composites for Construction* 3(2): 92-100.

Dorey, A. B., and Cheng J. J. R. 1996. The behavior of GFRP glued laminated timber beams. In Proceedings, *2nd International Conference Advanced Composite Materials in Bridges and Structures*, 11-14 August, Montreal, Canada, ed. M.M. El-Badry. 1:787-794. Montreal, Canada: Canadian Society for Civil Engineering.

Ebeling, W. D., and Fellow, F. 1990. Repair and rehabilitation of heavy timber trusses. *Journal of Performance of Constructed Facilities* 4(4):242-258.

Ehsani, M., Larsen, M., and Palmer, N. 2004. FRP laminates and epoxy help support new loads in an existing wooden gymnasium. *Structure Magazine* 11(2):19-21.

Falk, R. H., and Green, D. 1999. Stress grading of recycled lumber and timber. *Structures Congress-Proceedings*, 18-21 April, 1:650-653, New Orleans, LA: Structural Engineering in the 21 Century.

Falk, R. H., Green, D., Rammer, D., and Lantz S. F. 2000. Engineering Evaluation of 55-Year-Old Timber Columns Recycled From An Industrial Military Building. *Forest Product Journal* 50(4):71-76.

Foschi, R. O., and Barrett, J. D. 1976. Longitudinal shear strength of Douglas-fir. *Canadian Journal of Civil Engineering* 3(2):198-208.

Gentile, C., Svecova, D., and Rizkalla, S. H. 2002. Timber beams strengthened with GFRP bars: development and applications. *Journal of Composites for Construction* 6(1): 11-20.

Gilfillan, J. R., Gilbert, S. G., and Patrick, G. R. H. 2003. The use of FRP composites in enhancing the structural behavior of timber beams. *Journal of Reinforced Plastics and Composites* 22(15):1373-1388.

Green, D. W., Falk, R. H., and Lantz, S. F. 2001. Effect of heart checks on flexural properties of reclaimed 6 by 8 Douglas-fir timbers. *Forest Products Journal* 51(7-8):82-88.

Higgins, A. C. 1970. Veneer caps – new way to stop splitting in timbers. *Railway Track and Structures* 66(1):31.

Johns, K. C., and Lacroix, S. 2000. Composite reinforcement of timber in bending. *Canadian Journal of Civil Engineering* 27(5):899-906.

Keenan, F. J. 1974. Shear strength of wood beams. *Forest Products Journal* 24(9):63-70.

Lam, F., Yee, H., and Barrett, J. D. 1997. Shear strength of Canadian softwood structural lumber. *Canadian Journal of Civil Engineering* 24(3):419-430.

Lantos, G. 1970. The flexural behavior of steel reinforced laminated timber beams. *Wood Science Journal* 2(3):136-143.

Longworth, J. 1977. Longitudinal shear strength of timber beams. *Forest Products Journal* 27(8):19-23.

Mark, R. 1961. Wood-aluminum beams within and beyond the elastic range. Part I: rectangular sections. *Forest Product Journal* 11(10):477-484.

Mark, R. 1963. Wood-aluminum beams within and beyond the elastic range. Part II: trapezoidal sections. *Forest Product Journal* 13(11):508-516.

Moulin, J. M., Pluvinage, G., and Jodin, P. 1990. FGRG: fiberglass reinforced gluelam – a new composite. *Wood Science and Technology* 24:289-294.

Murphy, J. F. 1979. Strength of wood beams with end splits. *USDA Forest Service Research Paper FPL (Forest Product Laboratory)* (347):12.

National Bridge Inventory (NBI) 2005. Material type of structure by state. U.S. Department of Transportation, Federal Highway Administration Web Site. <http://www.fhwa.dot.gov/bridge/material.htm> (accessed March 2005, Last Updated February 2005).

Ou, F. L., and Weller, C. 1986. An overview of timber bridges. *Transportation Research Record* 1053.

Peterson, J. 1965. Wood beams prestressed with bonded tension elements. *Journal of Structural Engineering* 91(1):103-119.

Plevris, N., and Triantafillou, T. C. 1992. FRP-reinforced wood as structural material. *Journal of Materials* 4(3).

Plevris, N., and Triantafillou, T. C. 1995. Creep behavior of FRP-reinforced wood members. *Journal of Structural Engineering* 121(2).

Qiao, P., Davalos, J. F., and Zipfel, M. G. 1998. Modeling and optimal design of composite-reinforced wood railroad crosstie. *Composite Structures* 41(1):87-96.

Radford, D. W., Van Goethem, D., Gutkowski, R. M., and Peterson, M. L. 2002. Composite repair of timber structures. *Construction and Building Materials* 16(7):417-425.

Rammer, D. R. 1999. Evaluation of recycled timber members. *Materials and Construction, Proceedings of the Fifth ASCE Materials Engineering Congress (May)*:46-51. Reston, VA: American Society of Civil Engineers.

Rammer, D. R., and Lebow, P. K. 1997. Shear strength of solid-sawn Douglas-fir beams. *Journal of Materials in Civil Engineering* 9(3):130-138.

Rammer, D. R., and McLean, D. I. 1996. Shear strength of wood beams. *National Conference on Wood Transportation Structures*, 168-177, Madison.

Rammer, D. R., McLean, D. I., and Cofer, W. F. 1998. In-place shear strength of wood beams. *5th World Conference on Timber Engineering*, 17-20 August, Vol 1. Montreux, Switzerland.

Rowlands, R. E., Van Deweghe, R. P., Laufenberg, T. L., and Krueger, G. P. 1986. Fiber-reinforced wood composites. *Wood and Fiber Science*, 18(1):39-57.

Saucier, J. R., and Holman, J. A. 1975. Structural particleboard reinforced with glassfiber-progress in its development. *Forest Products Journal*, 25(9):69-72.

Sliker, A. 1962. Reinforced wood laminated beams. *Forest Products Journal*, 12(1):91-96.

Soltis, L. A., Ross, R. J., and Windorski, D. F. 1998. Fiberglass-reinforced bolted wood connections. *Forest Products Journal* 48(9):63-67.

Sonti, S. S., and GangaRao, H. V. S. 1996. Banding timber crossties using composite fabrics for improving their performance. *Materials for the new Millennium; Proceedings of the Fourth Materials Engineering Conference, 10-14 November, 2:1449-1457*. Washington, D.C.

Sonti, S. S., Davalos, F. J., Zipfel M. G., and GangaRao H. V. S. 1995. A Review of Wood Crosstie Performance. *Forest Products Journal* 45(9):55-58.

Sonti, S. S., Davalos, J. F., Hernandez, R., Moody, R. C., and Kim, Y. 1995. Laminated wood beams reinforced with pultruded fiber-reinforced plastics. *50th Annual Conference, January*, The Society of the Plastic Industry, Inc. 10(B):1-5.

Spaun, F. D. 1981. Reinforcement of wood with fiberglass. *Forest Product Journal* 31(4):26-33.

Svecova, D., and Eden, R. J. 2004. Flexural and Shear Strengthening of Timber Beams Using Glass Fiber Reinforced Polymer Bars-An Experimental Investigation. *Canadian Journal of Engineering* 31(1):45-55.

Theakston, F. H. 1965. A Feasibility Study for Strengthening Timber Beams with Fiberglass. *Canadian Agricultural Engineering* (1):17-19.

Triantafillou, T. C. 1997. Shear reinforcement of wood using FRP materials. *Journal of Materials in Civil Engineering* 9(2):65-69.

Triantafillou, T. C., and Deskovic, N. 1992. Prestressed FRP sheets as external reinforcement of wood members. *Journal of Structural Engineering* 118(5):1270-1284.

Triantafillou, T. C. 1998. Composites: a new possibility for the shear strengthening of concrete, masonry and wood. *Composites Science and Technology* 58:1285-1295.

Higgins. 1970. Veneer caps, new way to stop rail splitting in timbers. *Railway Track and Structures* 66(1).

Wipf, T. J., Ritter, M. A. and Wood, D. L. 2000. Evaluation and field load testing of timber railroad bridge. *Transportation Research Record* 1(1696):323-333.

Zaboklicki, A., and Gebski, M. 1997. Continuity of wooden beams as a method of reinforcement and preservation of timber structures at monumental buildings. *Structural Studies Repairs and Maintenance of Historical Buildings* 541-546.

Appendix A: Structural Analysis of Timber Stringers

Moment and shear diagrams, cross section properties, shear and bending stresses calculations are presented in this appendix.

Moment and shear diagrams

All stringers that were tested on a span of 4.2 m (13.6 ft) with 2 equal loads applied symmetrically at a distance of 457 mm (18 in.) from the centerline, to create a zone of constant moment (M) and shear (V) in the stringer, as shown in Figure A1. The maximum shear was equal to one-half of the applied load along the shear span. Shear forces in the stringer under the spreader beam had a value of zero. Bending moment, however, was a constant and maximum along the spreader beam.

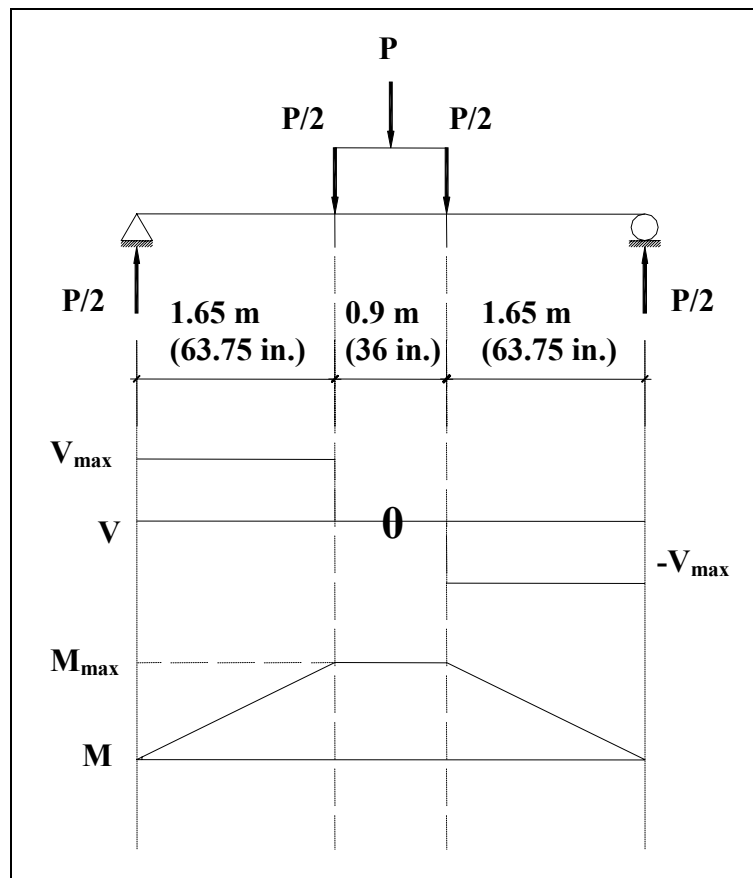


Figure A1. Moment and shear diagrams for timber stringers.

Cross-section properties

Width (w) and height (h) of the tested timber stringers were 191 mm (7.5 in.) and 406 mm (16 in.) respectively, as shown in Figure A2. Area of the stringers was 775.46 cm² (120 in.²).

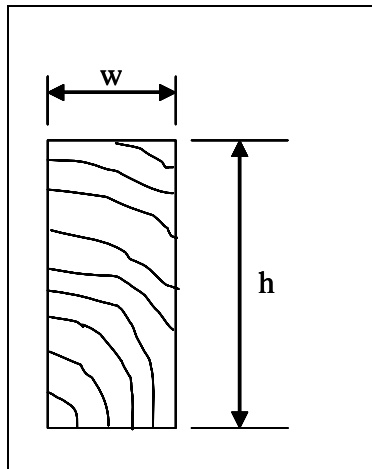


Figure A2. Schematic of cross section of a timber stringer.

The moment of inertia and the section modulus of the cross section was mm⁴ (2560 in.⁴) and mm³ (320 in.³), respectively. Moment of inertia and shear modulus was computed using equations A1 and A2:

$$I_x = \frac{1}{12} \times w \times h^3 \quad (A1)$$

and

$$S_x = \frac{I_x}{(h/2)} \quad (A2)$$

where

I_x = moment of inertia, in strong axes

w = width of the timber stringers

h = depth of the timber stringers

S_x = section modulus of timber stringers.

Shear strength of timber stringers

AFPA (1996) was used to compute the maximum shear stresses at failure and the force on the cross section of timber stringers. The maximum shear force and shear stress at failure on the cross section of the timber stringers was calculated using equation A3:

$$V' = \frac{2}{3} \cdot F'_V \cdot t \cdot w \quad (A3)$$

where

V' = Adjusted shear resistance of a flexural member

F'_V = Adjusted horizontal shear strength

t = Width

w = Depth

The adjusted horizontal shear strength was computed as using equation A4. Reference shear strength parallel-to-grain direction (F_V) for southern pine was 2.21 MPa (0.32 ksi). Since the aim was to find the ultimate capacity of the cross section in shear, adjustment factors were set to 1.

$$F'_V = F_V \times (C_m \times C_t \times C_H) \quad (A4)$$

where

C_m = 1.0 Wet Service Factor for dry use

C_t = 1.0 Temperature Factor for in service temperature range
 $<100^{\circ}\text{F}$

C_H = 1.0 Shear Stress Factor to account for increased shear strength in sawn lumber members with limited splits, checks or shakes.

Bending stress at ultimate load in timber stringers

Bending stress at ultimate load and moment capacity of the timber stringers were calculated using equation A5:

$$\sigma_b = \frac{M_{max}}{S_x} \quad (A5)$$

where

σ_b = bending stress at ultimate load

M_{max} = maximum bending moment at failure

S_x = section modulus of timber stringers.

Appendix B: Number of Hex Bolts and Lag Screws

This appendix presents the calculations used to determine number of hex bolts or lag screws to repair timber stringers in horizontal shear.

Hex bolts and lag screws as shear repair

AFPA (1996) mechanical connection concepts were used to calculate the required number of hex bolts and lag screws. A complete separation was assumed at the neutral plane, over the entire length of the stringers. The required number of hex bolts and lag screws were computed by modeling this system as a single shear connection, as shown in Figure B1.

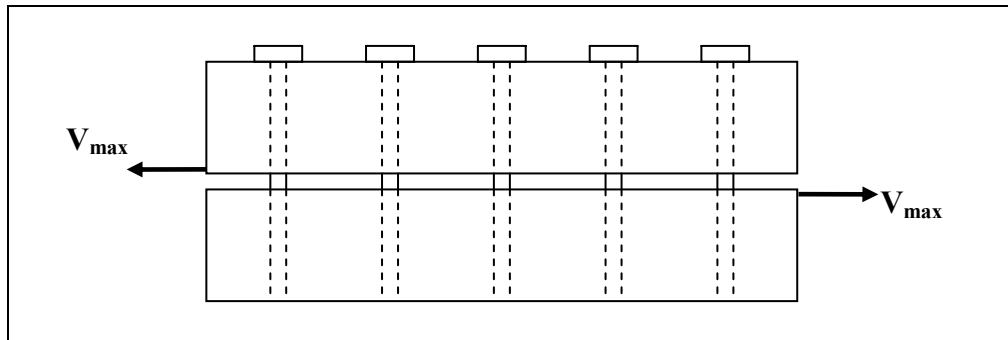


Figure B1. Single shear connection model for hex bolts and lag screws.

The purpose of the hex bolts and lag screws were to transfer the shear stresses along the length of the stringers. The reference lateral resistance of one hex bolt and lag screw was determined using Section 7.5 of AFPA (1996). For single shear connection Section 7.5 provides six different failure modes for hex bolts and three failure modes for lag screws. Among the failure modes which gave the smallest value controlled the capacity of the shear connection.

The yield modes use embedding strength, F_e , fastener yield strength, F_y , and connection geometry to predict a connection yield load for two- and three-member connections. Based on mechanics, six possible yield modes were identified for single-shear connections. Each mode is identified by number and action. Modes I and II actions are bearing dominated. Mode III results from the formation of a single plastic hinge in the dowel near

each shear plane. Mode IV exhibits two yield points in the fastener near each shear plane.

Yield mode equations for hex bolts

Yield modes for the hex bolts were computed using the equations given in Tables B1 which were taken from section Table 7.5-2 (a) in AFPA (1996).

Table B1. Yield mode equations for hex bolts.

Yield Mode	Applicable Equation
I _m	$Z = \frac{0.83Dt_m F_{em}}{K_\theta}$
I _s	$Z = \frac{0.83Dt_s F_{es}}{K_\theta}$
II	$Z = \frac{0.93k_1Dt_s F_{es}t_s}{K_\theta}$ where $k_1 = \frac{\sqrt{R_e + 2R_e^2(1+R_t + R_t^2) + R_t^2R_e^3} - R_e(1+R_t)}{(1+R_e)}$
III _m	$Z = \frac{1.04k_2Dt_m F_{em}}{(1+2R_e)K_\theta}$ where $k_2 = (-1) + \sqrt{2(1+R_e) + \frac{2F_{yb}(2+R_e)D^2}{3F_{em}t_m^2}}$
III _s	$Z = \frac{1.04k_3Dt_s F_{em}}{(2+R_e)K_\theta}$ where $k_3 = (-1) + \sqrt{\frac{2(1+R_e)}{R_e} + \frac{2F_{yb}(2+R_e)D^2}{3F_{em}t_s^2}}$
IV	$Z = \left(\frac{1.04D^2}{K_\theta}\right) \sqrt{\frac{2F_{em}F_{yb}}{3(1+R_e)}}$

where

D: diameter of hex bolts and lag screws
D = 13 mm (0.5 in.)

t_m and t_s : thickness of main and side members, respectively, in a connection

$$t_m = t_s = 191 \text{ mm (7.5 in.)}$$

R_t : Ratio of main to side member thickness in a connection

$$R_t = \frac{t_m}{t_s} = 1$$

θ : Angle loading to grain

since maximum shear force was along the direction of grain

$$\theta = 0^\circ,$$

$$K_\theta = 1 + 0.25\left(\frac{\theta}{90}\right) = 1$$

F_{em} and F_{es} : Dowel bearing strength of main and side members, respectively.

$$F_{em} = F_{es} = 42 \text{ MPa (6.15 ksi) for southern pine}$$

R_e : ratio of main to side member embedment strength in a connection

$$R_e = \frac{F_{em}}{F_{es}} = 1$$

Lateral resistance of one hex bolt was calculated as 13 kN (3 kips). The calculated connection lateral resistance per hex bolt for different modes is summarized in Table B2. Yield mode IV controlled the capacity of the single shear connection for hex bolts which shows two yield points in the fastener near each shear plane.

Table B2. Connection lateral resistance per hex bolt.

Yield Mode	Connection Lateral Resistance per Hex Bolt	
	kN	kips
I _m	85	19
I _s	85	19
II	40	9
III _m	36	8
III _s	36	8
IV	13	3

Yield mode equations for lag screws

Yield modes for the lag screws were computed using the equations given in Tables B3 which were taken from section Table 7.5-2 (c) in AFPA (1996).

Table B3. Yield mode equations for lag screws.

Yield Mode	Applicable Equation
I _s	$Z = \frac{0.83Dt_s F_{es}}{K_\theta}$
III _s	$Z = \frac{1.04k_3Dt_s F_{em}}{(2+R_e)K_\theta}$ where $k_3 = (-1) + \sqrt{\frac{2(1+R_e)}{R_e} + \frac{2F_{yb}(2+R_e)D^2}{3F_{em}t_s^2}}$
IV	$Z = \left(\frac{1.04D^2}{K_\theta}\right) \sqrt{\frac{2F_{em}F_{yb}}{3(1+R_e)}}$

where

D: diameter of hex bolts and lag screws

$D = 13 \text{ mm (0.5 in.)}$

t_m and t_s : thickness of main and side members, respectively, in a connection

$t_m = t_s = 191 \text{ mm (7.5 in.)}$

θ : Angle loading to grain

$\theta = 0^\circ$,

$$K_\theta = 1 + 0.25\left(\frac{\theta}{90}\right) = 1$$

F_{em} and F_{es} : Dowel bearing strength of main and side members, respectively

$F_{em} = F_{es} = 42 \text{ MPa (6.15 ksi)}$

R_e : ratio of main to side member embedment strength in a connection

$$R_e = \frac{F_{em}}{F_{es}} = 1$$

The lateral resistance of one lag screw was calculated as 13 kN (3 kips). The connection lateral resistance per lag screw for different modes is

summarized in Table B4. Yield mode IV controlled the capacity of the single shear connection for lag screws.

Table B4. Connection lateral resistance per lag screw.

Yield Mode	Connection Lateral Resistance per Lag Screw	
	kN	kips
I _s	85	19
III _s	85	9
IV	40	3

Required number of hex bolts and lag screws

The required number of hex bolts and lag screws was calculated using equation B1:

$$N_f = \frac{V_{max}}{q} \quad (B1)$$

where

V_{max} = Maximum shear capacity of timber stringers
 q = reference lateral resistance of one hex bolt or lag screw

The number of hex bolts and lag screws was determined by dividing the maximum shear force at the cross section by the capacity of one bolt. Yield mode IV controlled the capacity of a single shear connections for both hex bolts and lag screws. Lateral resistance of one hex bolt and lag screw was calculated as 13 kN (3 kips). Maximum shear capacity (V_{max}) of 191 mm by 406 mm (7.5 by 16 in.) timber section was 150 kN (33.6 kips). Number of hex bolts and lag screws (N_f) were then computed by dividing the maximum shear capacity of cross section by capacity of one hex bolt and lag screw.

The required number of hex bolts and lag screws along the length of the stringers was calculated to be 12; however, a total of 13 hex bolts and lag screws were used at every 305 mm (1 ft) to make field application simpler and prevent errors while measuring the spacing. Since the splits were not present over the entire length of the stringers, 7 hex bolts and lag screws were also used in experiments at every 610 mm (2 ft) to compare the effectiveness of the repair systems.

Appendix C: Number of Lag Screws to Attach Side Plates

This appendix presents the calculations used to determine number of lag screws to attach side plates in order to repair timber stringers in horizontal shear.

Side plates as shear repair

AFPA (1996) mechanical connection concepts were utilized to find out the required number of lag screws to attach side plates. A complete separation along the entire length of the stringers was assumed at the neutral plane as in previous section. The required number of lag screws was computed by modeling this system as single shear connection, as shown in Figure C1.

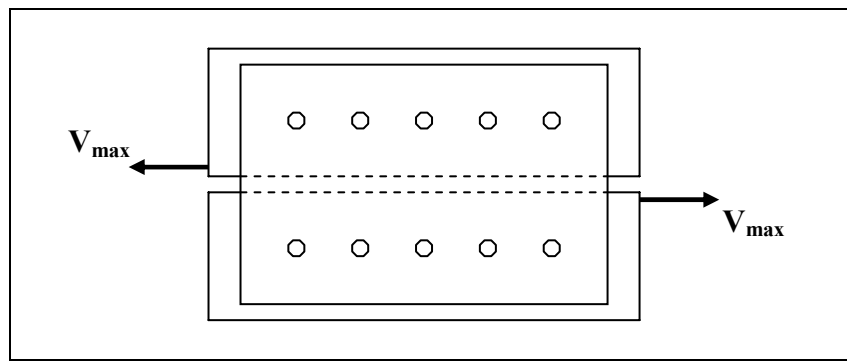


Figure C1. Single shear connection model for side plates attached using lag screws.

The purpose of the lag screws and side plates was to transfer the shear stresses along the length of the stringers. In the calculations bearing capacity of the side plates and timber beam was assumed to be equal. Side plates was also not used over the entire length of the timber stringers to prevent buckling problem due to bending of plates. Reference lateral resistance of one lag screw was determined using Section 7.5 of AFPA (1996). Section 7.5 provides three failure modes for lag screws for single shear connection. Among the failure modes the one which gave the smallest value controlled the capacity of the shear connection.

The yield modes use embedding strength, F_e , fastener yield strength, F_y , and connection geometry to predict a connection yield load for two- and three-member connections. Based on mechanics, six possible yield modes

were identified for single-shear connections. Each mode is identified by number and action. Modes I action is bearing dominated. Mode III results from the formation of a single plastic hinge in the dowel near each shear plane. Mode IV exhibits two yield points in the fastener near each shear plane.

Yield mode equations for lag screws

Yield modes for the lag screws were computed using the equations given in Table C1 which were taken from Section Table 7.5-2 (c) in AFPA (1996).

Table C1. Yield mode equations for lag screws.

Yield Mode	Applicable Equation
I _s	$Z = \frac{0.83Dt_s F_{es}}{K_\theta}$
III _s	$Z = \frac{1.04k_3Dt_s F_{em}}{(2+R_e)K_\theta}$ where $k_3 = (-1) + \sqrt{\frac{2(1+R_e)}{R_e} + \frac{2F_{yb}(2+R_e)D^2}{3F_{em}t_s^2}}$
IV	$Z = \left(\frac{1.04D^2}{K_\theta}\right) \sqrt{\frac{2F_{em}F_{yb}}{3(1+R_e)}}$

where

D: diameter of lag screws

$$D = 13 \text{ mm (0.5 in.)}$$

t_m and t_s : thickness of main and side members, respectively, in a connection

$$t_m = 191 \text{ mm (7.5 in.)}$$

$t_s = 6.4$ (0.25 in.) Thickness of the side plate

θ : Angle loading to grain

since maximum shear force was along the direction of grain

$$\theta = 0^\circ,$$

$$K_\theta = 1 + 0.25\left(\frac{\theta}{90}\right) = 1$$

F_{em} and F_{es} : Dowel bearing strength of main and side members, respectively
 $F_{em} = F_{es} = 42$ MPa (6.15 ksi) for southern pine.

It is assumed that the main and side members have same dowel bearing capacity.

R_e : ratio of main to side member embedment strength in a connection

$$R_e = \frac{F_{em}}{F_{es}} = 1$$

The lateral resistance of one lag screw was calculated as 2.84 kN (0.64 kips). The connection lateral resistance per lag screw for different modes is summarized in Table C2. Yield mode I_s controlled the capacity of the single shear connection. This mode was bearing yielding on side members, as expected.

Table C2. Connection lateral resistance per lag screw.

Yield Mode	Connection Lateral Resistance per Lag Screw	
	kN	kips
I _s	2.84	0.64
III _s	8	1.81
IV	11	2.49

Required number of lag screws to attach side plates

The required number of hex bolts and lag screws was calculated using equation C1:

$$N_f = \frac{V_{plate\ max}}{q} \quad (C1)$$

where

$V_{plate\ max}$ = Maximum shear force on each side plate

q = Reference lateral resistance of one lag screw.

Since separate side plates were used along the shear spans of timber beams, maximum shear force (V_{max}) on the cross section was divided by number of plates to find force on each plate. Yield mode I_s controlled the capacity of the single shear connections for side plates. Lateral resistance of one lag screw was calculated as 12.6 kN (2.84 kips). Shear force on each side plate was 37.5 kN (8.4 kips). Number of lag screws (N_f) to attach side plates was then computed by dividing shear force on each plate by capacity of lag screw.

The required number of lag screws to attach each side plate was calculated to be 13. However, a total of 12 and 14 lag screws were used to attach FRP and plywood side plates to make field application simpler and reduce possible errors while measuring the spacing.

